CRANFIELD UNIVERSITY

School of Applied Sciences

PhD Thesis

Academic Year 2005-2008

Amirreza Aref

Nanotechnology Applied to Stem Cell-Substratum Interactions

Supervisor: Professor Jeremy J Ramsden

Cranfield University

School of Applied Sciences

Nanotechnology Centre

Amirreza Aref

Nanotechnology Applied to Stem Cell-Substratum Interactions

Supervisor: Professor J. J. Ramsden

September 2008

This thesis is submitted in partial fulfilment of the requirements for the degree of Doctor of Philosophy

Table of contents

Nanotechnology applied to stem cell-substratum interactions

Abstract

The modulation of biological interaction with artificial surfaces is a vital aspect of biomaterials research. Perhaps the most challenging area is transplantation involving the introduction of stem cells into the body with their ability to differentiate; the response of stem cells to implanted biomaterials (or to the host tissue) provides a uniquely sensitive way to explore biocompatibility. An understanding of how to direct specific substratum-cellular responses is critical for the development of future biomaterials (e.g., for prosthesis).

Attachment and spreading of a cell to and on a substratum are the first part of the process that leads to the ultimate assimilation of the new cell or prosthesis with the host tissue. Together with conventional microscopy, I have exploited a uniquely powerful noninvasive optical technique (Optical Waveguide Lightmode Spectroscopy, OWLS) to quantify cell attachment and spreading of stem cells to artificial biomaterials, and determine how the cell environment (the substratum),the complex liquid medium bathing the cell, and the presence of congeners, influence attachment and spreading.

My results highlight that quantitative characterisation of interfacial interactions, including their kinetics leads to uniquely new insight into cell-protein-material interactions. This knowledge will be doubtless be useful in the development of new generations of biomaterials with improved properties designed for specific applications.

Preface

The fact is that a great number of people now are suffering from diabetes, kidney failure, spinal cord injury, Parkinson's disease and many types of cancers. Most of us share at least a piece of this experience, our loved ones, in times of pain or need, reaching out, looking to us for comfort, for a way to stop their suffering. This is the quest we join, together, when we contemplate the promise of stem cell research, debate its proper methods, and work toward making our hopes a reality curing disease and disability through stem cell derived therapies.

However, stem cell research starts with understanding its potential for you and me, our parents and children, our friends and families. For people with Parkinson's disease, stem cell research holds the promise of replacing destroyed specialised brain cells. For spinal injury patients, it offers the potential for regeneration of neural tissue, which would reconnect the pathways of sensation and motor control and allow them to walk again, or talk again, or hug their child again.

It may also provide solutions to the devastating complications of diabetes: blindness, kidney failure, amputation, and cardiovascular disease. Stem cell research offers hope for people with a great diversity of illnesses, for people of all age and genders and all backgrounds. It offers hope for each of us, and that hope is not measured by numbers.

Acknowledgement

I would like to express my gratitude to Prof. Jeremy Ramsden and Dr. Robert Horvath for allowing me to undertake this research and for their advices and useful suggestions.

I would also like to express to Prof. Geoff Ashwell who was my supervisor when I came to this university in the Nanomaterials group. I have been working for one year in the molecular electronics field under his supervision.

There are too many friends and colleagues at Cranfield to mention so I will single out a few. Most important are James McColl, Ghazal, Chris Shaw and Andrew Stallard for their help over the course of the work with technical issues. Enza, you are one in a million always happy and always helpful and all the other group members (Farah, Mohammad, Yun-Peng and Julie).

Finally, I feel it is time for me to thank my parents, for always encouraging me to do what I wanted, to go wherever I had to go, to my wife Sima, I thank you and love you dearly and thanks also to my lovely sister (Pooneh) for showing me the way, for their love and support and without whom I would not have had the opportunity to take on this scientific endeavour.

Papers arising from this work

Journals:

- J. McColl, R. Horvath, **A. Aref,** L. Larcombe, S. Morgan, I. Chianella, G. Yakubov, and J.J. Ramsden. Polyphenol control of cell spreading on glycoprotein substrates. *Journal of Biomaterials Science: Polymer Edition, in press*.

- **Aref, A.** Horvath, R, McColl, J, and Ramsden, J.J. Optical monitoring of stem cell-substratum interactions. *Journal of Biomedical Optics, in press.*

- **Aref, A.** Horvath, R, McColl, J, and Ramsden, J.J. Apparent retinoic acid instability results in a new morphology of human embryonal carcinoma stem cells. *Journal of Biological Physics and Chemistry. (Submitted).*

- **Aref, A.** Horvath, R and Ramsden, J.J. Quantitative spreading kinetics as a means of identifying stem cell differentiation. *(Submitted).*

Conferences:

- **A. Aref,** R. Horvath, F. Ansari and J.J. Ramsden. Attachment and spreading of human embryonal carcinoma stem cells on nanosurfaces using optical waveguides. Nanotech 2008, 11th Annual Conference, June 1-5, 2008. Boston, Massachusetts, USA.

- F. Ansari, **A. Aref**, S. Libor, R. Horvath, J.J. Ramsden. Adsorption kinetics of bacteria onto a thin Fe_3O_4 magnetic nanofilm, Nanotech 2008, 11th Annual Conference, June 1-5, 2008. Boston, Massachusetts, USA.

- **Aref, A**., McColl, J., Horvath, R. & Ramsden J.J.TC07-246: Attachment and spreading kinetics of stem cells using optical waveguide lightmode spectroscopy. The Royan International Twin Congress (3rd Congress on Stem Cells Biology & Technology), 5-7 Sep 2007. Tehran, Iran. *(Winner of the Best Poster Award).*

- J. McColl, R. Horvath, **A. Aref,** L. Larcombe, S. Morgan, I. Chianella, G. Yakubov, J.J. Ramsden."SSBII9: Polyphenol restoration of cell spreading inhibition on glycoprotein substrates. The 9th Annual Meeting, Design of Surfaces to Direct Cell Behaviour, 13-14 Sep 2007, Manchester, England.

CHAPTER 1

Introduction and Literature review

The objective of my research is to further understand the initial attachment[1] and subsequent spreading[2] and differentiation[3] process of stem cells. An important area of research is understanding the attachment and spreading kinetics in a mature organism that cause a stem cell population to proliferate and remain unspecialized until the cells are needed for repair of a specific tissue.

[1] Attachment (as a process): "The state of being fixed to an object; it implies that the object to which the attachment is made is larger or more secure, and that the object attached is free to move while remaining attached". The process of the cell arriving at a remaining within the close proximity of the substratum, while bring free to change the shape, and even the area of contact with the substratum. Note that nothing special is implied regarding the detailed micro- and nanomorphology of the cell-substratum contact.

[2] Spreading (as a process): Spreading is the transformation from sphere (i.e. the cell in culture, at the very instant of initial attachment) to segment. Note that this is an idealized (platonic) process. In reality the cell is not a perfect sphere initially, nor is the spread from a perfect segment. Biologically, it implies considerable internal remodelling of the cell, especially of the cytoskeleton, and possibly of the outer cell membrane, especially is protein components. Furthermore, the attainment of the spread state of often a prerequisite for functionally successful differentiation.

[3] Differentiation: In a general sense, the increasingly specialized organization of the different parts of an embryo as a multicellular organism develops from the undifferentiated fertilized egg; of cells, the development of cells with specialized structure and function from unspecialized precursor cells.
The modification that takes place in cells resulting in a change in the structure and function of the cell, and hence, when many cells are modified, a modification in the tissue composed of the cells, e.g. meristematic cells show no differences in function, but when they differentiate into permanent tissue, they become changed in structure, and altered in function, so the tissues composed of the differentiated cells are organized for the division of labour in the mature plant.

Many researchers have worked to bring recognition to the enormous potential that stem cells possess for genetic modification of organisms, regenerative medicine, and investigation in vitro of facets of development that are difficult to explore in vivo. The value of stem cells as resources for both basic and applied research is now acknowledged almost universally. Progress we are gaining a better understanding of both the enviroments and the basic differentiation biology process of these cells (Gardner, 2006).

Fundamental knowledge of cell-substrate interactions is important for tissue engineering, developmental biology, medical implants, and the drug screening. Cell-substratum attachment interaction may also explain differences in cell behaviour in vivo and in vitro. To gain insight into these interactions, a logical approach is to investigate the substrata on which cells attach and grow in living systems.

1.1What are stem cells?

Traditionally, approaches to restore tissue function have involved organ donation. However, despite attempts to encourage organ donations, there is a shortage of transplantable human tissues such as bone marrow, hearts, kidneys, livers and pancreases. Tissue engineering based therapies may provide a possible solution to improve the current shortage of organ donors. One of the major problems in this research areas use is the limit in available human cells.

Stem cells isolated from adults or developing embryos are a current source for cells for tissue engineering. These types of cells have the remarkable potential to develop into many different cell types in our bodies. A stem cell is a cell that, when it divides, can

produce a copy of itself as well as a differentiated cell progeny. This self-renewal capacity underlines the ability of adult stem cells, such as hematopoietic stem cells to constantly renew tissues that turn over rapidly in the adult (for review see Lanza, 2006).

Typically, stem cells can be divided into two broad categories, depending on their origin: embryonic stem cells (ES) and adult (somatic) stem cells (Gepstein, 2002). Both types share the capability to produce identical daughter cells (self-renewal), and produce daughters that are fated to differentiate whilst the former means that they can be expanded and used in large-scale production, the latter indicates that they can differentiate to produce desired cell types, either in vivo or in vitro and in terms of potentiality, stem cells can be classified as a three major groups: totipotent, pluripotent and multipotent stem cells (Watt and Hogan, 2000; Baharvand, 2006a).

It is a not inflexible classification of stem cell potency to call they pluripotent or multipotent. Indeed, it is evident that the distinction between pluripotent and multipotent is becoming growingly more unclear with some cells having greater plasticity than previously realised.

Determination potential of stem cell is dependent to a large extent on the genetic make-up of the cell and including a suitable genetic programme to make a particular cell type; Vats et al., 2002; Baharvand, 2006a). However, this is somewhat offset by the influence of the environment in which the stem cell is placed. For example, changes in cytokine gradients, cell–cell and cell–matrix contacts are important in switching ‘on’ and ‘off’

genes and gene pathways, thereby controlling the type of cell(s) that are generated (Bradley et al, 1984).

1.1.1 Embryonic stem cells (ESCs)

The first mammalian ESCs lines were derived by M. J. Evans and Kaufman in 1981 from mouse blasticysts. Embryonic stem cells (ESCs) are derived from the inner cell mass of the blastocyst and have an exhibit high proliferative capabilities and upon induction of differentiation, may form virtually any specialized tissue. However, because of their embryonic origin, ESCs differ from other stem cells in their ability to retain the potential to generate derivatives of all three germ layers (ectoderm, mesoderm and endoderm).

Figure 1.1 Human embryonic stem cell (gold) growing on a layer of supporting cells (fibroblasts). Image taken from, www.wellcome.ac.uk/en/bia/gallery.htm

Embryonic stem cells have since been shown to contribute to all cell lineages, including the germ line, following microinjection studies in murine embryos which give rise to chimeras, and the first successful derivation of human embryonic stem cell lines was reported by Thomson and colleagues in 1998. The availability of human embryonic cell lines provides a unique new research tool with widespread potential clinical applications (Nagy et al., 1993; Thomson et al., 1998; Baharvand, 2006a).

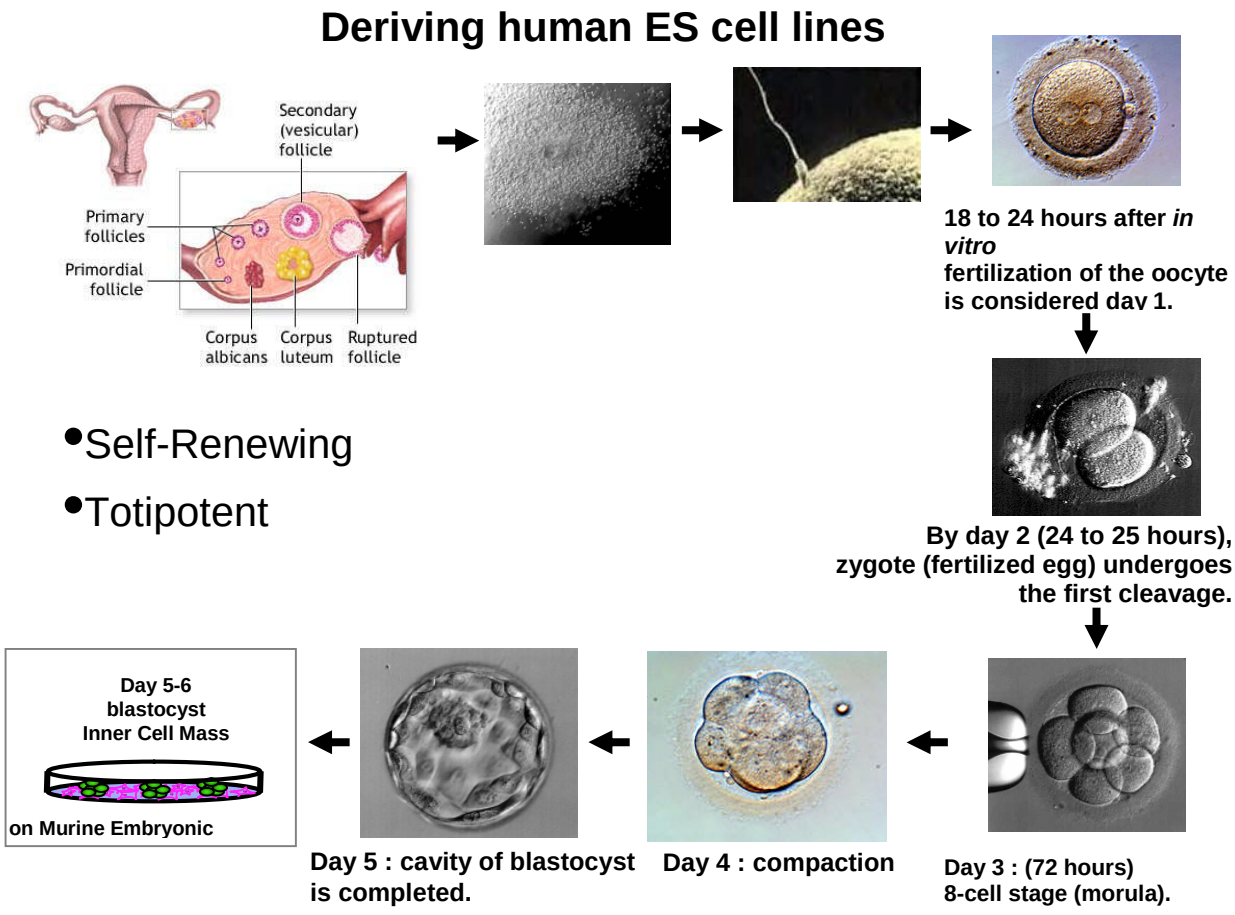

Figure 1.2 Derivation of human embryonic stem cell lines.

Control of ESC differentiation into specific cell types which can be maintained and cultured as pure populations, may provide an unlimited source of cells for transplant in

the treatment of several diseases. An important development in this field stemmed from establishment of human ESCs (Baharvand et al, 2005; Baharvand et al, 2006b). The unique properties of ESCs suggest they will be of great use in clinical applications such as transplantation and tissue regeneration therapies, as well as for studying basic developmental biology, cancer research, and intensive drug and toxic screening, as an alternative method for animal assays (Baharvand, 2006a).

1.1.1.1 Totipotent stem cells

"Totipotency is the ability to form all cell types of the conceptus, including the entire fetus and placenta" (Bongso and Richards, 2006). Some scientists do not believe that the totipotent cells are stem cells because the fertilised egg and the ensuing blastomers from early cleavage cannot divide to make more of themselves but anyway these cells have an unlimited capacity to give rise to any cell types that may form in the adult organism and in mammals the fertilised egg, zygote and the first 2, 4, 8, and 16 blastomeres from the early embryo are examples of totipotent cells (Baharvand, 2006a).

1.1.1.2 Pluripotent stem cells

Pluripotency is the ability to differentiate into several cell types, which represent cells derived during embryonic gastrulation and comprise those of the three distinct germ layers (ectoderm, mesoderm and endoderm), but not of the whole organism. Pluripotent stem cells are classified in four classes: 1) embryonic carcinoma cells (ECCs), 2) embryonic germ cells (EGCs), 3) embryonic stem cells (ESCs), 4) multipotent adult

progenitor cells (MAPCs) from bone marrow this 4th classes was recently discovered, see Baharvand, 2006a).

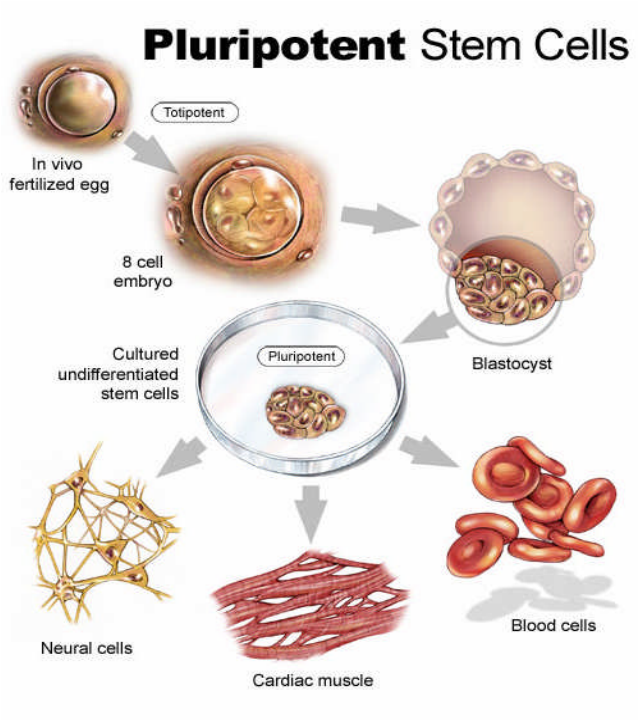

Figure 1.3 Pluripotent stem cell. Image taken from www.csa.com/discoveryguides/stemcell.

In 1970, early mouse embryos grafted into adult mice were found to produce teratocarcinomas (Solter et al., 1970; Stevens, 1970). Previous studies investigating spontaneously occurring teratocarcinoma indicated that the undifferentiated component, embryonal carcinoma, could be propagated in culture. This also occurs in embryo-derived teratocarcinoma (Smith, 2001; Baharvand, 2006a).

Teratoma carcinomas stem cells, which were used in my work, are generally isolated and established as embryonal carcinoma cell lines from teratocarcinomas whatever their

origin providing that there is a resident population of stem cells and their morphology of such cells, in that all murine and human EC linages (Przyborski, 2007). Embryonal carcinoma cells grow robustly in culture providing that they are maintained under optimal conditions. It appears that cell density is the single most significant variation in culture condition that most affects the maintenance of the EC stem cell phenotype.

The majority of the following protocols have been used in my work for the culture of sub-lineages of the well established EC cell line, TERA2, originally derived by Fogh and Trempe in 1975 (review e.g. Przyborski, 2007). Particular sub-lines of the TERA2 lineage, (Andrews, 1984) and TERA2 (Przyborski, 2001), have proved useful as models to investigate the molecular mechanisms that control cell fate in the ectoderm and the formation of terminally differentiated neurons (review: Przyborski et al. 2004).

1.1.1.3 Multipotent stem cells

"Multipotent cells can form a small number of cells/tissues that are usually restricted to a particular germ layer origin" (Kuo and Tuan, 2003) (e.g. bone marrow stromal or mesenchymal stem cells. Multipotent adult stem cells are located in somatic tissues and are known to maintain and regenerate tissues and organ systems (Slack, 2000; Baharvand, 2006a). The cellular basis of these properties is the capacity of adult stem cells to self-renew and to recruit the various cell types of the tissue. In adults, a highly regulated process of stem cell self-renewal and differentiation may help to sustain tissues with high cell turnover (Nagy et al., 1990).

1.1.2 Adult stem cells

Adult stem cells exist in postnatal tissues has been recognized since the 1960s, with the first conceptual proof that blood or bone marrow contains cells that can rescue humans and animals from bone marrow failure. The ability of adult tissue such as skin, haemopoietic system, bone, and liver to repair or renew indicates the presence of stem or progenitor cells. In adult somatic stem cells generally have been thought as tissue-specific and able to be lineage restricted and therefore they typically can differentiate into a relatively limited number of cell types (Dennis, 1999; Javazon, 2001). However, several recent studies suggest that "these cells might be able to break the barriers of germ layer commitment" (Hermann et al., 2006) and differentiate in vitro and/or in vivo into cells of different tissues (Orlic, 2001; Sekiya, 2002).

Moreover, transplanted bone marrow cells contribute to endothelium and skeletal muscle myoblasts and acquire properties of hepatic and biliary duct cells, lung, gut, and skin epithelia as well as neuroectodermal cells (Krause, 2001; Mezey, 2003). Recently, shown bone marrow was shown as a potential source of germ cells that could sustain ocyte production in adulthood. Furthermore, neural stem cells (NSCs) may repopulate the hematopoietic system, and muscle cells may differentiate into hematopoietic cells (Shih, 2002; Johnson, 2005).

1.1.2.1 Mesenchymal stem cells

In recent years "adult mesenchymal stem cells or marrow stromal cells (MSCs) have generated a great deal of interest as a potential source for cell-based therapeutic

strategies in stem cells research field" (Baksh et al., 2007). Mesenchymal stem cells are the adult tissue multipotential stem cells that give rise to cells of the skeletal connective tissues. MSCs are multipotential nonhematopoietic progenitors found in the bone marrow that can be isolated by their adherence to tissue culture plastic with a triple potential of osteo adipo and chondrogenesis. These cells readily generate single-cellderived colonies that can be highly expanded and differentiated into a variety of cell types, including chondrocytes.

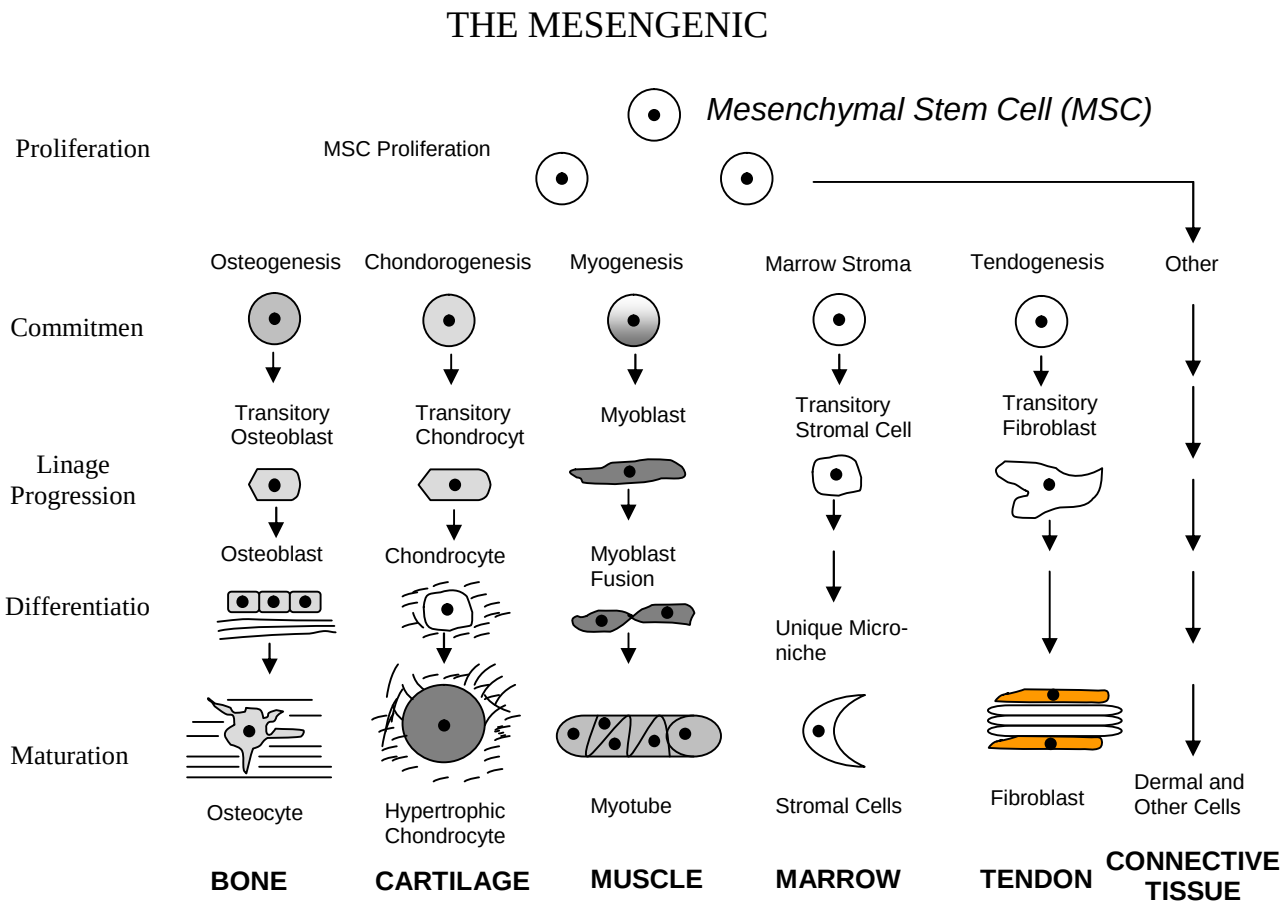

Figure 1.4 The mesengenic process depicts mesenchymal progenitor cells entering distinct linreage pathways that contribute to mature tissues.

The summary diagram in figure 1.4 is therefore a composite of many individuals' efforts and was fashioned to mimic the fundamental aspects of the hematopoietic pathway. Adult mesenchymal tissues all have unique turnover dynamics, some relatively rapid, like bone, and others relatively slow, like cartilage. In all case, turnover means that differentiated cells in the tissue die and are replaced by newly created cells. MSCs must be everywhere mesenchymal tissue turns over. To date, mesenchymal progenitors have been isolated from marrow, muscel, fat, skin, cartilage, and bone. Moreover, every blood vessel in the body has mesenchymal cells on the tissue side of the vessel (some of these are MSCs), although names like pericytes have been given to these multipotent cells (Chen et al., 2006; Caplan, 2006).

1.1.2.2 Hepatopoetic stem cell

Adult stem cells are in attendance in most self-renewing tissues, including the skin, the intestinal epithelium and the haematopoietic system. The best-characterized adult stem cell is the haematopoietic stem cell (HSC) (Wilson and Trumpp, 2006). This rare cell residing in the bone marrow give rise to all blood cell linages and bone marrow transplantation is widely employed for the treatment of congenital, malignant, and degenerative diseases. Although adult HSCs are an important target for genetic modification, success has been limited by difficulty expressing genes in HSCs and by challenge of maintaining and expanding HSCs in culture. Thus, embryonic stem cells as a source of HSCs would make it easier to genetically modify stem cell populations for example in vivo, to discover small molecules that impact blood development, to study genetic and epigenetic influences on hemapoietic cell fate, and to empower preclinical models for gene and cellular therapy (Daley, 2005).

1.2 Cell attachment and spreading

The study of attachment and spreading kinetics is one of the most effective methods for extracting further the parameters which characterise the cell environment. The advances in label-free sensing (Ramsden, 1995a) have led to a better understanding of the widely studied cell attachment and spreading at solid liquid interfaces. Even half a century there was much effort toward elucidating the mechanism of adhesion processes, as well as the interaction of cells with their substrata (Stocker and Rubin, 1967). The attachments of cells to a surface and their subsequent spreading on a supporting substrate have profound effects on the growth and behavior of many mammalian cells (Folkman and Moscona, 1978; Grinnell, 1978).

The importance of fundamental understanding of these processes is ever increasing, since the growth of many cell lines used for the production of pharmaceutically relevant biomolecules is often anchorage-dependent (e.g., human diploid fibroblast), i.e., they require a surface substratum for attachment and growth, and other cell lines produce only poorly in suspension culture.

Numerous attempts were made in the last decades to modify substratum surface properties by coating with certain substances, such as fibronectin, collagen, gelatin, dextrin, etc., in order to enhance the adhesion and spreading of cells on surfaces and thus improve the growth and production performance of the cells (Barngrover, 1986; Butler, 1988). However, before more insights can be gained into the interaction between cells and their substrata, there is need for a precise measurement method for the quantification of the adhesion as well as the spreading processes (e.g. Li et al., 1994).

The measurement of adhesion processes has been hitherto mostly achieved by enumerating the cells using optical or scanning electron microscopy (SEM). These methods, however, are often tedious, and the interpretation of results is subjective. Moreover, SEM requires the cell is killed and the force of adhesion can be obtained by determining the centrifugal force necessary to dislodge the cells (Guarnaccia and Schnaar, 1982).

Hug et al., (2000) have taken the possibility of label-free sensing (optical waveguide lightmode spectroscopy) as a whole cell sensor by looking at cell adhesion and morphology changes of fibroblasts in the presence of analytics.

Pioneering work by Hug et al., (2002) demonstrated the strength of OWLS for monitoring the adhesion and proliferation of anchorage dependent cells in applications where an on-line indicator of the total biomass is needed. In addition OWLS provides metabolic information through detection of the cell mass in close contact with the waveguide.

Horvath et al., (2005) have been reported the effect of the attachment and spreading of living cells on the modes of a grating-coupled reverse waveguide sensor is investigated in real time. Their results indicate that the new design of waveguides (reverse design) has increased probing depth into the sample making, it well suited for the monitoring of cell morphology and the significant changes in the incoupling peak height and peak shape were observed during cell attachment and spreading. He suggested that “the area

under the incoupling peaks reflects the initial cell attachment process, while the mean peak position is mostly governed by the spreading of the cells".

McColl et al (2008) have developed the ability to manipulate the surface characteristics provide a mechanism for directly influencing cell behaviour by OWLS. Their results show the application such as medical implants and tissue engineering require biocompatible, stable surfaces for controlling cell behaviour. Mucin-coated surfaces inhibit cell spreading compared with poly-l-lysine in vitro. Possible applications for a composite glycoprotein polyphenol layer include medical devices, in particular for those operating at mucosal interfaces such as the oral, tracheal or gastrointestinal tract cavities, wound healing, cancer control and the controlled growth of therapeutic cell cultures. (This work is fully described in appendix B.)

One of the most intriguing problems in biocompatibility is how to design the surface of an artificial implant, when the surrounding biological tissue strives to modify the surface for its own purposes (Ramsden, 2008). The principal means for accomplishing this is via the microexudate, a mixture of proteins and other biopolymers secreted by the cells and adsorbed on the implant surface (the substratum). The general problem is how to design an artificial surface that is able to control this living modification. Cell-surface contact involves initial adhesion followed by attachment and spreading which occur prior to growth and interaction of materials in our body.

A thorough understanding of the cellular and molecular mechanisms of these processes should enable them to be controlled; a prequisite for such understanding is their

quantification. Presently, only a few methods are available for measuring attachment and spreading. Certain microscopic techniques, such as interference reflexion and total internal reflexion fluorescence microscopies allow one to visualize the processes directly, but it is very difficult to analyze the results quantitatively.

In my work, is described a novel quantitative method for measuring the number of cells attached to a planar surface and their spreading, in real time on different substrates, different seeding numbers and during differentiation process. It is based on the change in the reflectance of a surface engendered by the presence of the cells. Quantitative expressions are derived relating the measurable change in reflectance parameters to the number, shape, and size of the attached cells.

A quartz crystal microbalance method has been used to determine the kinetics of adhesion in situ (Gryte et al., 1993), their result show that the frequency decreases observed during Vero cell attachment to the gold surface of the QCM are consistent with an effective increase in mass on the resonator surface and (QCM) was applied to continuously monitor the attachment and detachment of the QCM results in decreases in the QCM resonant frequency that can be monitored conveniently in real time. Lysis and detachment of Vero cells caused by vesicular stomatitis virus (VSV) infection can also be monitored readily but no information about spreading can be obtained by these methods. In our work (McColl et al., 2008), a novel method capable of quantitatively characterizing and measuring the attachment and spreading is presented. It is based upon the effective refractive index change for a guided wave caused by the cells.

1.2.1 Spreading cell model[4]

Spreading cell model indicates that the contact between a cell and a solid planar substratum. Figure 1.5 shows of the types of contact between a cell when reaches to the solid planar substratum. (a) A cell cultured in bulk medium that has just landed on the surface, and still retains its spherical shape; (b) an idealized spread cell of the same volume as its spherical precursor, and making closely parallel contact with the substratum; and (c) a more realistic representation of a spread cell, showing the somewhat irregular shape of the cytoplasm, and the presence of filopodia some tens of nanometer long between the main body of the cell and the substratum (Ramsden, 2008).

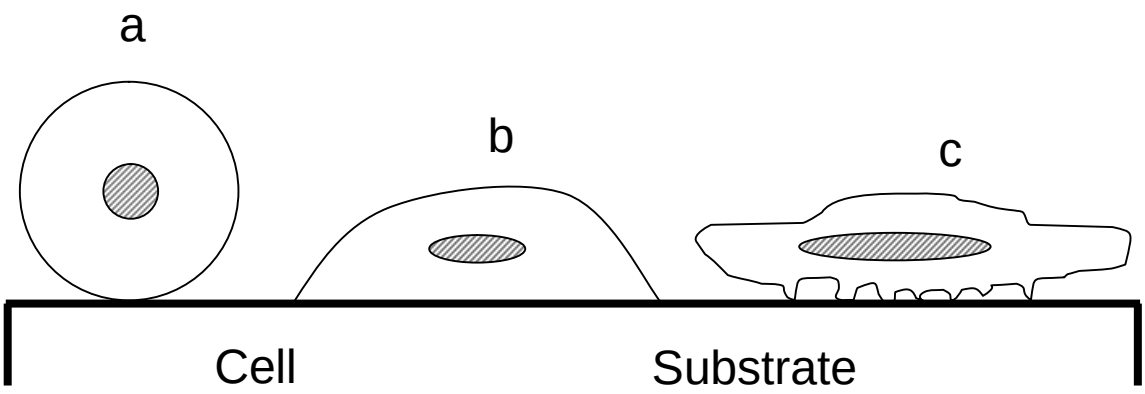

Figure 1.5 Sketch of the types of contact between a cell and a solid planar substratum. The DNA-rich nucleus of the cell is represented by the hatched zone (Ramsden, 2008).

[4] Definition of model: A model is a simplified representation of the entity under consideration, incorporating only is salient features, useful to explain is essential aspects.

1.3 Nanotechnology and where is it used now

Nanotechnology has become one of the most important and exciting fields during the last few years uniting physics, chemistry, engineering and biology. It shows great promise for providing us with breakthroughs that may change the direction of technological advances in a wide range of applications (for a review, see e.g., Poole and Owens, 2003). Nanotechnology is thus defined and concerned with the design, synthesis, characterization, and application of materials and devices with control at least one dimension on the nanometre scale (see, e.g., Ozin and Arsenault, 2005).

The real meaning of nanotechnology is therefore size and control. The consideration of nanotechnology is rather new, but it is by no means is based with atoms and molecules. In fact, “the disciplines of physics, chemistry and biology have long dealt with atoms and molecules, their behaviour and their manipulation; and quantum mechanics is already firmly established as the science of the absolutely small” (Ramsden, 2005).

It was first described in 1959 by Feynman in his famous talk ‘‘There’s plenty of room at the bottom’’. He introduced the idea of making things smaller, so small that ultimately the manipulation of single atoms would be possible. He proposed that such an improvement in physics would eventually find applications in other sciences such as biology, chemistry and electronics (Feynman, 1959). Despite Feynman’s vision and enthusiasm the progress of nanotechnology really took off in the 1980s when the development of apparatus such as the scanning tunnelling microscope (Binnig and Rohrer, 1982) resulted in the opportunity to “see” things at the nanometre scale.

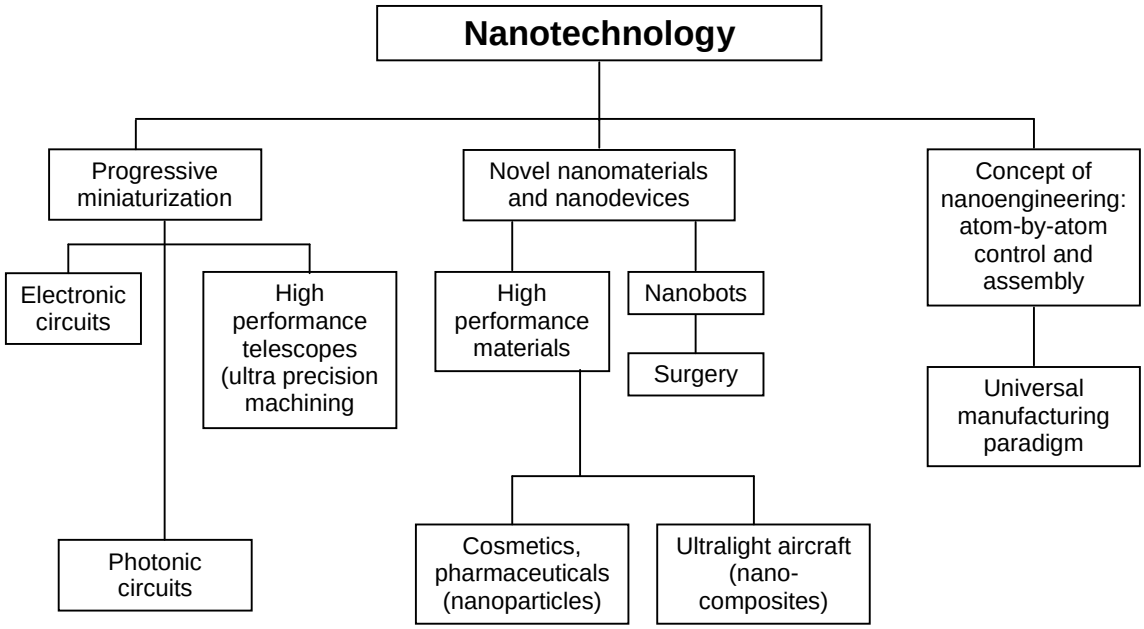

Figure 1.6 From left to right, the indirect, direct and conceptual branches of nanotechnology, with examples (Ramsden, 2005).

1.4 Nanotechnology and biology

Nanotechnology and biology are young and rapidly evolving fields of research at the junction of biotechnology and nanoscience, these two areas, each of which combines advances in science and engineering. Although the field of nanobiotechnology is still in a fairly embryonic state and the applications identification process are also used to generate related to health and environmental issues. Currently, nanobiotechnology is a field that concerns the utilization of biological systems optimized which capable the evolution such as cells, cellular components, nucleic acids, and proteins, to fabricate functional nanostructured comprised of organic and inorganic materials. Bionanotechnology and nanobiotechnology refer, respectively, to the materials and processes at the nanometer scale that are based on biological, biomimetic or biologically

molecules and also concern the modification and application of instruments that can precisely control the biological systems and initially designed to generate and manipulate nanostructured materials, to basic and applied studies of fundamental biological processes (for a review, see e.g., Niemeyer, 2004).

Nanotechnology is beginning to help advance the equally pioneering field of stem cell research, with devices that can precisely control stem cells and provide nanoscaffolds and magnetic tracking systems.

1.4.1 Nanotechnology and the cellular environment

Most biological systems are highly complex systems which have evolved over time to respond to various changes in a cell's environment. In general cellular behaviour is derived from intrinsic and extrinsic factors. The intrinsic factors are the internal genetic make-up of a cell defined by gene regulatory networks. The regulation of the gene networks is through stochastic and deterministic intracellular events. Although these events regulate the cell behaviour at times in an autonomous manner, many of the signals that regulate cellular behaviour are extrinsic and derived from the surrounding environment. The ability to control cell behaviour is important for a wide range of applications in biotechnology and tissue engineering. Developmental biology has shown that the environment plays an important role in controlling cellular differentiation, proliferation and of particular interest in controlling the cellular environment is to control the interactions at the nano-length scales. In the body, cells interact with their surrounding tissues on a sub-cellular level as well as on a tissue level. For example, many ECM fibres are on the multinanometer length scales. Therefore the ability to

control the in vitro cellular environment on the nano-length scales by using engineering and materials sciences approaches is of great interest in controlling cell behaviour (for review, see e.g., Khademhosseini et al., 2006).

Nanotechnology has been increasingly used to control the cellular environment. For example, nanomaterials such as self-assembled peptides and electrospun nanofibers are emerging as powerful technologies to generate 3D structures. In addition, nanoscale topography has been shown to be a powerful regulator of cell behaviour such as alignment, migration and differentiation (See e.g. Khademhosseini, 2008)

1.4.2 Nanotechnology and stem cells

During the last few years, stem cell biology has pioneered a rapid advancement, leading to rising hopes that stem cells, migrating towards a lesion target area, will contribute to functional improvement. Stem cell research area has recently generated more public and professional interest than almost any other topic in biology. One reason stem cells capture the imagination of so many is the promise that understanding their unique properties may provide deep insights into the biology of cells in general as well as a path towards treatments for a variety of degenerative illnesses. And although the field of stem cell biology has grown rapidly, there exists considerable confusion and disagreement as to the nature of stem cells (for review, see e.g., Lanza, 2006)

Therefore there is a need to develop methods for visualising transplanted stem cells and for quantifying their behaviour for a better understanding of their migrational dynamics and differentiation process and of their regeneration potential. Initial cell surface

reactions may trigger multiple responses, which in turn result in either spreading or detachment of the cell. Cell adhesion and mobility depend strongly on the interactions between cells and extracellular matrix (ECM) substrates (Zamir and Geiger, 2001).

1.4.3 Cell binding mechanisms (morphology)

Suspended cell morphology is that of a sphere and when attaching to a surface they first bind and then spread as they become more established. Figure 1.7A depicts rodent fibroblasts 10 minutes after attachment with the cells still mainly spherical in appearance. The same cells at 180 minutes are fully spread, morphologically distinct and well established (Figure 1.7B).

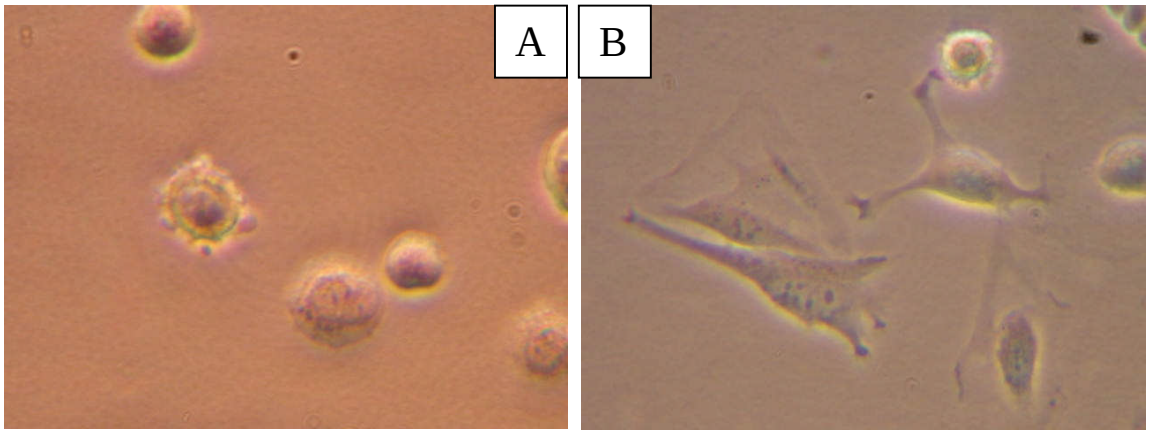

Figure 1.7 Fibroblasts cells (3T3 cell line) attachment after 10 minutes (A) and after 180 minutes (B).

The cells of multicellular organisms bind to the exteracellular matrix (ECM) and each other. The (ECM) consists of macromolecules secreted by cells such as collagen, proteoglycans and glycoproteins (e.g. fibronectin and laminin) that interact with the cell

through integrin receptors at the cell surface. The glycoproteins give an ordered structure to the extracellular matrix and the integrins bind to these. Integrin receptors are attached to filaments within the cell cytoplasm, span the cell membrane and attach to arginine-glycine-aspartate (RGD) domains on the proteoglycan (Pritinder and Li, 2000; McColl, 2007).

1.4.4 Cell-cell signalling and internal cell signalling

Cell to cell signalling involves the release of a signalling molecule from one cell which binds to a specific receptor on another cell. This can be paracrine, endocrine of autocrine and in addition cells can also communicate via gap junctions. Binding of the signalling molecule results in a receptor conformational change which initiates secondary signalling cascades that travel through the cell's internal machinery (Pennisi, 1998). By changing the cell's environment, one also changes the cell's genetic expression. Genes that are normally expressed can be up-regulated or down-regulated, while genes that normally are not expressed at all may be turned on. This may lead to very different functionality in cultured cells compared to their in vivo counterparts (Khademhosseini, 2008).

1.4.4.1 Cells behavioural on bionanomaterials

Attachment and spreading is a key behavioural indicator of living cells. Nanoobjects materials offer many possibilities for the modification of various materials turning them into nanomaterials, such as nanofibers and nano carbon tubes for optimal attachment, proliferation and spreading of different kinds of cells (reviewed see e.g., Dinesh et al., 2006). Once cells plated onto artificial adhesive surfaces, cells first flatten and deform extensively as they spread. At the molecular level, the interaction of membrane-based integrins with the extracellular matrix (ECM) has been exposed to initiate a complex flow of signalling events, which subsequently triggers cellular morphological changes and results in the generation of contractile forces (Griffith, 2002).

Stem cells are a useful tool at this stage for investigation methods relating to the extraction of specific cell types from mixed cell population and to study the differentiation events. Studies of the interactions between substrate topography and stem cells have been encompassed a wide variety of cell types and substratum features including grooves, ridges, steps, pores, wells, nodes, and adsorbed protein fibers.

1.5 Biomaterial surfaces

The area of biomaterials and in particular the rapidly developing field of stem cells and tissue engineering require the ability to control cellular responses to materials. Driving these research areas is the need for better materials in the clinic and the desire for new tissue regeneration strategies. Biomaterials can be classified in four main groups of materials: polymers; natural materials (including plants and animals, ceramics (carbons,

glasses) and metals and in some other classifications composites are a fifth class of biomaterials. Recently, many biomaterials surface engineers have developed polymers and natural biomaterials in combination with living cells and apply practically in the field of tissue engineering and organs (see e.g. Ratner et al., 2004).

Cell-surface interactions dictate biomaterial compatibility, when a cell interacts with a biomaterial; it senses the surface topography and will respond accordingly. If a suitable site for adhesion is detected, focal adhesions and actin stress fibers are formed, later, microtubules are recruited, which stabilize the contact (Gallagher, 2002; Dalby et al., 2002). It was reported that regular nanotopography significantly reduces cell adhesion (Curtis, 2001). It is also believed that small fiber diameter and the overall porous structure aid in the adhesion and migration of cells into the scaffold (Yoshimoto, 2003).

One key area of research achievement extensively attention during the past quite a few years is tissue engineered scaffolds. These scaffolds can be constructed of a range of materials and shapes depending on the application. Chu et al. (2002) used a 3D porous biodegradable hydrogel on a nonwoven fabric structure which an alternate concept developed by Karamuk et al. (2000) uses a 3D embroidered scaffold from a tissue-engineered substrate. Prospect in the future, various novel concepts will be undergoing development. Heim et al. (2002) reported on the development of a textile-based tissue engineered heart valve. These concepts will provide new and novel implantable products for advancing medical treatments and cell therapies in the future (for review see e.g. Ratner et al., 2004).

1.5.1 Prospects for smart biomaterials

Smart or intelligent materials are polymers which respond with sharp, large property changes to small changes in physical or chemical conditions. These materials can take many forms; they may be dissolved in aqueous solution, adsorbed, attach on aqueous-solid interface or cross-linked in hydrogel (Ratner et al., 2004). One of the most promising areas of research into biomaterials surfaces is ways in which such surfaces can be made “smart”, which typically means responsive to their environment (Ramsden, 2008). Polymers that are made smart may be physically or chemically conjugated mixed to biomolecules such as proteins and oligopeptides, sugars and polysaccharides, RNA and DNA. These combinations produce a new, smart “biohybrid” system that can combine the individual properties of the two components to yield new properties (Ratner et al., 2004).

1.5.2 Bioactive coatings

The concept of bioactive coating is in effect to transform biomedical substrates such as scaffolds into the physiology of the host organism. The kinds of activities that are of interest are the encouragement of cell attachment, the prevention of cell proliferation or inhibit spreading. The two ways in which bioactivity is achievable are: 1) Coating with fragments of biomacromolecules (polypeptides or polysaccharides); 2) Incorporating a reservoir of small molecules such as drugs, growth factors and hormones within the implant. Bioactive coatings are very interesting and important research area in biomaterials science and very useful for promoting the adhesion or adhesion-inhibiting coating of cells to an implant (Ramsden, 2008).

1.5.2.1 Cell adhesion-promoting coatings

Controlling cell attachment on synthetic scaffolds is essential to successfully recreate the complex chemical and topographical cues cells would normally receive in the body hence cells need to be encouraged to attach, proliferate and differentiate into the correct phenotype as would be expected naturally in the body. The most extensively adhesion-promoting researched are based on the tripeptide motif arginine-glycin-aspartic acid (RGD), which is a fragment of the ubiquitous adhesion protein fibronectin. This fragment is a receptor for a particular integrin present on the surface of endothelia cells and fibronectin contains many other fragments acting as receptor for other kinds of cells (Ramsden, 2008).

1.5.2.2 Cell adhesion-inhibiting coatings

Cell adhesion inhibiting coating on solid surfaces is important to study the developmental properties of the cells, e.g. differentiation, adhesion, motility and proliferation. There are very promising as biomaterials agents that coating can slowly release or generate in situ bioactive substances. For instance, the simple molecule nitric oxide, NO, is a well-known inhibitor of platelet adhesion and activation (Ramsden, 2008)

1.5.3 Natural materials

Natural polymers (materials) offer the advantage of often identical to macromolecular substances which the biological environment is prepared to recognize and to deal with

metabolically (table 1.1). An interesting characteristics of natural polymers is their ability to be degraded by naturally taking place enzymes, a virtual guarantee that the scaffold will be ultimately metabolized by physiological mechanisms (for review see e.g. Ratner et al., 2004).

1.5.3.1 Mucin (nanobiomaterial)

Originally the word mucus corresponded to viscous and slippery secretions from humans and various animals and mucins are the main constituent and play a major role in the defense mounted by mucus layer in our body, which contains a heavily glycosylated glycoprotein. Mucins were probably the first type of compounds to be clearly recognized as glycoproteins and they have been based on their chemical composition (from 50 to 80 % carbohydrate) and molecular mass (from several hundred to several thousands kDa). Mucins are high molecular weight glycoproteins (Figure 1.8) with rheological properties (viscosity, elasticity) important for their physiological function: for instance, the efficiency of the mucociliary escalator in the airways, buccal cavity, gastrointestinal tract, and surface of the eye (Roussel and Delmotte, 2004). There are 19 mucin genes (Perez and Hill, 1999) characterised for humans (for review e.g. McColl, 2007). Many of the 19 mucin genes are tissue-specific and the glycosylation configuration within a tissue can also vary between individuals suggestive of a detection role for these molecules.

The physical properties of the mucins are important for the protection of the underlying mucosae and from a general point of view, mucins can interact with endogenous molecules from different origins (mucosae, inflammatory cells). However, it is obvious

that due to their high glycosylation, many functions of these molecules should depend on their carbohydrate chains, which offer wide possibilities on interactions with their environment (Roussel and Delmotte, 2004).

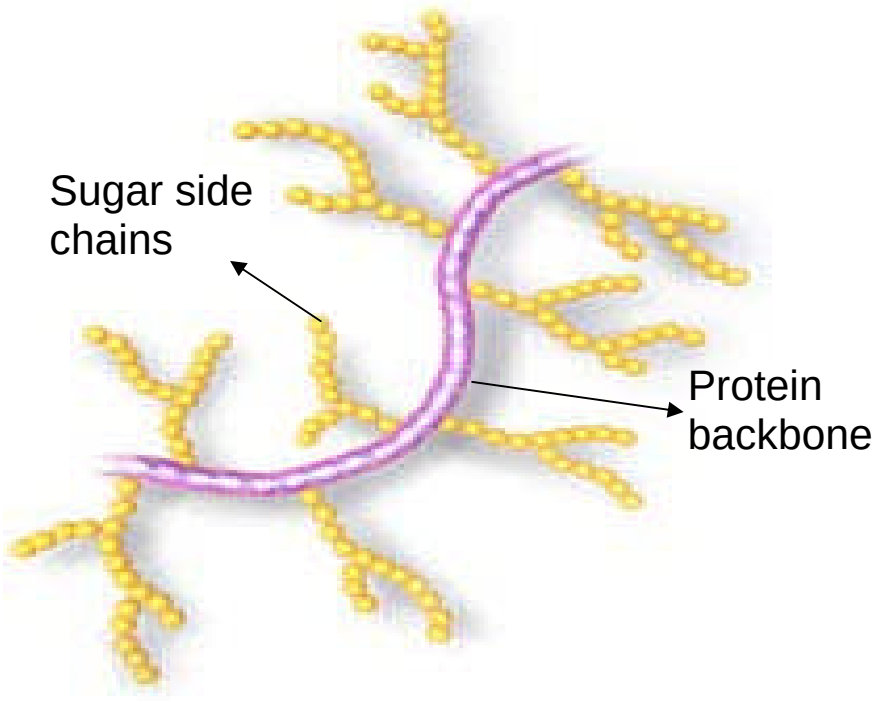

Figure 1.8 Schematic diagram of mucin molecule which consists of a central protein core with branched glycosylated side chains (Roussel and Delmotte, 2004).

1.5.3.2 Mucin structure

Mammalian mucins in general contain fucose, galactose, N-acetylglucosamine, N-acetylgalactosamine and sialic acid with a relatively small quantity of mannose also present. Mucin has diverse roles ranging from lubrication (Bansil et al., 1995; Proctor and Carpenter, 1998), also are probably able to bind to many other molecules, for

example, human neutrophil elastase, a product of the inflammatory response, can be inhibited by human airway mucins.

The outstanding lubricating properties of mucin have been linked to its ability to adhere to particles and may have a role as biological lubricants, facilitating the movement of bacteria, sloughed off cells and non-digested particles in the gastrointestinal tract. This creates a repulsive force that greatly reduces friction between surfaces (Berg et al., 2003; Berg et al., 2004).

Mucins are therefore key components of saliva and the ability of saliva to adsorb onto surfaces is due to mucin's film forming properties (Levine, 1987; Hatton, 1987; McColl, 2007). Therefore when mucin-based saliva replacements are tested they lubricate and reduce wear better than their saliva complements (Chrissterson, 2000; Turrsi, 2002).

During tumor development both membrane-bound and secreted mucins have a role (Moniaux, 2004); for instance the reduction of cell adhesion due to corrupted expression, discharges cells into circulation thus facilitating metastasis (Wesseling, 1996).

Table 1.1 General properties of certain natural biomaterials

	Polymer	Incidence	Physiological function
A. Proteins	Silk	Syn by arthropods	Protective cocoon
	Keratin	Hair	Thermal insulation
	Collagen	Connective tissue	Mechanical support
	Gelatine	Collagen	Industrial product
	Fibrinogen	Blood	Blood clotting
	Elastin	Neck ligament	Mechanical support
	Actin	Muscle	Contraction, motility
	Mucin	Muscle	Contraction, motility
B. Polysaccharides	Cellulose	Plants	Mechanical support
	Amylose	Plants	Energy reservoir
	Dextran	Syn by bacteria	Matrix for growth
	Chitin	Insects	Provide shape and form
	Glycosaminoglycams	Connective tissue	Contributes to mechanical
C. Polynucleotide	DNA	Cell nucleus	Direct protein biosynthesis
	RNA	Cell nucleus	Direct protein biosynthesis

1.5.4 Poly-l-Lysine (PLL)

Cell interactions with foreign materials are usually mediated by a biological intermediate, such as adsorbed proteins and synthesized molecules. By adsorbing or covalently grafting ligands for cell-surface adhesion receptors to the material surface this mediation can be mimicked. Poly-L-lysine (PLL) is a synthetic molecule used to increase cell attachment to plastic and glass surfaces (McKeehan, 1984). Tissue culture plastic has a negative surface charge which is produced by plasma treatment of the

polystyrene. While many researches have shown that reduced serum culture can be significantly enhanced by coating the culture surface with positively charged polymers, i.e., Poly-L-lysine surface treatment improves adhesive properties by altering the charge on the vessel surface from negative to positive.

Considerate the cellular response to the ECM or external environment would give close into the ability to control cell behaviour. PLL is not broken down by the proteases released by cells in culture and it does not stimulate biological activity in the cells cultured and also PLL dose not introduce impurities carried by natural polymers (Ham and McKeehan, 1979).

1.5.5 Nanomaterials

The role of the surface chemistry on cell behaviour has been explored extensively in the past decades (Senesi et al., 2007). Substratum topography has direct effects on the abilities of cells to orient themselves, migrate, and produce organized cytoskeletal arrangements (Meng et al., 2006). The nanorevolution offers great promise for new creation of biomaterials and biomedical surfaces.

Nanostructured surfaces, such as polyamide nanofibers, nanoparticles, and carbon nano tubes are considered for various applications in stem cell biology and technology. Most nanomaterials in various physical or chemical forms may be able to enhance the cell response selectively for biological application in tissue integration.

Bionanomaterials based on nanostructures define in the 1-100 nm range; have been used to create materials that have novel properties and functions. In particular, nanofibers, carbon nanotubes and magnetite nanoparticles are now used to target synthetic ECM and plasmids to specific cell types while protecting these macromolecules from enzymatic degradation (Chavany et al., 1994; Janes et al., 2001). Additionally, "nanoparticles have been proposed for the treatment of many diseases that need constant drug concentration in the blood or drug targeting to specific cells or organs" (Braydich-stolle et al., 2005).

Nanomaterials can be classified as two main groups: natural or manmade. The former are produced naturally: such as proteins in the body, which control things like transfer of information or repairing cells.

A living cell is a gorgeous example of a highly sophisticated, controlled system of nature's nanomaterials, proteins and other biomolecules, which self-assemble into various supermolecular architectures and interact in a well-defined manner at the nanometer scale. Nanocomposites permit materials combining a greater variety of attributes than is possible with simpler materials (Ramsden, 2008) and also nanodevices permit the development of information processing and thus responsivity to be incorporated into coatings, combined with ultracompact artificial sensors.

Flemming et al. (1998) have described the topography of the basement membrane and reviewed the effects and fabrication of synthetic nanostructured surfaces on cell behaviour.

Rosenthal et al. (2001) have prepared serotonin-labeled nanocrystals and demonstrated that these nanocrystals inhibit serotonin transport activity in transfected cells.

1.5.5.1 Carbon nanotubes

Another class of nanomaterials are carbon nanomaterials, which are a macromolecular form of carbon with high potential for biological applications due in part to their unique mechanical, physical, and chemical properties. Carbon nanomaterials are strong, flexible, may conduct electrical current, and can be functionalised with different molecules, properties that may be useful in basic and applied biological research. Carbon nanotubes (CNTs) have attracted a great deal of attention due to their unique structural, electrical, and mechanical properties (Paradise and Goswami, 2007). Recently, there has been an intense interest in exploring some of their novel properties, such as superior strength, flexibility, electrical conductivity, and availability of chemical functionalisation (Chen et al., 1998) for biological applications both at molecular and cellular levels.

Studies of the interaction between CNTs and living cells are still limited. Mattson et al. (2000) reported the feasibility of using CNTs as a substrate for neuronal growth. Hu et al. (2004) have reported chemically functionalized CNTs as substrates for neuronal growth and studied fully interaction between CNTs and living mammalian cells and their results show that the chemical fictionalization of multiwall carbon nanotubes (MWCNTs) possess a diameter almost 100 nm and aspect ratios that are similar to those of small nerve fibbers.

That idea of reconnecting the pathway of sensation signal after neuronal injury such as spinal cord injury is not new and during a few last years advances in nanotechnology have stimulated a renewed interest in the development of novel neural biomaterials that could potentially be used for reconnecting neurons. CNTs are a novel form of carbon made of a rolled layer of grapheme, which appears well suited to the design of novel neural biomaterials (Lovat et al., 2005).

1.5.5.2 Nanofibers

Nanofibrous scaffolds structured by electrospinning certain polymers are highly porous have a high surface area to volume ratio, and morphological properties similar to collagen fibrils (Li, 2002; Li et al., 2005). These physical characteristics promote favourable biological responses of seeded cells within these scaffolds including enhanced cell attachment, proliferation, and maintenance of the chondrocytic phenotype (Li et al., 2003 and 2005). Attempts to make nano fibrous structures began for tissue formation to make scaffolds that are an artificial ECM substitute. These scaffolds aim to mimic collagen, a natural ECM component in tissues such as ligament, tendon, and bone and even skin and they reach scales between 50 and 500 nm (Smith and Ma, 2004).

1.5.5.3 Magnetite nanoparticles

Iron oxide nanoparticles are the end products of a wide variety of physical, chemical and biological processes and have attracted a considerable attention during the last decade and they have been of great interest in many important technological applications. The use of magnetite nanoparticles in clinical and medicine is important and has considerable promise for applications in the biomedical and diagnostic fields such as diagnostic medicine, targeted drug delivery, hyperthermic treatment for malignant cell, cell labelling, tissue repair and magnetic resonance imaging (MRI) (Berry and Curtis, 2003; Ansari et al., 2008).

Another application of magnetic nanoparticles is in separation because the reactivity of the particles can be adapted by modifying the surface coatings on the nanoparticles. The nanoscale particles can be recovered for reuse and they have very high surface areas. The magnetic nanoparticles which are widely used for biomedical applications are Fe_3O_4 and related oxides, which are chemically stable, nontoxic, non-carcinogenic and have useful magnetic properties.

1.6 Evaluation of toxicity of nanomaterials with stem cells

There is a serious lack of information concerning the effect of nanoparticles on human health and the environment, such widespread application of nanomaterials may cause significant potentials for human exposure. Therefore, appropriate risk assessment and management of nanomaterials should be performed to assess and regulate these nanomaterials to protect human health and the environment (Gonsalves et al., 2008).

Many nanomaterials are unique because their physical behaviour when measuring less than 100 nm changes from classical to quantum and they are small enough to penetrate even very small capillaries throughout the body and be widely disseminated to various organs and tissue (Revell, 2006). Thus, they can affect the physiology of any cell and cells exposed to foreign particles may initiate an immunological response. Also, particles may have an effect on the cellular transcription process and induce change at the molecular level.

This consideration is importance for the development of stem cells research, where the effects of nanoparticles on their potential for self-renewal and differentiation are largely unknown. Braydich-Stolle et al. (2005), by using mouse spermatogonial stem cell line as a model to assess nanotoxicity in the male germ line in vitro, demonstrated a concentration-dependent toxicity for all types of particles tested, whereas the soluble salts had no significant effect. Silver nanoparticles were the most toxic while molybdenum trioxide (MoO_3) nanoparticles were less toxic.

Single wall carbon nanotubes (SWNTs) in suspension in the culture medium were incorporated into the cell cytoplasm by macrophages and leukaemia cells without affecting the cell population growth (Cherukuri et al., 2004 and Shi, 2004). But it has been shown that CNT substrates decreased keratinocyte (Shvedova, 2003), glial (McKenzie et al., 2004), and HEK293 (Cui, 2005), cell survival significantly, raising important concerns about the biocompatibility of the nanomaterials.

Nanoparticles may also gain access to the body by ingestion or be generated within joints as wear particles from the bearing surfaces of a prosthetic replacement. The sites of deposition of these particles include the liver and spleen, in which organ there may be general consequences of exposure, for instance the stimulation of immune systems (Revell, 2006).

Despite there is a large body of evidence about the effects of nanoparticles on the living systems and specially cells from which they are constituted, these effects are largely unknown and remain to be investigated. In conclusion, nanoparticles represent a new challenge to those involved with toxicology and biocompatibility and little is known of the biological effects to nanoparticles. The increasing availability of sophisticated methods of evaluating biological phenomena, including developmental biology, drug discovery and molecular biology especially as it is applied in immunology and genetics, present opportunities for unfolding knowledge in this exciting and important area (Revell, 2006).

1.7 Attachment and spreading measurement techniques

To measure interaction of particles such as proteins, or cells, onto a surface several techniques, are used some of which are based on optical principles. Total internal reflection fluorescence (TIRF), scanning angle reflectometry (SAR), and ellipsometry are examples of optical based uses and the quartz crystal microbalance (QCM) is based on a weight measurement (See e.g. Ramsden 1993). Each of these methods or techniques offers various advantages and disadvantages (Brusatori, 2001). For instance, the disadvantage of the total internal reflection fluorescence is to require particles with either a natural or attached fluorescent label; and the quartz crystal microbalance technique requires careful accounting of viscous drag of the contacting liquid.

In contrast, optical waveguide lightmode spectroscopy (OWLS) suffers from neither of the problems (Brusatori, 2001), and has been shown to provide accurate and precise kinetic adsorption data for several protein or nanoparticle/surface systems (Kurrat et al., 1997; Ramsden and Mate, 1998). In my work, OWLS is used to obtain continuous measurements of attachment and spreading of cells (Ramsden et al., 1995b; Li et al., 1994).

Monitoring the attachment, spreading and the total biomass of cell growing in monolayers may be used as a control factor in a number of applications. These parameters are required in the development of new bioreactors. Image analysis techniques of any microscopic pictures depend on edge intensity and level and are normally restricted to subconfluent systems and the visible projected cell area is only an

indicator of the actual area in close contact with the surface. On the other hand, OWLS is a very sensitive method which can measures the effective refractive index above an solid surface and within a sensing region of about 500 nm (Ramsden, 1994).

The simple OWLS technique, described here allows the accurate determination of both the adhesion and the spreading kinetics of cells (Li et al., 1994) on various modified surfaces and in different kinds of medium. The chip surface may be readily modified using, for example, the Langmuir-Blodgett film technique or chemical methods to allow the investigation of cell interaction with other surface materials. Furthermore, the thickness of the protein adlayer needed to promote adhesion can be determined very precisely.

This technique (Li et al., 1994) helps us to select substrata to which cells adhere and spread and allows kinetic information on cell response to various media and on different substrata to be obtained. Thus, the optical waveguide is a powerful biological sensor for the detection of cell adherence and provides valuable information for microcarrier research.

1.7.1 Label-free sensing- OWLS

In recent years, imageless label-free techniques exploiting the evanescent field created by light guided in optical waveguides have been exploited, and it is already well established that the size, shape and average refractive index of the cell body can be determined (Li et al., 1994; Hug, 2000). Since the evanescent field decays exponentially away from the surface of the waveguide (i.e., the substratum), what is actually sensed

by the waveguide (via the propagation constants of its modes) is the Laplace transform of the cell geometry. It has been convincingly demonstrated that high resolution kinetics of the spreading transformation on substrata can be obtained by this method (Ramsden, 1995b). These nonimaging waveguide methods have been recently augmented by a powerful new development that enables the arrangement of the cells on the substratum to be simultaneously characterized (Horvath et al., 2001; Horvath et al., 2005).

1.7.1.1 Optical waveguide lightmode spectroscopy (OWLS)

The OWLS technique was developed in the mid-1980s and is based on multiple total internal reflection, which is used in studying adsorption, desorption, adhesion, of protein or other macromolecules onto the surface and biospecific binding processes (Ramsden, 1993; Kurrat et al., 1998). Linearly polarized light from a He-Ne laser guided light travelling along an optical waveguide in the form of a thin slab of high refractive index material surrounded by lower refractive index material (usually a glass substrate) exhibits a discrete spectrum of modes, and the guided light can be thought of as propagating along the waveguide in a zigzag fashion undergoing total internal reflexion alternately at the two boundaries of the waveguide (Ramsden, 1995a). The OWLS technique measures the refractive index within a thin film layer close to a surface (Ramsden, 1995b).

The evanescent field generated by the reflexions will interact with cells or indeed anything else sitting on the waveguide. Changes at the waveguide surface results in changes to the measured propagation constants of the guided modes.

Briefly, OWLS is based on the phase-shift which occurs when polarised light is totally reflected at the interface between the waveguide and the sample medium (Fig. 1.9). At the interface, light penetrates approximately 100 nm into sample medium, which corresponds to the penetration depth of the evanescent wave.

If molecules such as proteins or cells are adsorbed at the interface (within the penetration depth of the evanescent wave), the extent of the phase-shift depends on the total amount and polarisability of the adsorbed molecules. Due to this phase-shift the light intensities of both the electromagnetic (TE) and the magnetic (TM) modes reach their individual maxima at certain so-called coupling angles (Fig 1.9).

For more detail about the principle and equations of this technique see the experimental method chapter and appendix A.

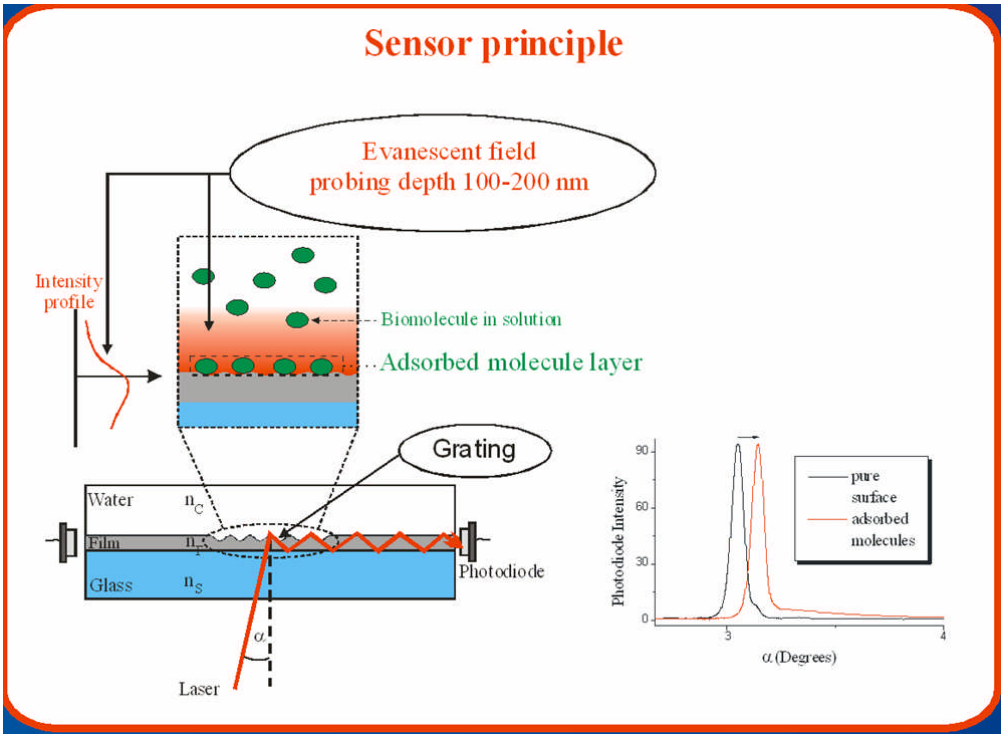

Figure 1.9 Schematic illustration of the adsorption of proteins and cells on the waveguide (Horvath et al., 2005)

1.7.1.2 The principle of OWLS

This method makes use of the grating coupler, which is the most common approach for measuring the propagation constants of the guided lightmodes (Ramsden, 1993). In the incoupling configuration, light from an external beam (typically a highly monochromatic, wavelength λ, linearly polarized laser) is made to fall on the grating and the angle of incidence α is selected to couple the light into the waveguide. The beam itself may have a diameter of several tenths of a millimetre, and the grating itself extends to typically 1–2 mm. The incoupling condition is:

$$N = \sin \alpha + \lambda\kappa/\Lambda$$

Where N is the effective refractive index of a given lightmode, $\kappa = 0, \pm 1, 2,...$ is the diffraction order, and Λ is the grating constant. N is a function of the refractive indices of the waveguide layers (Ramsden, 1993), including the cover material, which in the situation we are considering is heterogeneous, comprising cells and their surrounding liquid medium. Sweeping α while measuring the intensity of the incoupled light using a photodiode at the end of the waveguide produces a series of peaks (the lightmode spectrum, hence this technique is usually called optical waveguide lightmode spectroscopy, OWLS) corresponding to the allowed modes of the waveguide.

The incoupling is not infinitely sharp, but is somewhat broadened (Ramsden, 1993). When cells are present on the grating it is observed that the broadening is much greater than the limiting peak width (Horvath, 2001), depending on the actual construction of the waveguide, two peaks may even be observed (Horvath, 2005). Intuitively one might guess that the greatest broadening is observed when exactly half the substratum is covered by cells, and this has been confirmed by detailed calculations (Cottier and Horvath, 2008).

For a given surface coverage θ, the peak width also depends on the optical contrast between the covered and uncovered zones (i.e., the difference in refractive indices between the objects and the medium in which they are immersed). Note that the incoupling efficiency, and hence the peak heights, depends on the optical contrast between the waveguiding film and the cover materials, which will therefore also influence the composite peak width (Horvath, 2001).

1.7.2 Optical waveguides

Of practical importance is the confinement and propagation of light must somehow be trough into the waveguide. One way is to focus a laser beam on one edge of the waveguide. A far better approach is to use a diffraction grating to couple the light into the waveguide as shown in Figure 1.10.

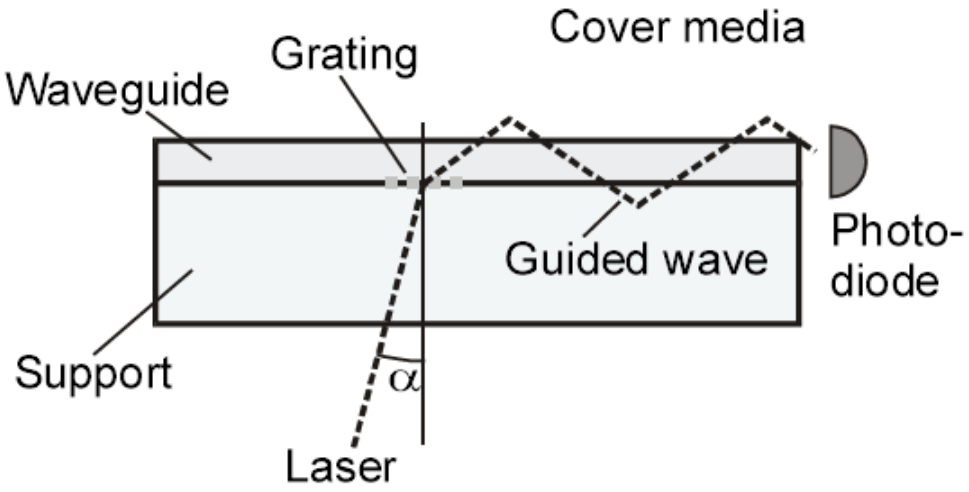

Figure 1.10 Schematic drawing of the grating coupler device

Tiefenthaler (1992) has fully described the theory of the OWLS. In practical, different size of particles for instance, particles or cells have different meaning of the OWLS biosensor. Foe example Hug et al, (2000) have shown that the Bovin Serum Albumin (BSA) which is a protein adsorbs as isotropic monolayer, whose thickness is far below the penetration depth of the evanescent field, and the OWLS can measure the total amount of BSA adsorbed.

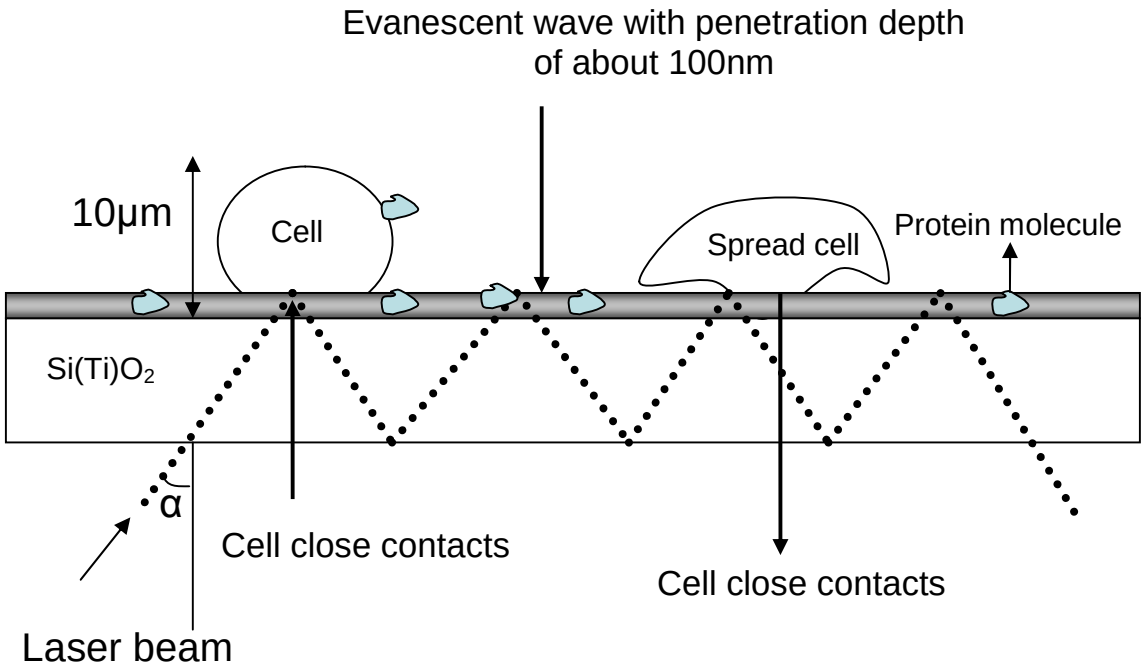

Figure 1.11 Schematic illustration of the adsorption of proteins and cells on the waveguide: Adsorption proteins are completely within the penetration depth of the evanescent wave. After adhesion cells may spread (Hug et al., 2000).

The signal of OWLS depends upon the cell morphology and area in close contact with the chip. In contrast, the height of an attached and fully spread cell is in the range of several µm and therefore only a part of the cell mass is located within the penetration depth of the evanescent field (figure 1.11). In the cell transformation from a globular to a flat shape the contact area between the chip and the cell increases. Since the change of the refractive mode index is proportional to the contact area of the cells, this change in the cell shape can be detected, although the adsorbed mass cannot be calculated (Hug et al., 2000).

“In contrast to protein adsorption and cell settling the adhesion and spreading of cells is in the order of hours. The contact area of the cells with the chip increases for several hours until the fully spread state of the cells, the steady state, is reached. Therefore, the selectivity between proteins and cells is based upon different rates of protein adsorption and cells adhesion and spreading, respectively” (Hug et al., 2000).

1.8 Application of OWLS in stem cell researches

One of the main current problems in the stem cell field is to determine the kinetics of differentiation, and how it is influenced by various environmental factors. At present, optical microscopy is the main observational tool in use. Although it is easy to implement experimentally, quantitative analysis of the results is rather difficult, and some degree of subjectivity in the interpretation is almost inevitable.

The spreading of a living cell in contact with the surface of a substratum is one of the fundamental responses of the cell to such contact (Taylor, 1961). There are myriads of cell types and environments—including here both the nature of the substratum and of the liquid medium bathing cell and substratum—and not all combinations thereof lead to spreading (see e.g. Li et al., 1994). Moreover, the actual temporal course of the spreading, i.e. its kinetics, depends sensitively on cell type and environment (Taylor, 1961; Li et al., 1994; Ramsden et al., 1994). It follows that these kinetics should be a sensitive indicator thereof, and, *a fortiori*, of differentiation, provided that an appropriately accurate way of measuring them can be found. Optical (e.g. (Taylor, 1961)) or electron (e.g. (Hanein, 1993)) microscopies are really unsuitable for this purpose, not only because of the difficulty of getting good time resolution (although

modern techniques of digital photography have to some extent overcome that difficulty), but also because the information obtained is typically rather incomplete (for example, just a cross section, i.e. either plan or elevation).

Sometimes, more complete information can be obtained, such as using techniques of confocal microscopy, but these have the disadvantage of requiring the cell to be fed with fluorescent dyes, thereby altering its physiology in usually unwanted ways.

Nevertheless, a suitably informative technique capable of high temporal resolution has been developed, notably optical waveguide lightmode spectroscopy (OWLS), which is based on perturbation of the evanescent field generated at the surface of an optical waveguide by the presence of the cells (Ramsden et al.,1995b). The method relies on the refractive index of material of the cell being different from that of the medium bathing the cell. Since the evanescent field decays exponentially from the waveguide surface (the cell substratum) into the medium, the perturbation depends on the number of cells per unit area, the refractive index of the cells and its distribution within them, as well as the size and shape of the cells (Ramsden et al., 1995b).

One of the main goals in current stem cell research is the controlled differentiation of a pluripotent cell into a specific end form. This is typically achieved by the addition of certain molecules to the ambient medium. Although some patterns of differentiation are well characterized empirically, the process as a whole depends on complex internal regulatory machinery inside the cell, and is not well understood. At present, the identity of a differentiated form has to be established by laborious morphological and other

ways of phenotypical characterization (including the expression pattern of selected genes), that may take days or even weeks to be concluded. It would therefore be a great advantage if an *in situ* technique were available with which the course of differentiation could be followed as it took place. In this work, I show that high resolution OWLS can be adapted to provide such a technique.

CHAPTER 2

Experimental techniques

This chapter focuses on the primary experimental technique used throughout the my work, an overview of the techniques and the physical principles underlying the technology are presented as are the experimental procedures used. The cleaning procedures and the cell culture and the imaging protocols are provided.

2.1 Stem Cell culture

The cells used for this project were human embryonal carcinoma stem cells TERA.2 cell line (provided by S. Przyborski, Durham University, UK). These were chosen as these cells can reform a teratocarcinoma in *vivo* and differentiate in vitro (Przyborski, 2007) and they provide a suitable model system to study cellular commitment and differentiation. These cells are derived from germ cell tumors are valuable tools for the study of embryogenesis and closely resemble embryonic stem cells. During embryonic development cells communicate with their local surroundings and receive information from their neighbors via secreted factors and membrane-bound molecules.

Cells were cultured at 37 ^{o}C in a 5% CO_2 environment with growth media relevant to their requirements in cell culture flasks. Cells were detached using 0.05% trypsin/EDTA and collected using centrifugation (1500 rpm for 3 minutes). Cells were counted using a haemocytometer in conjunction with an optical microscope.

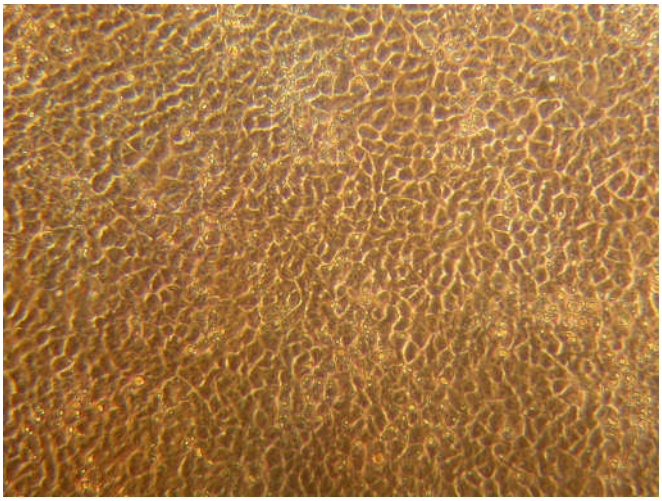

Figure 2.1 Typical confluent layer of TERA2 stem cells morphology in culture flasks.

Cells are typically stored for long time in a liquid nitrogen tank. The freezing process requires the addition of some dimethyl sulfoxide (DMSO; Sigma Aldrich, U.K.) and comprises slowly freezing the cells first in a -80° C by dry ice and transfer frozen cells into long-term storage facility, -190° C (liquid nitrogen).

2.2 OWLS

The principle method used in this work is optical waveguide lightmode spectroscopy (OWLS). In addition, several other methods have been used to get either complementary information to the OWLS signal or to characterise the surfaces before and after the experiments.

Smooth planar optical waveguides were made from amorphous silica-titania at a ratio of approximately 2:1, with a penetration depth of the evanescent field of the order of 100

nm, and incorporated a shallow (5–10 nm) grating coupler (type 2400 (MicroVacuum, Budapest), grating constant equal to 416.667 nm).

The incoupling resonance peaks for the TM0 mode of the waveguides were measured every 40s using a laboratory-built setup (Horvath, 2003; Horvath, 2005), and saved for subsequent analysis. The peak position and overall width were defined and determined according to (Horvath, 2005).

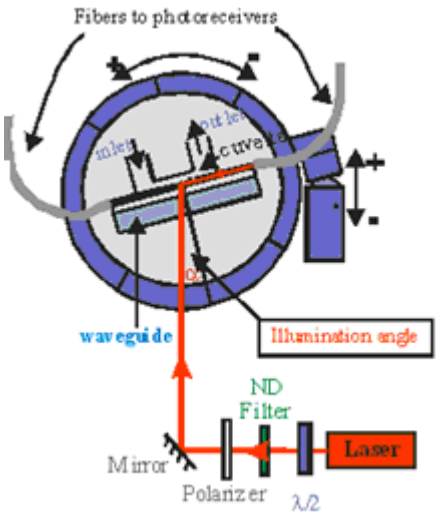

Figure 2.2 Setups for the optical waveguide lightmode spectroscopy (Horvath et al., 2005).

2.2.1 Waveguide sensor

Figure 2.3 shows a standard planar optical waveguide of Si(Ti)O_2 (thickness d_F ~ 200 nm and refractive index n_F ~ 1.8) with an incorporated shallow grating coupler (depth – 10 nm, grating constant Λ = 416.6 nm), obtained from MicroVacuum, Budapest (type 2400).

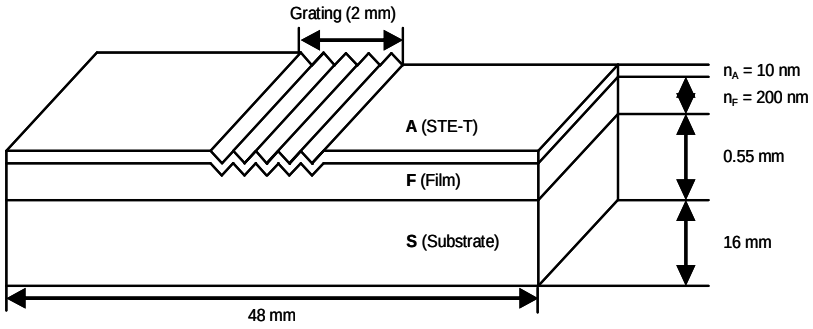

Figure 2.3 Schematic diagram of the optical waveguide grating coupler sensor chip

2.3 Substratum preparation

The cleaning process of the OWLS instrument is the most important factor for obtaining reliable results. Waveguides can be used several times to reduce costs and were cleaned after each experiment. Attached and spread cells on an uncoated waveguide can be removed easily using a weak acid solution while proteins that adhere aggressively require a tenside. In this work a number of cleaning protocols were used.

2.3.1 Plasma treatment cleaning

For cell experiments on the uncoated waveguides cleaning procedure was: under sonication in Roche "COBAS Integra" cleaning solution for 15 minutes, rinsing with ultrapure water, and treating with O_2 plasma (20 mW for 2 minutes). This was sufficient to remove all residues from the surface. The PLL attach strongly to the waveguide and Roche solution alone is not sufficient to remove them. A protocol using sonication in sodium dodecyl sulphate (SDS) (15 minutes), rinsing in ultrapure water and treating with O_2 plasma (20 mW for 2 minutes, figure 2.4) takes out all PLL from surface.

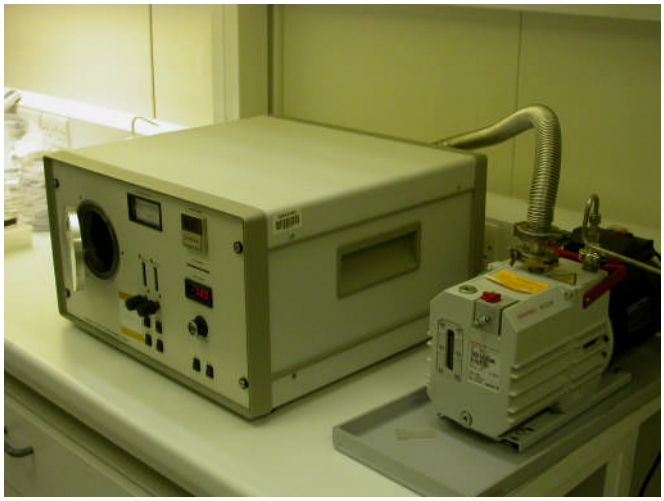

Figure 2.4 Plasma cleaning apparatus (placed in the clean room).

2.3.2 Chromic acid cleaning

Glycoproteins adsorbed on the waveguides cannot be removed by Roche solution or SDS/Roche treatment. Waveguides are immersing for 3 minutes in chromic acid (Fisher Scientific, U.K.) and then extensively rinsing with KOH (2M) and then sonication in ultrapure water for 30-40 minutes finally removes all adsorbed molecules.

2.4 Experimental procedures (OWLS)

OWLS is extremely powerful for investigating the kinetics of attachment and spreading of cells very close to the surface.

1. Attachment and spreading characteristics of human embryonal carcinoma stem cells (TERA.2) during differentiation to neurons and a new morphology.
2. Stem cell response to adsorbed mucin, poly-l-Lysine and silica titania

3. Attachment and spreading of human embryonal carcinoma stem cells (TERA.2) their response to adsorbed at different seeding numbers
4. Response to Nanofibers, nano carbon materials and nano-magnetic particles

2.4.1 Attachment and spreading during differentiation

For these experiments a suspension of single TERA2 cells were produced by incubating confluent cultures with 0.25% trypsin (2 mM EDTA) in phosphated buffered saline (PBS) for 5-6 minunes. Cells were harvested and the cell number determined. Next the cells were seeded at $2x10^4$ cells/cm^2 and placed in the first culture flask in growth medium containing 10 μM retinoic acid (20 μL of the 10 μM stock in DMSO freshly added to 20 mL of growth medium immediately before use) and in the second culture flask the protocol differed from first culture flask as the retinoic acid was handled differently, a large supply of10 μM retinoic acid dissolved in growth medium was prepared and stored at 4 $^{\circ}$C in the dark.

Cells adhere to the both flasks surface within 24 hours and produce a loosely confluent monolayer in 3-4 days. Cell density increases although the culture will not overgrow as the vast majority of cells begin to differentiate and eventually become postmitotic. In the first culture flask neuron populations become visible within 19-21 days and in the second culture flask new morphology population become visible 12-14 days.

In this experiment waveguides were uncoated and following baseline measurement (0.1M Hepes buffered) an aliquot of 5×10^4, cells of both morphologies (neurons and new morphology) in 300 μL buffered SGM were added directly to the open cuvette of

the custombuilt OWLS system using a micropipette whilst the incoupling peaks was continually monitored and saved.. Cells were counted using an optical microscope in conjunction with a haemocytometer, with the number of cells and surface coverage (50-60%) confirmed using phase contrast microscopy inspection of the waveguide after the experiment.

2.4.2 Stem cell response to mucin, PLL and silica titania

In this experiment the waveguides were coated with either 0.1% w/w poly-l-lysine, 0.1% w/w mucin in water. The stock solutions were made up and pre-equilibrated overnight. Solutions were applied to the substrata for 20 minutes, washed twice with ultrapure water and incubated for at least 40 minutes in cell growth medium, (Invitrogen, U.K. See Appendix A for details) and incubated for 40 minutes (37 ^{o}C, 5% CO_2 environment) in cell growth medium [SGM]. Following the baseline measurement (0.1M Hepes buffered SGM) an aliquot of 5 x 10^4, TERA.2 stem cells in 300 μL buffered SGM were added directly to the open cuvette of the custom built OWLS system using a micropipette whilst the incoupling peaks was continually monitored and saved. Cells were counted using an optical microscope in conjunction with a haemocytometer, with the number of cells and surface coverage (50-60%) confirmed using phase contrast microscopy inspection of the waveguide after the experiment.

TERA2 human EC cell lines were cultured according to (Appendix A). Waveguides were cleaned at room temperature with chromic acid as described in (McColl, 2008). The PLL (0.01% solution; Sigma) and mucin (0.1% w/w) stock solution were made up by dissolving weighed dry material in ultrapure water and pre-equilibrated overnight.

Solutions were applied to the waveguides for 20 min and then washed twice with ultrapure water. This is sufficient to completely coat the waveguides (McColl, 2008), which were then incubated overnight in cell culture medium buffered with 10 mM HEPES-NaOH, pH 7.0. Cells were detached from the culture flask (Appendix A), and introduced into a customer-designed open microcuvette, 7 mm diameter, of which the waveguide formed the bottom.

2.4.3 Attachment and spreading (seeding number)

Initially the attachment and spreading characteristics at different number of TERA.2 stem cells were investigated using OWLS. For these experiments the waveguides were uncoated and kept into the stem cell growth medium, (Invitrogen, U.K. See Appendix A for details) overnight. Following the baseline measurement (0.1M Hepes buffered SGM) an aliquot of different concentrations, 1×10^4, 4×10^4, 7×10^4, TERA.2 stem cells (Durham University, UK) in 300 μL buffered SGM were added directly to the open cuvette of the custom built OWLS system using a micropipette whilst the incoupling peak was continually monitored and saved. Cells were counted using an optical microscope in conjunction with a haemocytometer, and confirmed using phase contrast microscopy inspection of the waveguide after the experiment.

2.5 Polyamide nanofibers

Polyamide nanofiber discs were obtained from the Donaldson Co. (Minneapolis, MN). The electrospinning process uses an electric field to create nanofibers.

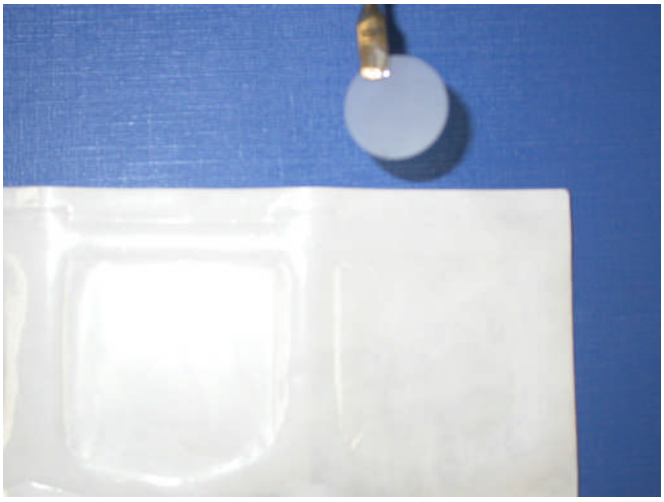

Figure 2.5 Polyamide nanofiber discs obtained from the Donaldson Company.

Coverslips coated with polyamide nanofiber discs were placed into 12-well plates, sterilised under ultraviolet light for 15 minutes, and used as a 3D nanofibrillar surface for stem cell culture. Cell suspension of single TERA2 cells were produced by incubating confluent cultures with 0.25% trypsin (2 mM EDTA) in phosphate buffered saline (PBS) for 5-6 minutes.

2.6 Magnetite nanoparticles

Magnetite nanoparticles coated with PEG were prepared and characterized. Briefly, a solution of a mixture of $Fe(NO_3)_3$ and $FeSO_4$ in an equimolar ratio (0.9 M : 0.9 M) was prepared and an equal volume of a solution of 20% (w/v) poly(ethylene glycol) in

distilled water was then mixed with the iron solution, and kept at room temperature under nitrogen for 30 min. Sodium hydroxide was then dissolved in 125 mL of distilled water to achieve the desired concentration (0.5 M). The basic solution was purged with nitrogen and then heated in a mantle. When the reaction temperature reached 65 °C, the solution of iron salts was added dropwise to the basic solution. Black precipitates formed immediately upon addition of the iron salt solution. The reaction mixture was mixed vigorously for 30 minutes. The aggregates were then removed by centrifugation for 5 minutes at 3000 g. The supernatant was discarded by decantation and the particles were rinsed three times with approximately 150 mL of distilled and deoxygenated water by centrifugation at 3000 g for 5 min to remove excess ions in the suspension.

Finally the particles were rinsed with approximately 100 mL of 0.01 M HCl to neutralize them. The particles were then collected, and were dried in an oven at 80 °C overnight. The magnetic nanoparticle concentration was expressed in terms of dry weight per volume of suspension medium (Ansari, 2008).

Coverslips were coated with 0.1% w/w magnetic nanoparticles in water and a suspension of single TERA2 cells were produced by incubating confluent cultures with 0.25% trypsin (2 mM EDTA) in phosphated buffered saline (PBS) for 5-6 minutes. Cells were counted using an optical microscope in conjunction with a haemocytometer.

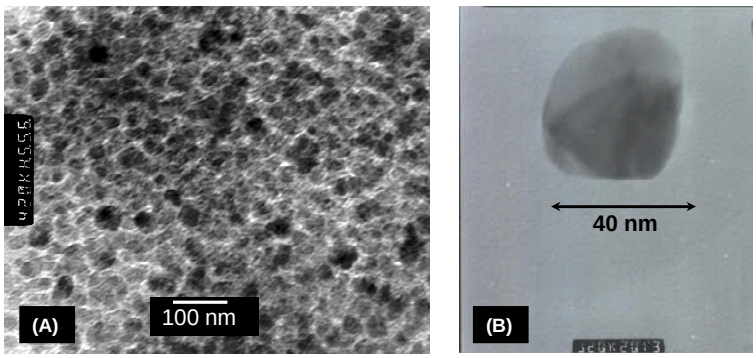

Figure 2.6 (A) TEM image of a 40 nm Fe_3O_4 particle. (B) is a high resolution image of one the synthesized particles (Ansari, 2008).

2.7 Carbon nanomaterials

Carbon nanomaterials and nanofibers related research has led to the development of new production routes and the suggestion and realization of many fascinating applications, and interest is growing rapidly around the world (Boskovic, 2007).

Carbon nanomaterials were obtained from Thomas Swan Company and the coverslips were coated with 0.1% w/w carbon nanomaterials in water.

Figure 2.7 Carbon nanomaterials were obtained from Thomas Swan.

2.8 Microscopy images

Optical microscope, (model XDS-1A Inverted Microscope, GX. Ltd) was used to confirm and support the OWLS experiments. Stem cells on the culture flasks and on the substratum are monitored by optical microscopy.

2.8.1 Cell staining

Optical waveguide light spectroscopy is powerful technique for investigating the kinetics of attachment and spreading cells which are very close to the surface, however a drawback is the lack of images. To obtain a clear picture and also confirmatory evidence of cell spreading on carbon nanotubes, nanofibers, magnetic nanoparticles, mucin, PLL and silica taitania, substrates (cover slips) were washed with fresh PBSand put it 20 minutes under UV light before adding 1×10^5 cells to each cover slip. Following 120 minutes of attachment and spreading cells were fixed using ice-cold

methanol and were stained and imaged. The cells were visualised using hematoxylin (Molecular probes, U.K.).

2.9 Preparation techniques

2.9.1 Cell Culture

The cells have been used in this work were human embryonal carcinoma stem cells TERA2 cell line which were chosen as these cells can differentiate in vitro and they provide a appropriate model system to study cellular commitment and differentiation. All preparation techniques of TERA2 stem cells are fully described in (Przyborski, 2007).

Growth medium:

- 90% Dulbecco's Modified Eagles medium (DMEM; high glucose (4500mg/L); pyridoxine HCl; $NaHCO_3$; without L-glutamine) (Sigma).
- 10% fetal calf serum (FCS, Invitrogen), batch tested, heat inactivated at 56°C for 30min in a shaking water bath.
- 2mM L-glutamine (Sigma).
- Antibiotics (optional) - penicillin (2.5U/ml) / streptomycin (2.5U/ml) (Invitrogen).

Collection medium:

- 100ml growth medium supplemented with antibiotics (penicillin 25,000U; streptomycin 25 mg; kanamycin 10 mg; amphotericin B; all from Sigma). Store up to 2 weeks at 4 °C.

Freezing medium:

- 10% DMSO (Sigma)
- 40% FCS
- 50% growth medium

Glass beads:

- Glass beads (3 mm diameter, Merck) require acid washing before use.
    a) Incubate beads in concentrated HCl overnight in fume cabinet.
    b) Remove acid and wash beads well in tap water.
    c) Wash beads x3 with ddH_2O and drain prior to autoclaving.
    d) Dry in oven (~150°C) 1-2 days to remove any moisture.
    e) Aliquot ~15 beads per capped test tube and autoclave beads in tubes, beads are now ready to use in cell culture.

Retinoic acid:

All *trans*-retinoic acid (Sigma). Produce a 10mM stock solution in sterile DMSO (purchased sterile in ampules, Sigma). Do not filter. Aliquot 500 µL per vial. Store at -70 °C. Light sensitive.

Protocols:

Routine passaging and harvesting of EC cells: There are two ways in which this can be achieved. The Method (A) relies on mechanical disruption which is quick, simple and avoids complete dissociation of the cell culture. This is important since the maintenance of cell contacts and high confluency is known to limit spontaneous differentiation within the culture. The second method uses enzymatic treatment to completely dissociate the culture into a single cell suspension. This is necessary to determine cell number using a haemocytometer or preparing the cells for flow cytometry. Method (B) can be used occasionally to passage the cells but it is not recommended for routine passaging since it may change the nature of the cells over time. In both the following methods, cells from a confluent 75 cm^2 tissue culture flask (T75) have been processed (Przyborski, 2007).

Method (A) – mechanical dissociation (for a 1:3 split):

a) Aspirate growth medium from cell culture and rinse with 5 ml PBS.
b) Add ~15 acid-washed 3 mm glass beads and 5ml growth medium.
c) Carefully rock the flask from side-to-side, backwards-and-forwards to roll the beads over the cells to dislodge them from the surface. Be careful not to tip the contents into the neck of the flask.
d) Collect the dislodged cells with a 10ml pipette and gently pipette the suspended cells up and down a couple of times with the tip of the pipette resting in the bottom corner to disrupt the larger aggregates.
e) Collect the cell suspension with the same pipette and transfer this to a new T75 flask containing 50ml growth medium.

f) Ensure the suspension is completely mixed before splitting the culture equally between x3 new T75 flasks (20 ml per flask) (Przyborski, 2007).

Method (B) – enzymatic dissociation:

a) Aspirate growth medium from cell culture and rinse with 5 ml PBS lacking calcium and magnesium.
b) Add 1 ml trypsin-EDTA (0.25% trypsin, 1mM EDTA in calcium- and magnesium-free PBS) and tip the flask to ensure the monolayer of cells is covered.
c) Incubate the cells at 37°C until they round up and begin to detach (3-5min). Dislodge the remaining cells with a sharp lateral motion delivered by tapping the side of the flask with the palm of the hand.
d) Add 9ml growth medium and flush over entire culture surface for maximum harvest. Gently pipette up and down a couple of times to break up any clumps.
e) Count the cells with a haemocytometer. Generally, cell viability is greater than 95% and this can be checked by a simple dye exclusion assay (for example, staining with 0.4% trypan blue or 0.15% erythrosine B)
f) Reseed the cells into fresh tissue culture plastic-ware at $5x10^4$ cells/cm^2 (equivalent of $3.75x10^6$ cells per T75 flask) containing the appropriate amount of growth medium (20ml per T75 flask).

Notes:

EC stem cells adhere and recover rapidly forming a fully confluent monolayer in 3-4 days when maintained at 37°C under a humidified atmosphere of 5% CO_2 in air (Figure

3). Cells should not require feeding during this time. Passages involving 1:2 to 1:4 split ratios can be used depending on the confluency of the culture prior to passaging. It is not necessary to wash the cells for passaging after collection using trypsin, provided that sufficient growth medium containing FCS has been added to inactivate trypsin.

Freezing cells:

a) Harvest cells according to procedure described above and pellet at 1500rpm for 3min.
b) Remove supernatant and re-suspend pellet in freezing medium (3ml per T75 flask; 1ml per T25 flask).
c) Aliquot 1ml suspension per cryogenic vial.
d) Label vial with name of cell line, passage number, date.
e) Slowly freeze samples overnight by placing vials in an insulated box and transferring the box into the -70°C freezer.
f) Transfer frozen samples next morning into -140°C long-term storage facility.
g) Ensure records are up dated and accurate.

Thawing cells:

a) Remove cells from storage facility and transfer to portable liquid nitrogen storage canister.
b) Thaw vial rapidly in a 37°C water bath.
c) Transfer contents of vial into a 15ml centrifuge tube containing 10ml growth medium at 37°C.
d) Spin down cells at 1500rpm for 3min and remove supernatant.

e) Re-suspend cells in 20ml growth medium and split equally between two T25 flasks.
f) Culture cells overnight and inspect the next day. Change growth medium.
g) Ensure records are up dated to reflect removal of cells from storage facility (Przyborski, 2007).

2.9.2 Waveguide cleaning

Cleaning processes were set up throughout in this work. To remove weak (concentrations up to 0.1 % w/w) mucin solutions from the waveguide surfaces Roche was used. The rinse step involves filling the centrifuge tube with fresh water and pouring out.

Roche Protocol

Sonicate in water for 10 minutes at 50^{o}C

Rinse

Rinse

Sonicate in Roche 'Cobas Integra' solution for 10 minutes at 50^{o}C

Rinse

Rinse

Rinse

Dry with filtered nitrogen

O_2 plasma treated at 20 mW for 2 minutes

For higher concentrations of mucin (up to 3%) Roche was not good enough at removing the extremely well bound layer. A Sodium dodecyl sulphate step was introduced into the protocol.

SDS – Roche Protocol

Sonicate in water for 10 minutes at 50^{o}C

Rinse

Rinse

Sonicate in SDS for 10 minutes at 50^{o}C

Rinse

Rinse

Rinse

Sonicate in Roche 'Cobas Integra' solution for 10 minutes at 50^{o}C

Rinse

Rinse

Rinse

Dry with filtered nitrogen

O_2 plasma treated at 20 mW for 2 minutes

At very high mucin concentration (10%) and for mucin or PLL solutions the layer formed was very stable and Chromesulphuric chromic acid was used to clean it.

Chromesulphuric acid

Fully submerge in chromesulphuric acid for 3 minutes

Dip in potassium hydroxide (KOH)

Sonicte in water (room temerature) changing water frequently

Dry with filtered nitrogen

O_2 plasma treated at 20 mW for 2 minutes

CHAPTER 3

Monitoring and characterization of the differentiation process of TERA2 stem cells

A major current problem in stem cell research is to determine the kinetics of differentiation, and how differentiation is influenced by various environmental factors. In this chapter the chance discovery of a new morphology of human embryonal carcinoma stem cells are described, and then it is demonstrated that measurement of the spreading kinetics via perturbation of the evanescent field generated at the surface of an optical waveguide can allow the unambiguous determination of the differentiated state after only a few minutes of observation, independently of the need for lengthy visual observation and a possibly subjective judgment.

3.1 Differentiation of EC cell lines by retinoic acid (RA)

Scientists have long been looking for a tool for basic research of the growth of human neurons, including the study of the nervous system, toxicological testing, and drug discovery. Embryonal carcinoma (EC) stem cells, which are derived from germ cell tumours and closely resemble embryonic stem cells, are especially useful to study the growth of human neurons in vitro (Schmeichel and Bissel, 2003; Beningo et al., 2004). During embryonic development cells communicate with their local surroundings and receive information from their neighbours via secreted factors and membrane-bound molecules; such interactions play a pivotal role in the modulation of cell differentiation

and the determination of cell fate (Luthi et al., 1998; Cukierman, 2001; Witte and Kao, 2005). Embryonal carcinoma cells provide a source of pluripotent stem cells that are often used as surrogates for investigating the mechanisms that regulate cell differentiation during embryonic development. When human TERA2.cells are exposed to retinoic acid and grown as adherent monolayers they differentiate into neurons. These primary cultures of terminally differentiated neurons have mostly been used as models to study the development and function of neurons in vitro (Thompson et al., 1984; Reynolds and Weiss, 1992a; Carpenter et al., 1999) but it is always important to consider that transformed cell lines may not share the exact features of primary neural tissue, these terminally differentiated neurons have recently been used in clinical trials as post-stroke replacement neural tissues (Jones-Villeneuve et al., 1982).

All-*trans* retinoic acid (RA) (Figure 3.1), a member of the retinoid family and the active derivative of vitamin A, is actually essential for vertebrate embryonic development. Both the lack and excess of RA result in developmental malformations. The importance of its role in morphogenesis (Vescovi et al., 1993; Drager and McCaffery, 1997) is well illustrated by cell determination from a tail bud to an additional limb in frog, while is promoted by (Müller et al., 1996). Other roles include differentiation (Miano and Berk, 2000) and homeostasis control at both embryonal and postnatal life stages (DeLuca, 1997).

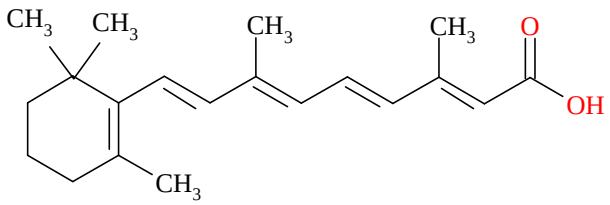

Figure 3.1 Chemical structure of all-*trans* retinoic acid

During the last decade, several groups have isolated mammalian neural progenitor cells from the embryonic nervous system and explored the responses of these cells to molecules such as RA, epidermal growth factor (EGF), bone morphogenic protein 4 (BMP4), and basic fibroblast growth factor (bFGF). Under these conditions, neuroprogenitors grow as suspended aggregates of cells commonly referred to as neurospheres (Reynolds and Weiss, 1992b; Reynolds, 1996; Svendsen, 1998). Pioneering work by Jones-Villeneuve et al. (1984) demonstrated that murine EC stem cells differentiate in response to retinoic acid forming populations of neurons and glial cells (Sun, 2002).

Regulation by RA is mediated by retinoic acid receptors (RAR) located on target cells and by retinoic acid binding proteins (RBP), soluble proteins bind the hydrophobic RA molecule within the cell cytoplasm (e.g. CRABPI and CRABPII) and in the extracellular environment (e.g. serum RBP) (Noy, 2000). Maintaining control of RA degradation and synthesis during embryogenesis is extremely important; imbalances have been implicated in disease states such as spina bifida and cleft palate (Niederreither et al., 2002).

3.1.1 My discovery

Since the TERA2 system offers a convenient and robust model for studying the commitment of human EC stem cells to the neural or non-neural lineages, I was growing these cells adherent monolayers and exposing them to a freshly prepared solution of RA, whereupon the TERA2 cells form terminally differentiated neurons. By chance, I found that aging the RA in aqueous growth medium results in the TERA2 cells differentiating into completely different (non-neural) morphology.

3.1.2 Experimental procedure and results

Detailed procedures for the growth and differentiation of murine P19 EC stem cells have been adapted and applied to EC stem cell differentiation (Macpherson and McBurney, 1995). The two protocols are: A for the growth of cells as neuron adherent monolayers, typically used to induce cultured human EC to form neural derivatives; and my new protocol, B, which differs only from protocol A in that the RA in the growth medium is handled differently. This induces a new cell morphology.

Protocol A-differentiation into neurons

A suspension of single TERA2 cells were produced by incubating confluent cultures with 0.25% trypsin (2 mM EDTA) in phosphated buffered saline (PBS) for 5-6 min. EC stem cells were harvested and the cell number determined. Next the cells were seeded at $2x10^5$ cells/cm^2 and placed in growth medium containing 10 μM retinoic acid (20 μL of the 10 μM stock in DMSO freshly added to 20 mL of growth medium

immediately before use). Cells adhere to the flask surface within 24 hours and produce a loosely confluent monolayer in 3-4 days. Cell density increases although the culture will not overgrow as the vast majority of cells begin to differentiate and eventually become postmitotic. Neuron populations become visible within 20-21 days (Figure 3.2).

For the first 21 days retinoic acid containing growth medium was replenished every 3-4 days. Thereafter the culture was dissociated with trypsin solution and 10 mL of growth medium then added. A single cell suspension was produced by gently pipeting the cells. These were then split (1:4) and cultured in the growth medium containing no retinoic acid for a further 4-6 days. During this time, neurons were readily identified above a background of flat non-neuronal cells (Przyborski, 2000; Przyborski, 2007).

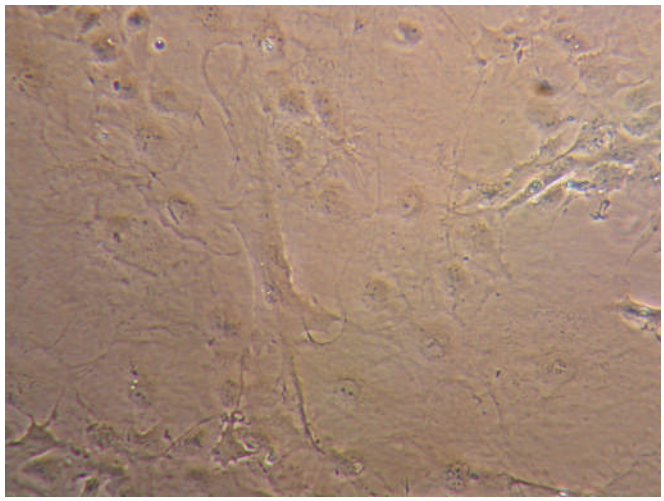

Figure 3.2 Differentiation into neurons (Protocol A).

Protocol B-differentiation into a novel morphology

This protocol differed from protocol A as the retinoic acid was handled differently. Here a large supply of 10 μM RA acid dissolved in growth medium was prepared and stored at 4 ˚C in the dark. The growth medium was replenished every 3-4 days and a new TERA2 stem cell morphology found after 12-14 days (Figure 3.3).

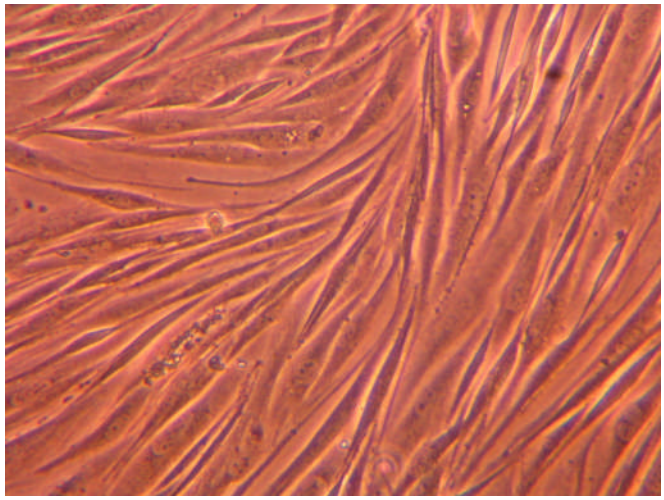

Figure 3.3 Differentiation into new morphology (Protocol B).

To investigate the effect of RA concentration cells were grown in media (following protocol A) containing concentrations spanning 0.5μL, 1μL, 5μL, and 10μL stock solution. Following Protocol A, but at lower concentration (5, 2.5 and 0.5 μM). This resulted in no differentiation at all – the TERA2 cells simply proliferated and overgrew each other (Fig 3.4). Hence the proteins in the medium do not simply sequester free RA.

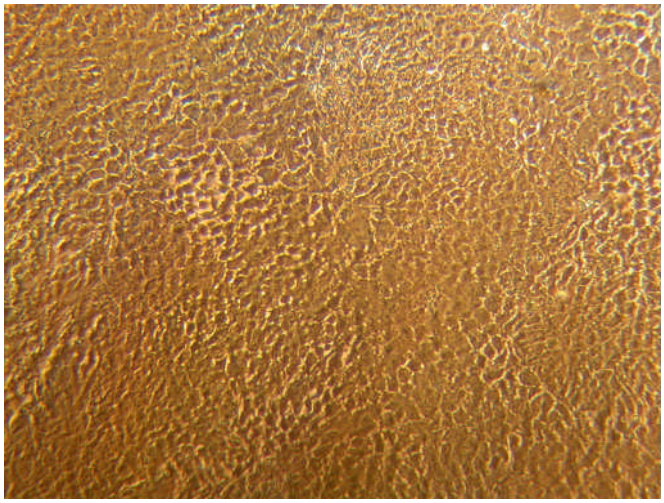

Figure 3.4 TERA2 cells were grown according to protocol A except that the concentration was 0.5 µM. The width of the image is 850 µm.

The effect of storage temperature on RA's ability to alter cell morphology was investigated by storing the 10 mM storage stock solution in DMSO at 4 ^{o}C (instead of -70 ^{o}C) before making up fresh dilutions (e.g. Protocol A, figure 3.5).

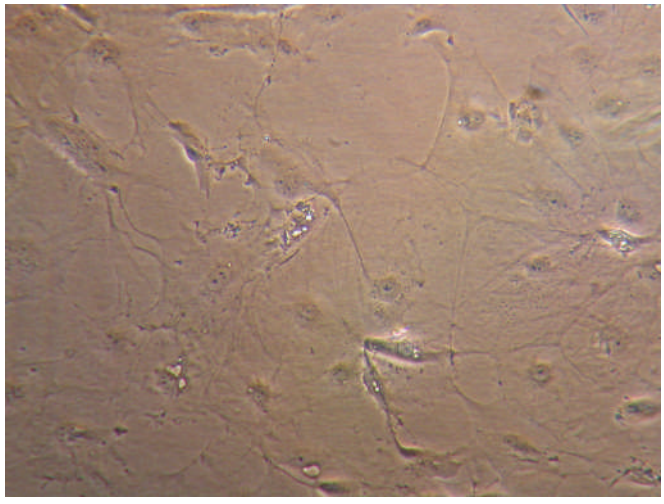

Figure 3.5 TERA2 cells were grown according to protocol A, except that the storage temperature at 4 $^{\circ}$C. The width of the image is 850 µm.

For protocol A (with freshly diluted RA) neurons form, whilst prior storage of the diluted in the aqueous growth medium (Protocol B) dramatically changes the morphology of the differentiated cells (Figure 3.6).

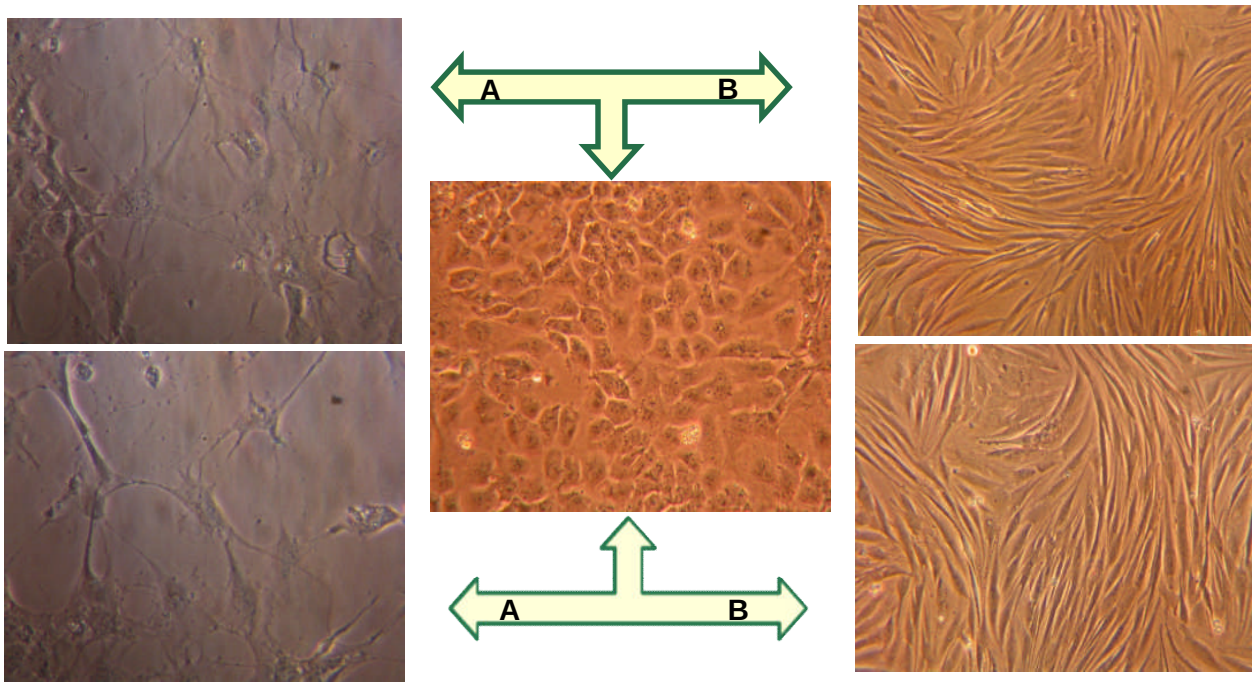

Figure 3.6.Differentiation of neurons. Protocol A (left) using fresh 10 µM retinoic acid. Protocol B (right) using 10 µM retinoic acid aged in the medium, both derived from undifferentiated TERA2 cells (centre). The widths of the images are 850 microns.

The temporal dependence of retinoic acid activity is remarkable. RA can become unstable under unfavourable conditions (such as high temperature) and as such needs to be stored at -70 ^{o}C. One might expect that storing the RA at lower temperatures may be the cause of the effects demonstrated here. Our inability to detect any new morphology

changes by the RA stored at 4 ^{o}C in DMSO alone suggests that this effect is not temperature-related. It is most likely medium-related. Table 3.1 summaries the results.

Table 3.1 RA concentration for differentiation process.

Retinoic acid concentration	Stem cell (TERA2) morphology
0	Undifferentiated stem cells
10 μM RA (Protocol A)	Neurons (after 21 days)
10 μM RA (Protocol B)	New morphology (after 14 days)
20 μM RA (Protocol A)	Dead cells (after a few days)*
5 μM RA (Protocol A)	Undifferentiated stem cells
1 μM RA (Protocol A)	Undifferentiated stem cells
0.5 μM RA (Protocol A)	Undifferentiated stem cells
10 μM RA (Prot. A with storage at 4 °C)	Neurons (after 21 days)

3.1.3 Discussion

How to explain? Free available RA concentration is diminished: it is well known that Retinol is bound by circulating serum proteins in vivo and that RA is bound both intra and extracellular (Noy, 2000). Sequestering of RA by these proteins (over time) could therefore lead to the reduction of available active retinoic acid in the media. But, my concentration results suggest however that the effect of storage retinoic acid in growth medium dose not simply lead to the sequestering of free RA. Hence the proteins in the

* Due to the high DMSO concentration.

medium do not simply sequester free RA. Similarity, simply storage RA at 4 $^{\circ}$C (in DMSO) results in the usual differentiation, so RA is not so excessively unstable (Figure 3.5). The most likely explanation for these observations is that the RA is functionally regulated by proteins in the growth media.

Although it would be desirable to determine what is RA complexation product that results in such a dramatic new form, the complexity of the growth medium in which it is stored precludes systematic (bio) chemical characterisation. We also note that even minor deviations in the growth medium composition typically result in morbidity or death of the cell, severally limiting the possibilities to approach the problem by systematically exposing the cells to simplified media.

The next question is that what else could be done to characterize the new morphology? Considerable effort is needed to address what is going on here and whether are any new molecular or biological insights. At a molecular level, a whole set of markers would need to be identified, either by polymerase chain reaction (PCR), or using antibodies with flow cytometry, monitored over time following treatment. Also, if it is not RA itself that is responsible for the phenotype then are would have to try to identify what is the derivative product, is it a breakdown product in combination with protein, etc. this would need comprehensive biochemistry on the medium, and might not even be realizable.

3.2 Quantitative spreading kinetics as a means of identifying stem cell differentiation

Stem cells undergoing development leading to a differentiated state were periodically removed from their culture environment and allowed to settle upon a planar substratum. The kinetics of cell spreading on the substratum were followed by analysing the perturbation of an optical evanescent field generated from light guided along the substratum. A logistic law was fitted to the high resolution kinetic spreading data, which could be quantified using three parameters, exploratory eagerness, spreading constraint, and time to decision. To culture environments were considered, leading to quite different terminal differentiated states. Using our method, I could demonstrate that the three parameters markedly differ between the processes leading to the two states.

I recently discovered that two distinctly different morphologies can be generated from TERA2 stem cells treated with all trans retinoic acid (RA) by slightly changing the manner in which the RA is introduced to the cells. Protocol A is the "standard" procedure that has been established elsewhere (Przyborski, 2007), and which generates neurons. Protocol B is our novel procedure generating a striated morphology, not yet definitively identified[5]. I have used this as a model system for establishing our methodology. Monitored of the coupling of light into a waveguide via a grating is used to investigate the attachment of human embryonal carcinoma stem cells during differentiation as two protocols. Microscopy images, although it has yielded an initial characterization of the process, cannot provide high resolution information and kinetics.

[5] Details of the protocols and of the identification are fully described in the first section of this chapter.

3.2.1 Results

Figure 3.7 shows optical micrographs of the development according to protocol A, leading to end-differentiated neurons 21 days after initiating treatment with RA, and figure 3.8 shows the same according to Protocol B, leading to a novel morphology. Figure 3.9 shows the corresponding changes in incoupling angle for the two protocols, at different times after initiating the treatment leading to differentiation.

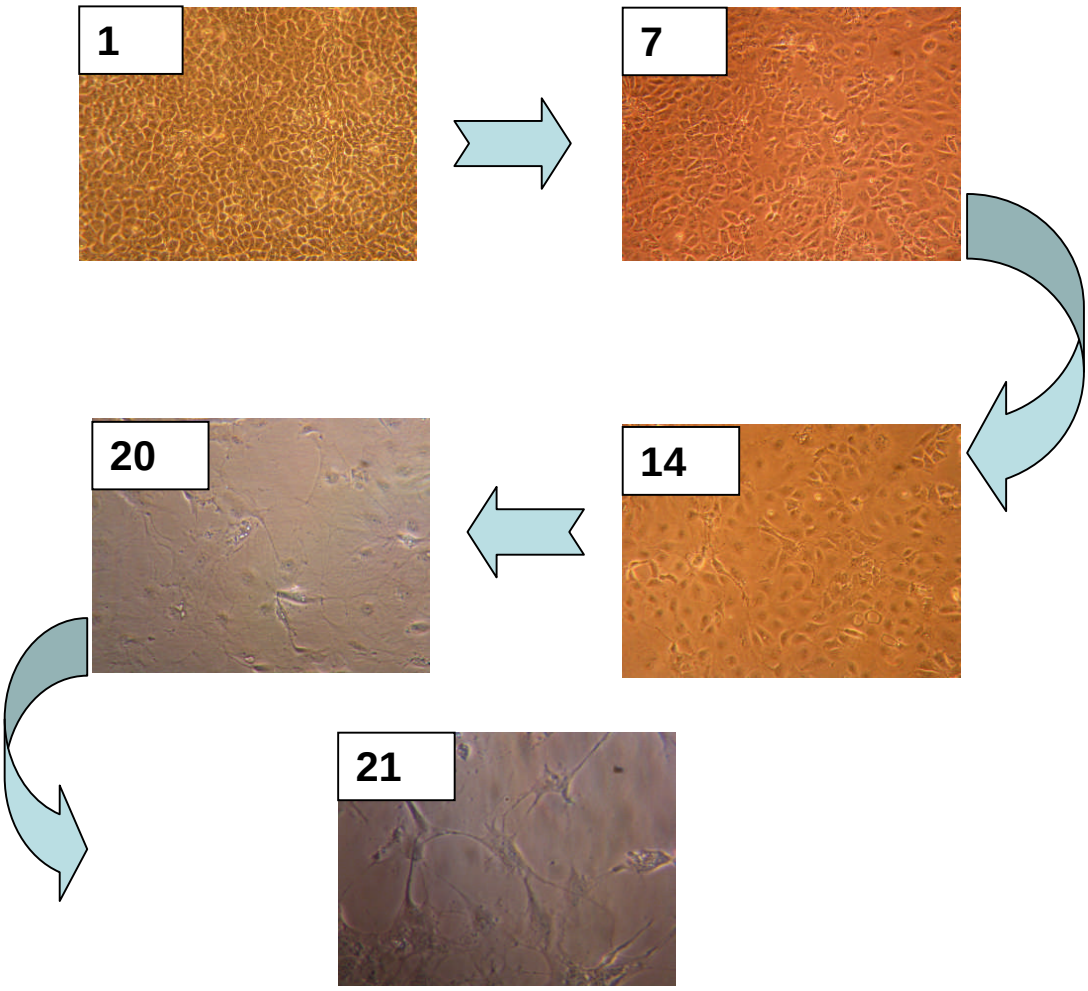

Figure 3.7 Differentiation of TERA2 cells according to Protocol A. The number in the upper left-hand corner gives the number of days after initiating treatment with retinoic acid.

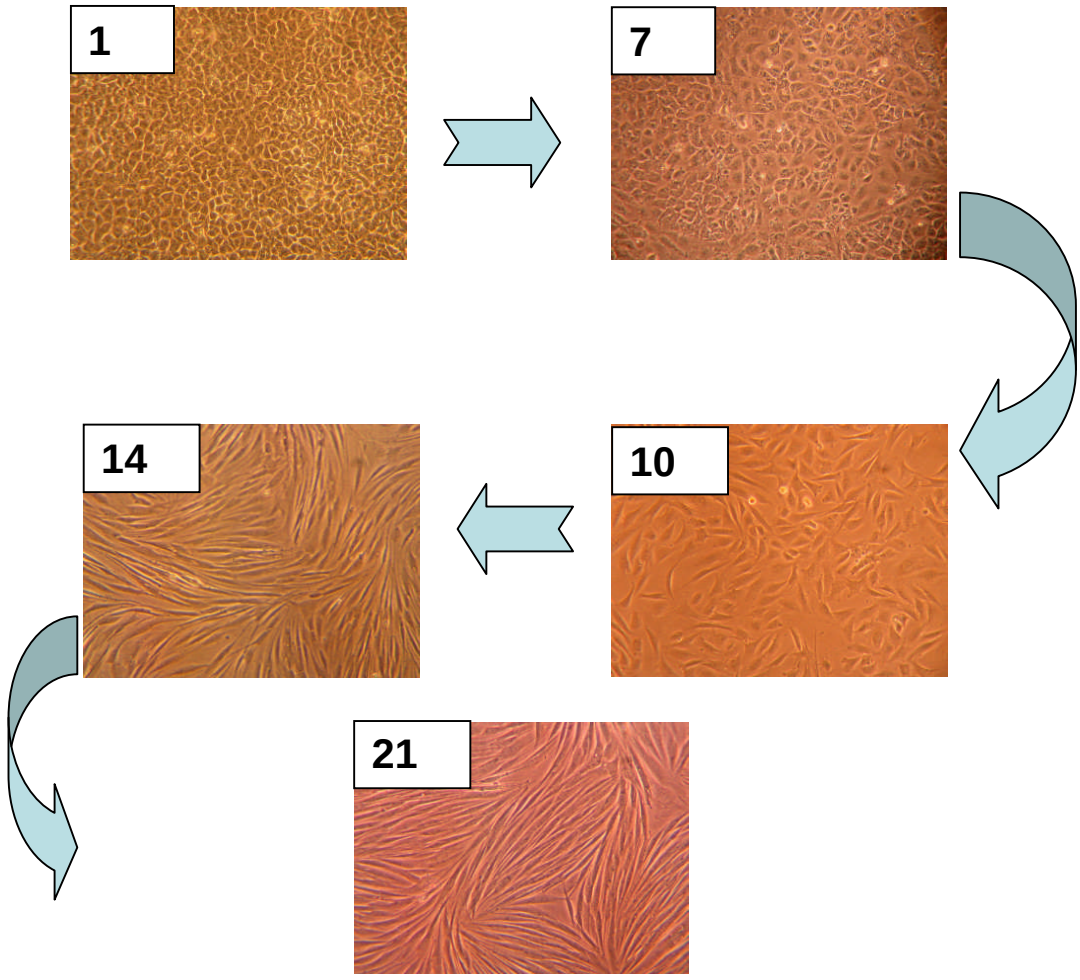

Figure 3.8 Differentiation of TERA2 cells according to Protocol B. The number in the upper left-hand corner gives the number of days after initiating treatment with retinoic acid.

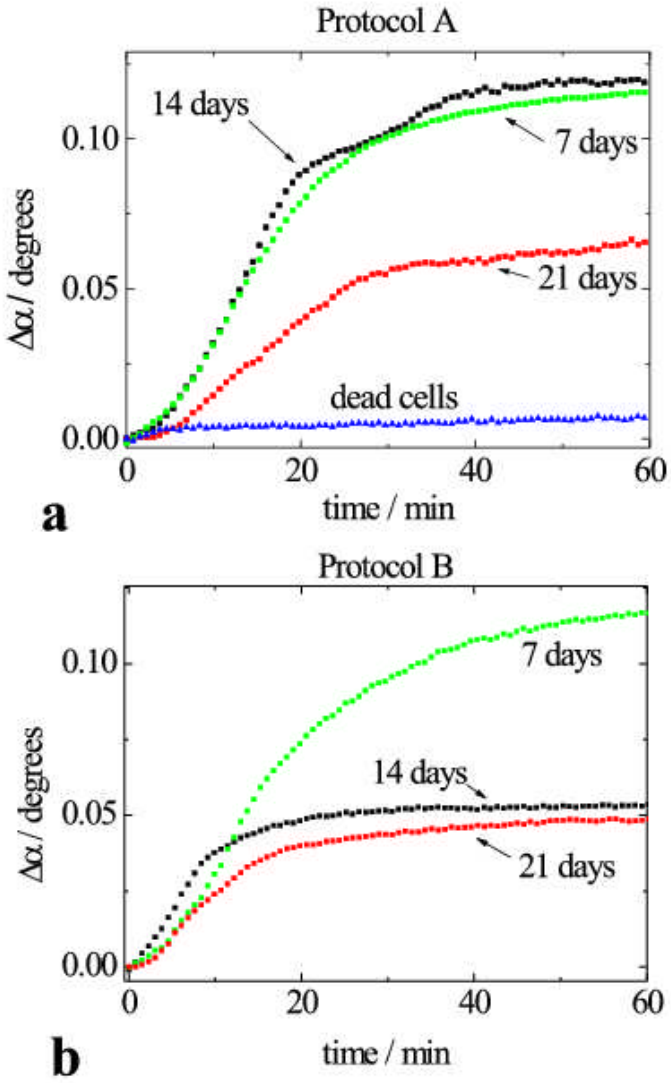

Figure 3.9 Typical changes in incoupling angle of the zeroth transverse electric (TE) modes, measured using OWLS for cells having experienced different numbers of days of differentiation-induced treatment, according to Protocol A and B.

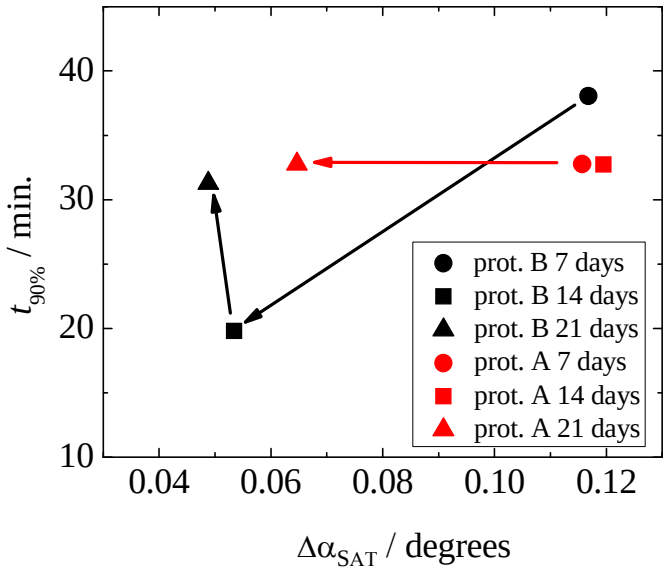

Figure 3.10 Two dimensional "phase diagram" of cell spreading during the differentiation. X axis: saturation values from OWLS. Y axis: time to reach the 90% of the saturation value.

It is intriguing that what might be considered to be cells are spreading completely differently as two protocols. Figure 3.10 shows the two dimensional "phase diagram" of cell spreading process during differentiation.

3.2.2 Analysis

The change in incoupling angle $\Delta\alpha$ is approximately equal to the "area of contact" *a* between the cell and its substratum (Ramsden et al., 1995b). In that previous work, Ramsden et al. considered the spread cell to have the idealized form of a segment with its planar surface in apposition to the (planar) substratum, in other words the true nature of the "contact", whereby the approximately planar underside of the cell is actually

resting on a forest of filopodia each several tens of nanometres long, was neglected. This approximation was just one of several, including the assumption that the refractive index of the entire volume of the cell (i.e., the volume enclosed by the cytoplasm) has a uniform value. I believe, however, that it can be safely asserted that these approximations, together with the assumption that there is a uniform number of filopodia per unit area of cell surface, do not change the essential points, namely that $\Delta\alpha$ is proportional to the number of filopodia. We take this quantity, f, as the one of fundamental interest. Our task is therefore to determine the temporal evolution of f, which is what we in effect directly measure with OWLS.

3.2.2.1 Models of the cell

A survey of the literature that followed the early observations of spreading reveals a broad consensus insofar as the cell is considered as a deformable sac, and the spreading process is therefore determined by the interfacial free energy (per unit area) between the surface of the cell and substratum, and the deformability of the cell. It is usually supposed that both the cell cytoplasm, dominated by the cytoskeleton, especially the cell "cortex", comprising the filamentous network of proteins associated with the bilayer lipid membrane, contribute to the deformability[6]. Furthermore, the interfacial free energy depends not only on the average composition of the cell surface (and hence accessible through standard techniques), but also on specific cell adhesion molecules (Dembo et al., 1988) (especially important if the substratum is mimicking the basement membrane on which cells usually spread *in vivo*, see e.g. (Virtanen et al., 1982; Dunon

[6] Bulk cytoplasm is viscous rather than elastic.

et al., 1996)) (e.g., Bereiter-Hahn et al., 1990; Bruinsma, 1996; Bruinsma and Sackmann, 2001; N'Dri et al., 2002; Pesen and Hoh, 2005)).

The models resulting from such considerations are quite complicated, and since they tend to have rather more parameters than can be measured independently, their application to the problem is not wholly satisfactory. Another difficulty is that much of the science assumes that the cell is in equilibrium (e.g., (Bell et al., 1984)), whereas it is in fact a highly dynamical system, whose shape is constantly evolving in response to contact with the substratum.

The filopodia seem to play a key role in guiding this response. Albrecht-Buehler (Albrecht-Buehler, 1976) has already pointed out their important exploratory role. I therefore propose to give unique precedence to the filopodia in our explanation.

3.2.2.2 Cell spreading kinetics

As Bardsley and Aplin (1983), pointed out some time ago, spreading very typically follows sigmoidal kinetics. This has since been confirmed and made more precise in subsequent work using OWLS to quantify the contact area (Ramsden et al., 1994; Li et al., 1994), and fully corroborated by our present results (Figure 3.9). An obvious choice of mathematical function to represent the kinetics is therefore the well known logistic law (Feller, 1940), frequently invoked to represent biological growth:

$$\mathrm{d}f/\mathrm{d}t = bf\,(1 - f/a) \qquad (1)$$

where f is the number of filopodia in contact with the substratum, b represents the exploratory eagerness of the cell, and a represents a constraint on this eagerness, which might arise from energetic limitations, or material ones, or both. The solution of this differential equation is:

$$f(t) = a / [1 + \exp(-b(t - m))] \qquad (2)$$

where m, the arbitrary constant of integration, gives the time at which the point of inflexion occurs (the "decision point"). The ordinate of the point of inflexion is ecessarily $f = a/2$. In proposing this equation, we are fully aware that many other equations will also fit the data equally well or better, and that even though the present choice has a minimum number of parameters, each of which has a direct biological-physical significance, other mechanisms amenable to a simple mathematical description might also be found (Feller, 1940).

3.2.2.3 Fitting standard function to the observed experimental data points

Protocol	Days	a/º	b/º min $^{-1}$	m/min
A	7	0.12	0.0057	16
A	14	0.12	0.0057	16
A	21	0.065	0.0029	16
B	7	0.11	0.0046	15
B	14	0.053	0.0046	6
B	21	0.048	0.0046	10

Table 3.2 Parameters fitting equation (2) to the experimental data reported in Figure 3.9.

3.3 Discussion

Protocol A. Qualitatively, and with the knowledge from the optical micrographs that the cells only reach their end state of differentiation (neurons) after 20 days, we can say that the spreading kinetics are well correlated with the degree of differentiation. In the undifferentiated state, the cells are characterized by a high exploratory eagerness. In the terminal differentiated state, this is presumably scarcely necessary. Furthermore, their spreading is much more constrained. However, the decision point occurs at the same time regardless of the state of differentiation.

Protocol B. The main differences, compared with Protocol A, are: (i) differentiation is more rapid (clearly corroborated by the optical micrographs; it is essentially complete after 14 days); and (ii) exploratory eagerness is undiminished even in the differentiated state; and (iii) the decision point shows a minimum immediately upon attaining the differentiated state. On the other hand, even though the differentiated state is very different from neuron-like, it is subject to a similar constraint regarding the possible maximum degree of spreading.

3.3.1 Calibration of the degree of spreading

Given the approximate linear relationship between $\Delta\alpha$ and the product of contact area and cell number (Ramsden et al., 1995b), without troubling to carry out the calculations after Ramsden et al., one can calibrate the OWLS data using the optical micrographs. The mean areas of the differentiated neurons and non-neurons (Figs 3.7 and 3.8 respectively) are 4.6±13.98 and are 0.43±1.5 μm^2 respectively.

CHAPTER 4

Stem cell-substratum interactions

Up until now cell biologists investigating the attachment and spreading of *living* cells at solid-liquid interfaces, the quantification of which is a fundamental part of studies of the biocompatibility of medical devices for example, have had little alternative but to use optical microscopy, but effective exploitation of this technique (e.g. using a confocal arrangement) requires the cells to be fed on relatively large quantities of toxic dye molecules, which to a greater or lesser degree affect the physiology and hence behaviour of the cells. A nonimaging alternative based on analysis of the perturbation of the evanescent field generated at the surface of an optical waveguide has been developed more recently, but this does not allow signals emanating from the cell to be separated from signals emanating from proteins, e.g. microexudate from the cell, deposited on the waveguide. The significant advance reported in this work describes how a deeper and more extensive analysis of the waveguide signals enables protein deposition, and/or focal adhesions, to be measured separately from overall cell shape changes. The method is immediately applicable to high throughput screening.

Modulation of the coupling of light into a waveguide via a grating is used to investigate in the first section the attachment of human embryonal carcinoma stem cells to three substrata, silica-titania (representative of artificial implants), poly-L-lysine (a commonly used laboratory cell culture substrate) and mucin (the coating of the mucosa) and in the second section the attachment at different seeding number of cells. By analysing

selected optical parameters of the cell-waveguide system we distinguish the formation of filopodia, and the overall change in its shape (spreading). Moreover, were obtained the kinetics of these processes with excellent time resolution.

4.1 Kinetics, substrates interactions (PLL, mucin, silica-titania)

Within the (eucaryotic) cell, the nucleus, rich in nucleic acids, has a higher refractive index than the cytoplasm; and spreading typically implies movement of the nucleus nearer to the substratum, increasing the optical contrast between the covered and uncovered zones. The micro-morphology of the cell-substratum “contact”, already referred to, will also affect the optical contrast sensed by the exponentially decaying evanescent wave. We can already remark here that tight binding presumably implies a high density of filopodia. Finally, the cell may secrete macromolecules as part of its adaptive response to the substratum.

These diverse effects are taking place simultaneously and are prima facie difficult to separate from one another. Here we show that by simultaneously comparing the evolution of the incoupling peak width with the evolution of the incoupling peak position (which depends on the propagation constant of the guided lightmode) it is possible to separate microexudate secretion (which does not affect incoupling peak width), filopodium formation, and cell body spreading, without perturbing the cell. Such observations are not possible with optical microscopy, let alone with high time resolution.

This work were investigated three distinctively different cell substrata. Silica-titania is representative of artificial implants (titanium is the most common material used for prostheses (Ramsden, 2008), and in the body is invariably oxidized; the salient surface energetic features, most notably the Lewis acids/base parameters, of titanium are almost the same as those of silicon (Cacace, 1997), poly-l-lysine (a very commonly used cell culture substrate in the laboratory) and mucin, found ubiquitously coating the mucosae (Griffith, 2002), of which it is the major macromolecular component; mucins comprise a family of heavily glycosylated, high molecular weight glycoproteins with carbohydrate side chains that make up some 50–80% of the molecule by weight (Shi, 2000).

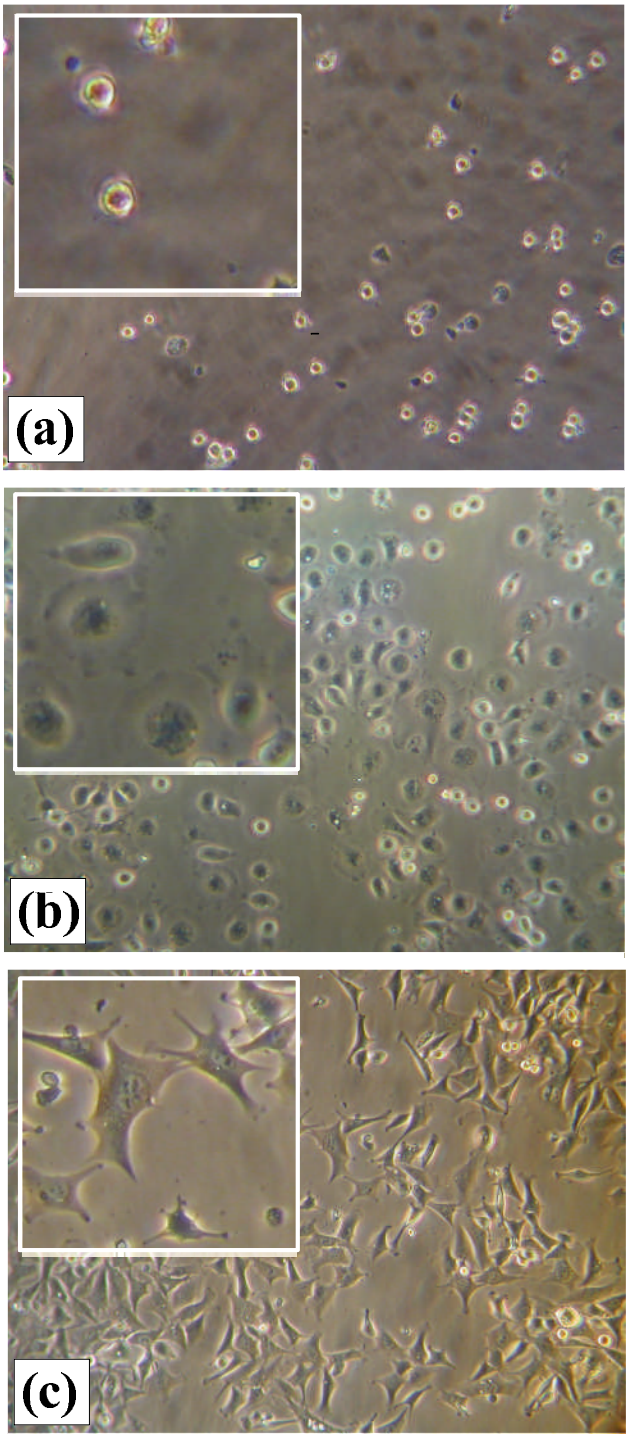

Figure 4.1: Optical micrographs of TERA2 stem cells on (a) mucin, (b) PLL, (c) Si(Ti)O2 after 120 min of culture. Each main image is 850 µm wide; the insets are 170 µm wide.

4.1.1 Experimental results

Figure 4.1 shows the microscope images of the cells on the three different substrata. Even visually, it is very apparent that the cells have not spread on the mucin, have significantly spread in a circularly symmetrical fashion on the PLL, and have spread in an elongated fashion on the $Si(Ti)O_2$. The corresponding kinetic data showing the evolution of the incoupling angle (directly related to the waveguide propagation constant, eq: $\alpha = \sin \alpha + \lambda\kappa/\Lambda$) and the incoupling peak width are shown in Fig. 4.2. The results observed that cells that had not undergone at least one passage behave somewhat differently (Fig. 4.3).

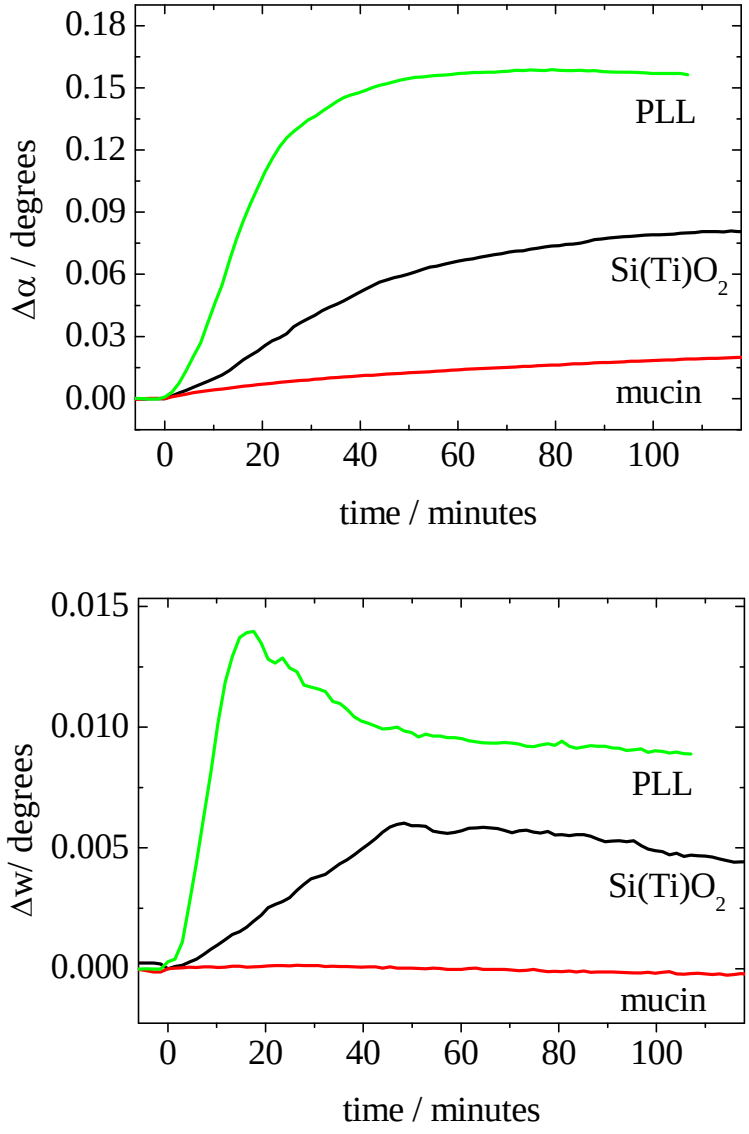

Figure 4.2: (Upper panel, a) incoupling angle, given as the difference Δα between the actual value and the value immediately prior to seeding the waveguide with 5×10^4 TERA2.spl2 stem cells, grown for at least two days with at least one passage, in a total volume of 550 µL on (from top to bottom) PLL, Si(Ti)O2, and mucin. (Lower panel, b) incoupling peak width, given as the difference Δw between the actual value and the value immediately prior to seeding the waveguide with the cells.

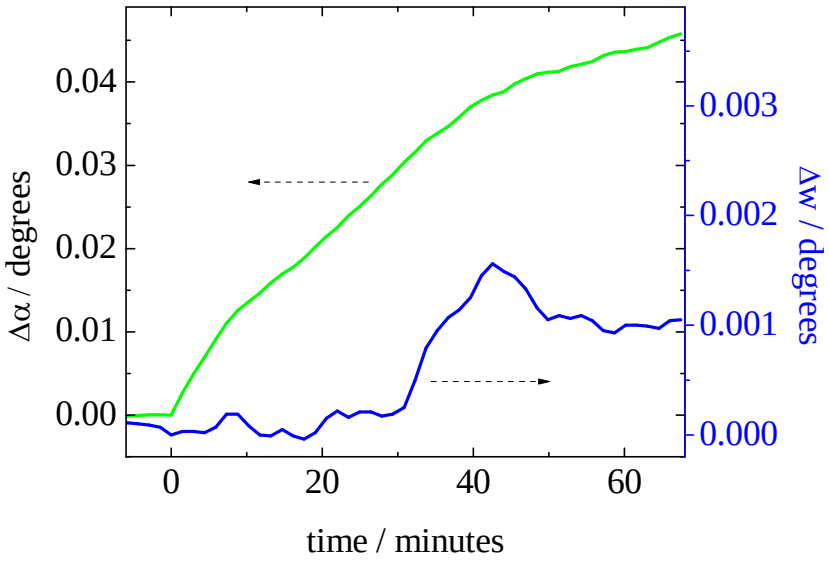

Figure 4.3: Plot of incoupling angle (left-hand scale) and the incoupling peak width (right-hand scale) following the seeding of a PLL-coated waveguide (at t = 0) with 5×10^4 TERA2.spl2 stem cells not having undergone passage.

4.1.2 Discussion

There are very striking differences between the cell responses to the three substrata. From Fig. 4.2 (a) it is clear that the cells spread well on PLL, less well on Si(Ti)O_2, and perhaps not at all on mucin; this merely confirms the visual observations. Fig. 4.2 (b) however clearly implies that the cells do not spread at all on mucin, and the small and slow increase in $\Delta\alpha$ for the cells on mucin is likely due to microexudate, i.e. the extracellular matrix molecules secreted by the cell in an attempt to render an uncongenial substratum congenial. In fact, this is suggested by two facts: (i) the absence of any change in incoupling peak width; and the absence of the sigmoidal kinetics of increase of propagation constant, which appears invariably to be associated with cell

spreading (e.g., (Ramsden, 1995b)), whereas protein deposition kinetics usually give the hyperbolic behaviour seen here (e.g., (Ramsden, 1994)).

The evolution of Δw reaches a peak when 50% of the surface is covered by the cells. That cells on PLL reach this peak much faster than on $Si(Ti)O_2$ is not surprising, given the more rapid evolution of Δα. What is revealing is that the value of Δα at the moment when Δw reaches its peak is much greater for PLL than for $Si(Ti)O_2$. We propose that this indicates that in cell-substratum contact is stronger (especially through more filopodia) for the former than for the latter. The fact that the Δw peak height is much greater for the PLL also corroborates this inference, for it implies that the optical contrast between the cell-covered and the uncovered regions of the waveguide is greater. We might emphasize here that such information can not be obtained via optical microscopy.

It is intriguing that what might be considered to be a cell that has not fully recovered from the storage in liquid nitrogen shows very different behaviour (Fig. 4.3; compare with 4.2). Firstly the temporal evolution of Δα is not sigmoidal, but hyperbolic. Secondly, there is a distinct lag before Δw starts to increase. Assuming that the initial increase of Δα is due to protein secretion (which cannot cause w to increase; note also the hyperbolic kinetics, characteristic of protein deposition, e.g. (Ramsden, 1994), we estimate the amount of protein after 30 min to be about 1.6 ng/mm^2. From the rather low value of the Δw peak height, we also infer that the cell-substratum contact is weaker than for cells that have undergone more passages. This can be made quantitative: we propose that the value of Δα at the instant when Δw is at its peak is equated with the

cell-substratum adhesivity (a composite quantity indicating the strength of the cell-substratum contact).

4.1.3 Summary of cell-substratum interactions

In conclusion, the evanescent field of lightmodes guided in an optical waveguide is perturbed by the presence of cytoplasm, its shape and composition, and by secreted macromolecules. Simultaneous examination of both the incoupling peak position and width (unaffected by macromolecular secretion and deposition on the waveguide), and their temporal evolution, allows these contributions to be separated. The methodology described in this work can be anticipated to be of value for high throughput experiments (cf. Fang, 2006), since a single set of simultaneous measurements, not requiring labelling, yields the rate of cell spreading, the rate of macromolecular secretion, and the adhesivity (density of filopodia).

In the results described in this section, the waveguide surface was seeded with a fixed number of spherical cells fresh from culture. Depending on the nature of cells, the medium in which they are immersed, and the substratum, the cells may undergo a spreading transformation from sphere to segment (Li and Ramsden, 1994). This causes the surface coverage to increase. A number of features of actual living cells complicate the apparently simple relation between composite incoupling peak width and surface coverage. If the cells spread to a very great extent, they may become thinner than the penetration depth of the evanescent wave, lowering the optical contrast between the covered and uncovered zones.

4.2 Dependence of attachment and spreading on seeding number

In this series of experiments OWLS was applied as a quantitative method for measuring the attachment and spreading of human embryonal carcinoma stem cells at different cell surface densities: I investigate the behaviour of cells spreading on silica-titania chips, and use the results to assess the biocompatibility of such surfaces as scaffolds. Microscopy images, together with OWLS kinetics data, suggest that the surface densities can control cell spreading on substrates.

TERA2 stem cells were used for all experiments, cultured at 37 °C in a 5% CO_2 environment with growth medium. Cells were counted by eye using a haemocytometer, with the number of cells and surface coverage confirmed using phase-contrast microscopy inspection of the waveguide after the experiment.

Similar to the previous experiment, waveguides were made from amorphous silica:titania at a ratio of approximately 2:1, with a penetration depth of the evanescent field of the order of 100 nm, and incorporated a shallow (5–10 nm) grating coupler (type 2400 (MicroVacuum, Budapest), grating constant equal to 416.667 nm). The incoupling resonance peaks for the TM 0 mode of the waveguides were measured every 40 s using a laboratory-built setup (Horvath, 2003; Horvath, 2005), and saved for subsequent analysis. The peak position and overall width were defined and determined according to Horvath et al., (2005).

4.2.1 Experimental results

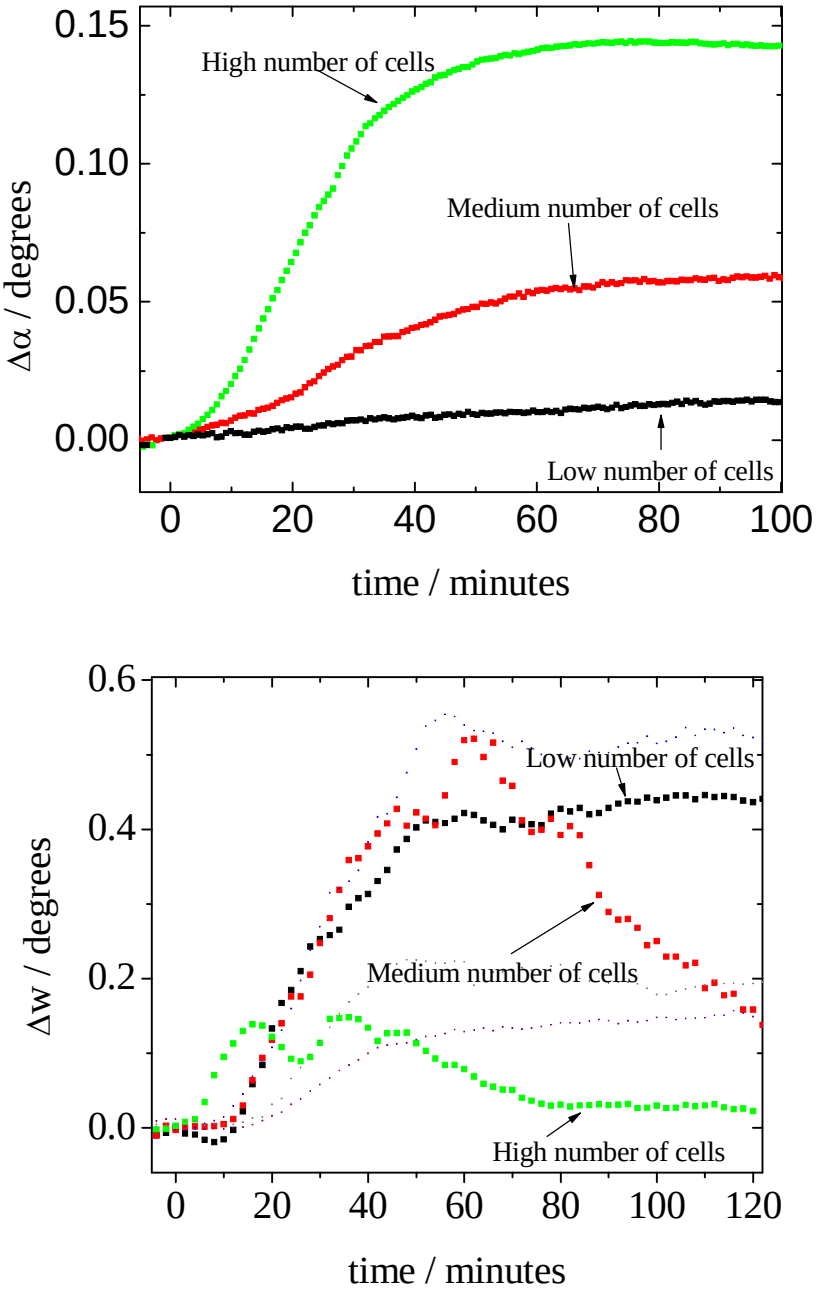

Figure 4.4 incoupling angle, given as the diference Δα between the actual value and the value immediately prior to seeding the waveguide.

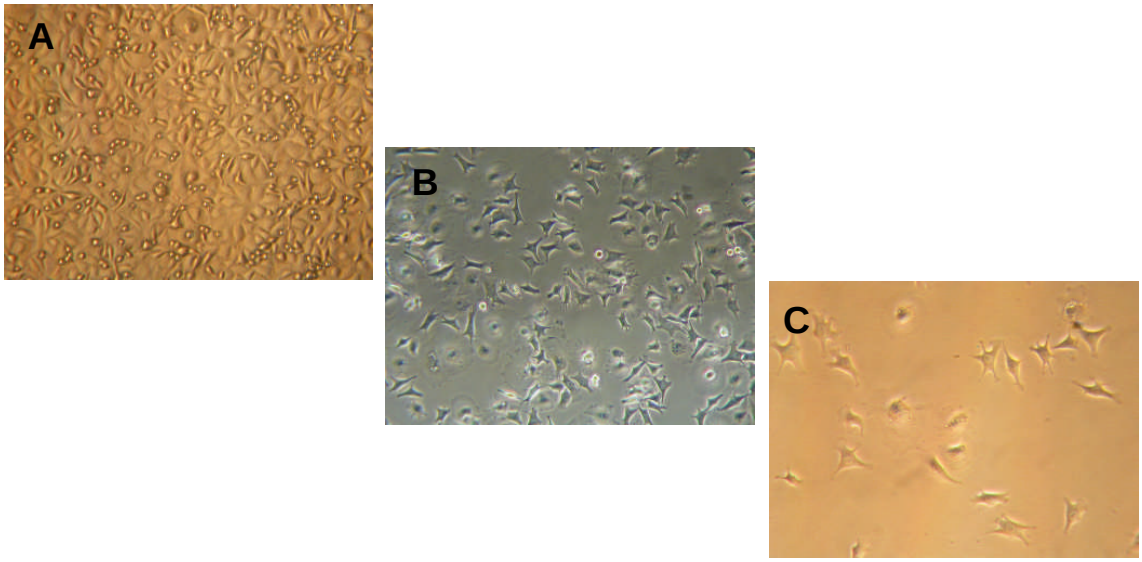

Figure 4.5 Optical micrographs of TERA2 stem cells on a silica-titania substratum; each main image is 850 µm wide; the insets are 170 µm wide.

Figure 4.4 shows the (Upper panel) incoupling angle, given as the difference Δα between the actual value and the value immediately prior to seeding the waveguide with (from top to bottom) 75×10^4 cells per 50 µL of TERA2 stem cells, 40×10^4 cells per 50 µL of TERA2 stem cells, 10×10^4 cells per 50 µL of TERA2 stem cells grown for at least two days with at least one passage and the (Lower panel) incoupling peak width, given as the difference Δw between the actual value and the value immediately prior to seeding the waveguide with the cells. Figure 5.5 shows the optical micrographs of TERA2 stem cells on a silica-titania substratum, (A) high concentration (75000 cells per 50 µL), (B) medium concentration 40000 cells per 50 µL, (C) low concentration of cells (10000 cells per 50 µL) after 100 minutes of culture.

4.2.2 Discussion

OWLS and microscopy data both support the conclusion that spreading strongly depends on the surface density of cells. The peak width data (see e.g. Cottier and Horvath, 2008), (figure 4.4-lower panel) clearly implies that the cell-covered area is larger for lower surface density because the cells have more space to spread. It is clear that for the intermediate (red) curve, the cells are attached and spread very well.

The incoupling peak position change (figure 4.4, upper panel) suggests that the quantity and movement (figure 4.4, lower panel) of optically refractive material, either intra-cellularly (e.g., the nucleus or cytoskeletal components) or extracellularly towards the substratum. During early cell spreading these may be key factors for long term cell viability. This is clear if one compares $\Delta\alpha$ for high surface density and low surface density at 25 minutes (figure 4.4). There is a twofold increase in $\Delta\alpha$ for high surface density; more highly refractive material is localised close to the surface. On the other hand, upon contacting the substratum stem cells (and many other cell types) will modify it by synthesising and releasing onto the surface the requisite for the extracellular matrix. These observations are confirmed by the optical microscopy (figure 4.5).

4.3 Nanosubstrates of differing morphologies and chemistry

The major factors influencing the behaviour---attachment and spreading---of cells, especially stem cells in vitro, have been studied for various materials with different properties, differing in surface roughness, or electrical or chemical characteristics. Nanoparticles have been shown to increase or decrease proliferation, or modulate differentiation processes of different kinds of cells (Gutwein and Webester, 2004). ECM proteins (Tourovskaia et al., 2002) and a range of other surface modifications, including self assembled monolayers, have also been shown to influence cell attachment (Kommireddy et al., 2006).

We need to find out what are optimal surface properties for promoting new tissue growth. Since surface properties vary with the grain size of a material, there is excitement concerning the use of nanomaterials in stem cell-substrata interactions research, because nanotechnology allows the size-precise fabrication of surface features. Transplanted stem cells in artificial scaffolds for cell attachment have been an interesting area of study for a recent stem cell researches and various method and techniques have been proposed and implemented (Webster et al., 2004). One of the main applications of nanomaterials is surface modification of implantable materials---the modifications can increase or inhibit cell attachment considerably (e.g. McColl et al., 2008). One of the methods of surface modification for cell attachment is assembly of nanoparticles on a substratum, and after adding the cells their attachment and spreading are visualized during the first attachment period. Morphological differences of TERA2 stem cells were evaluated during 1-2 hours. Stained microscopy images of stem cells on four different substrates after 90-100 minutes show the organelle

distribution of the cell (figure 4.6). Figure 4.6 shows clearly different spreading on (A) polyamide nanofiber compared with (B) CNTs--- on the latter, the cells are spread very differently--- much more, with some connections between cells not appearing on the polyamide nanofiber, nor on the two other substrata (figure 4.6).

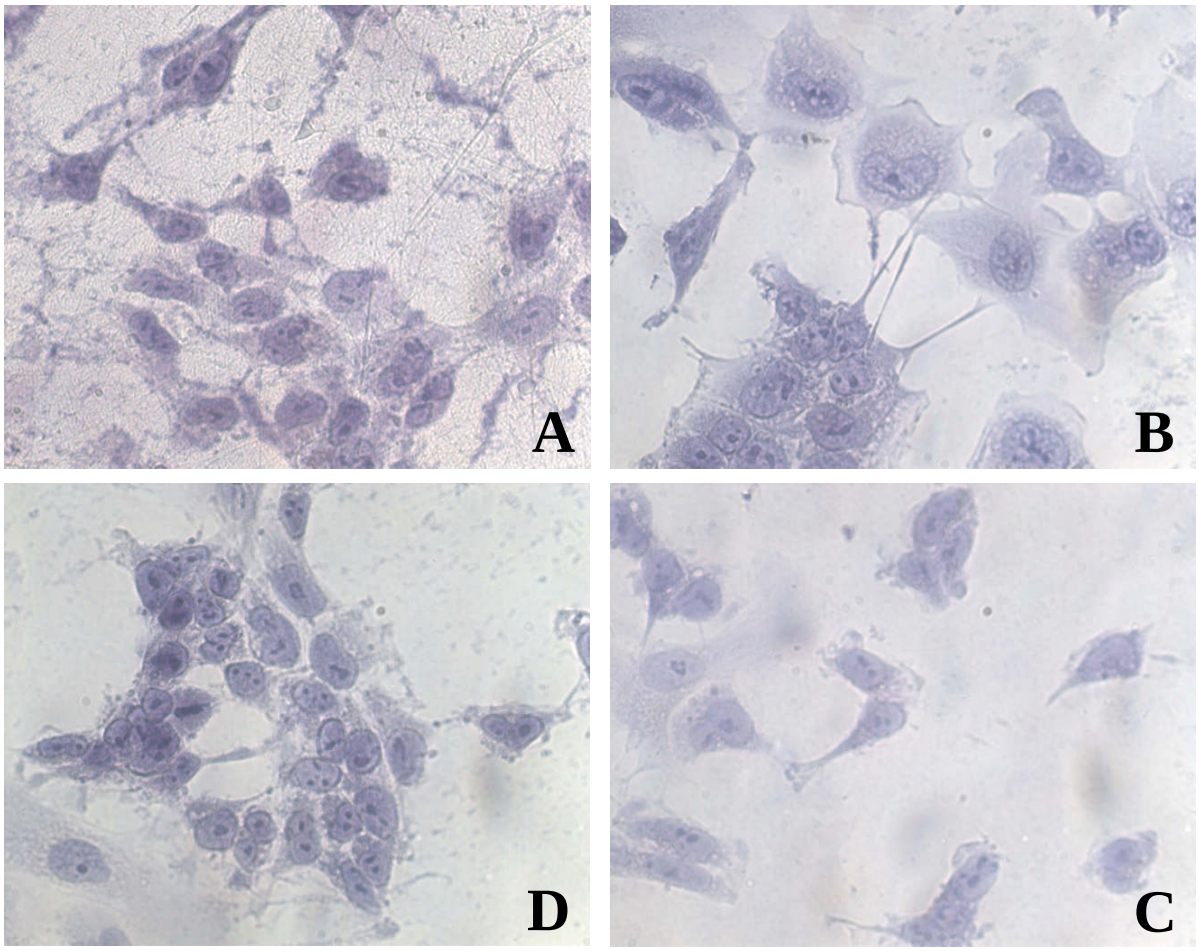

Figure 4.6 Morphologies of TERA2 stem cells. Cells ($1x10^5$ per 1 mL) were added to cover slips which were fixed and stained using hematoxylin. (A) On polyamide nanofiber discs, (B) On CNTs, (C) On silica-based glass cover slip (D) On magnetite nanoparticles. The widths of the images are 500 microns.

Cells on the magnetite nanoparticles (MNPs) cluster very close to each other and are not spread well compared to the polyamide nanofibers and the CNTs. Glass (C) shows that cells are attached and spread completely differently from the other substrates.

4.3.1 Discussion

I have used the image analyzer program designed by Jeremy Ramsden in this experiment to parameterize differing morphologies. This program helped me to quantify the spread area on four different substrates (Table 4.1). Figure 4.7 clearly demonstrated that cells are attached and spread on four substrates but the spreading areas are completely different.

Table 4.1 Summary of morphological change of TERA2 on different substrata

Nanosubstrata	Attachment	Spreading	Spreading area / μm^2	Microscopy morphology
Polyamide nanofibers (A)	Very well	Well	12.4 ±1.35	Seems that cells are "happy"
Carbon nanotubes (B)	Very well	Extremely wide	81.6 ±39.95	Cytoplasm is largely spread
Silica Glass (C)	Well	Well	15.8 ±3.65	Cytoplasm is normally spread
Magnetite nanoparticles (D)	Well	Well	10.4 ±2.65	Cells are spread closely each other

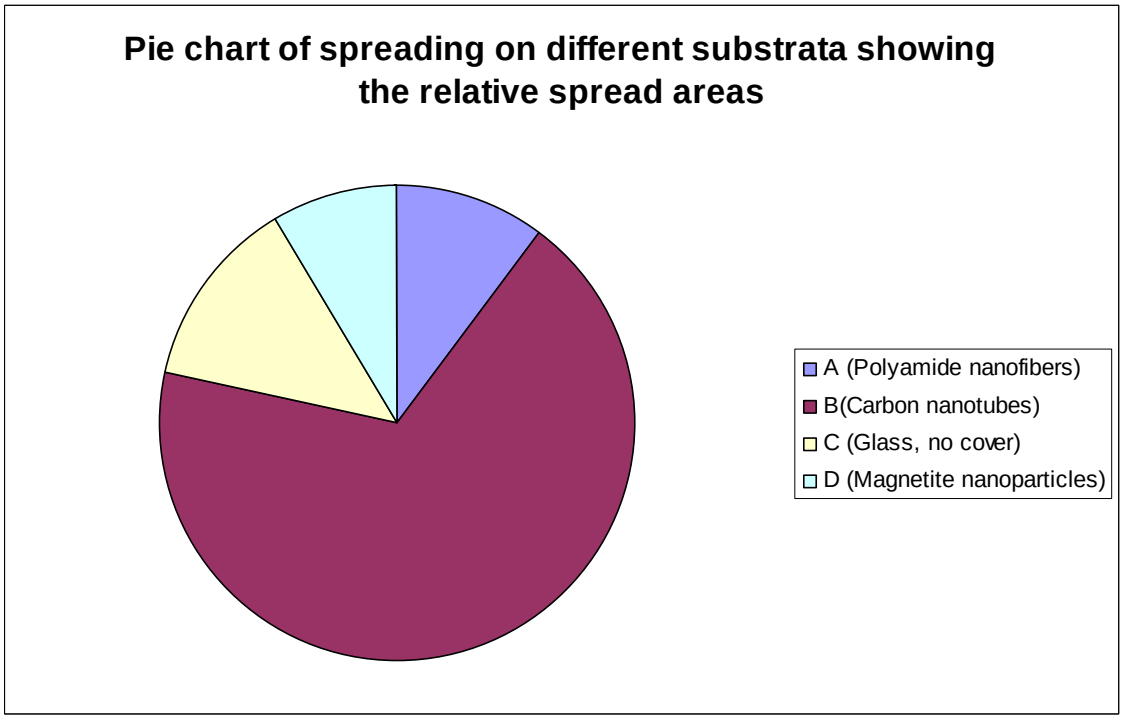

Figure 4.7 Spreading area distributions on the substrata.

Cells on the carbon nanotubes (B) spread almost seven times more than on any of the three other substrates, and develops some connections between cells. Cells on the magnetite nanoparticles (D) are very much clustered together and they spread to the lowest area compared with the other three substrata.

After this experiment, I concluded that a combination of cell adhesion biochemistry and CNT thin film surface properties make this material a good candidate for further studies with TERA2 stem cells.

Polyamide nanofibers do not have an especial effect on spreading, but these nanomaterials had a different effect on differentiation process during my work. As described in chapter 3 (differentiation of EC cell lines by RA, section 3.1), I discovered how to differentiate cells into A, neurons and B, new morphology i.e. two different morphologies. I applied these protocols on the polyamide nanofibers exactly in the same ways, but although the TERA2 cells differentiated to neurons as before, they do not differentiat to the new morphology (figure 4.8), but produce something even stronger.

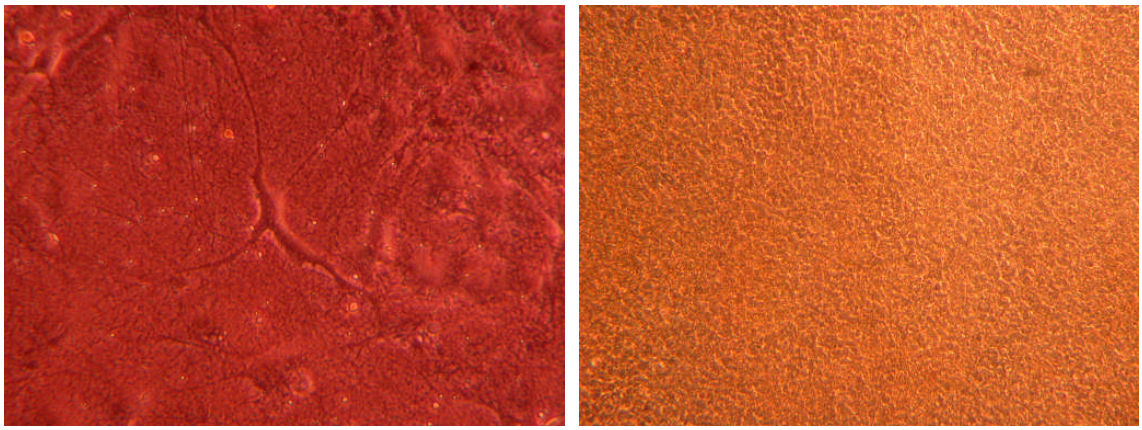

Figure 4.8 TERA2 cells differentiate to neurons on polyamide nanofibers, (Protocol A, section 4.1, left), but they do not differentiate to the new morphology (right). The widths of the images are 850 microns.

CHAPTER 5

Conclusion and global understanding

The future success of designing biomaterial substrata such as scaffolds for engineered tissue growth depends on an understanding of the mechanisms of interactions between cells, proteins and surfaces. My work deals with the effects of cell-substrata interactions arising from different substrata on the cells, such as morphological changes, including during differentiation of stem cells, as a means of quantifying cellular responses. These responses were investigated *in vitro*.

One of the present limitations hindering progress has been the lack of a suitable measurement technique for quantitatively and accurately characterizing cell state. This limitation is overcome by the introduction of optical waveguide lightmode spectroscopy (OWLS).

Future development in this area will doubtless require surfaces which are derived from an understanding of the processes that lead to protein adsorption and subsequent cellular responses. As the *in vivo* cell environment presents a complex array of chemical and topographical cues it would be logical to further explore how surface chemistry and topography can be used to elicit desired bimolecular surface interactions. This thesis takes significant first step along this road.

The development of OWLS has been required in order to study *in vitro* and *ex vivo* sample. *In vitro* measurements, although an important step in understanding interfacial interactions, do not completely explain *in vivo* interactions. This thesis clearly demonstrates that the OWLS holds great promise for gaining further insight into cell-substratum interactions. For exploitation of the OWLS technique to monitor cell interactions in real time, however, may require even better understanding of the influence on the OWLS signals of substrates and cell cytoskeleton reconstruction leading to the goal of understanding how the substratum influence the cytoskeleton. This should ultimately lead to a complete model to interpret the OWLS parameters in terms of the detailed cellular interactions with substrata.

In biotechnology, the ability to optimize bioprocess conditions to maximize the synthesis of desired biomolecules is of great interest; in a similar way, controlling cell behaviour is important for developing tissue cultures and artificial tissues that can be used as predictive models of biological systems, and 3D structures for tissue engineering. An example of the importance of controlling the cellular microenvironment is found in the drug discovery process, in which the effects of specific chemicals within a large library of chemical molecules are tested on cells, to identify candidate drugs. The ability to predict the toxicity and functionality of a candidate drug is important for classifying these drugs and eliminating costly animal experiments and failures in clinical trials. Therefore, it is important to have predictive tissue models in vitro, OWLS then provides the means to quantitatively monitor the cell response. Another example that demonstrates the importance of controlling cellular behaviour in culture is related to generating a renewable source of cells for regenerative

medicine. In most cases the cells of an adult organism cannot proliferate to the extent required to generate a renewable tissue. However, it is possible to utilize stem cells that are either derived from the adult organism or from embryonic sources to generate a renewable source of cells. A critical challenge in stem cell based therapy is how to uniformly direct the differentiation of stem cells into desired cell types. My results show how nanotechnology can help to achieve this goal.

CHAPTER 6

Future work

The aim of this final chapter is to suggest some possible future areas of research and highlight areas that may either emphasize this work or answer any questions which were not addressed. Nanotechnology involves the creation and manipulation of materials at the nanoscale level to create unique products that exploit novel properties. Recently, nanomaterials such as carbon nanotubes, nanofibers, and quantum dots have received enormous national attention in the creation of new types of analytical tools for biotechnology and the life science (De Wild, 2003). Of much greater interest, however, is the use of nanomaterials to directly influence cell behaviour, as I have demonstrated (Section 5.3).

Of interest therefore would be further investigations into nanostructures, giving further insights into the dynamics of the cells. A possibility here is to use modified waveguides capable of supporting additional modes. These should give more information about the cell structure and as such would help to understand the differentiation process.

An area which we have not investigated at all is polyelectrolyte films and their impact on cell differentiation process. To reduce the differentiation period polyelectrolyte films such as PSS and PAH multilayered films, when terminated by PAH, induce strong adhesion of stem cells that spread and keep their phenotype on glass and these coatings allow rapid---within only two weeks compared with two months for classical coating (Berthelemy et al., 2008).

The new morphology of TERA2 stem cells requires further work to characterise it, e.g. using immunocytochemistry. We could not yet characterise the “new” cell type. It is also important to establish what other derivatives of RA can modulate cellular phenotype. RA is apparently extremely unstable in aqueous solution and deteriorates quickly. It can also interact with culture media.

Appendices

Appendix A

Optical waveguide lightmode spectroscopy:

(Principle)

A.1 Reflection, refraction and total internal reflection

When light travels across medium of differing refractive indices (for example F and C) some light will be reflected back and some will be refracted. This is commonly known as Snells law although Harriot had initially discovered it sometime before Snell (Fig. B. 1).

$$n_F \sin \theta_F = n_C \sin \theta_C \qquad \text{(A1)}$$

where n_F and n_C are the refractive indices of media F and C respectively where $n_C > n_F$. θ_F is the angles of incidence and θ_C the angle of refraction.

A

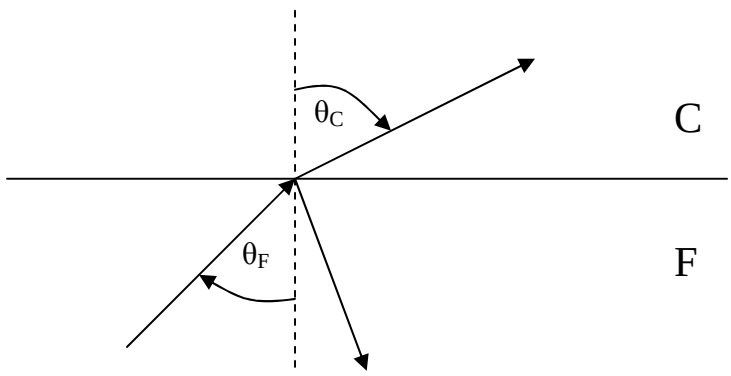

B

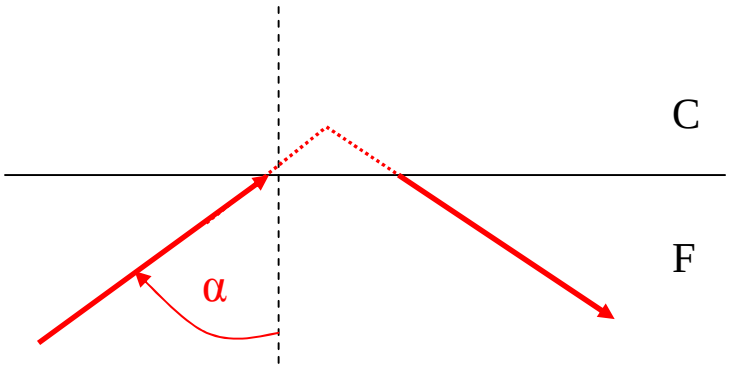

Figure A. 1: Refraction, reflection and total internal reflection. A. Light travelling into media F (dark arrow) will refract into media C and reflect back into media F with the C/F relationship dependent on the angle of incidence θ_F. B. Total internal reflection (red arrow) will occur above a critical incidence angle, here no light is rerfracted. The Goos-Hánchen shift is shown as the dotted red lines.

Above a critical angle (α), total internal reflection will occur. This only occurs when the light is travelling from a high to low refractive index material. The light confined within two reflecting interfaces will travel as a standing wave between the surfaces and as an evanescent wave beyond (Fig. A. 2). The light penetrates into C before returning to F, resulting in a phase shift, D (Tien, 1977).

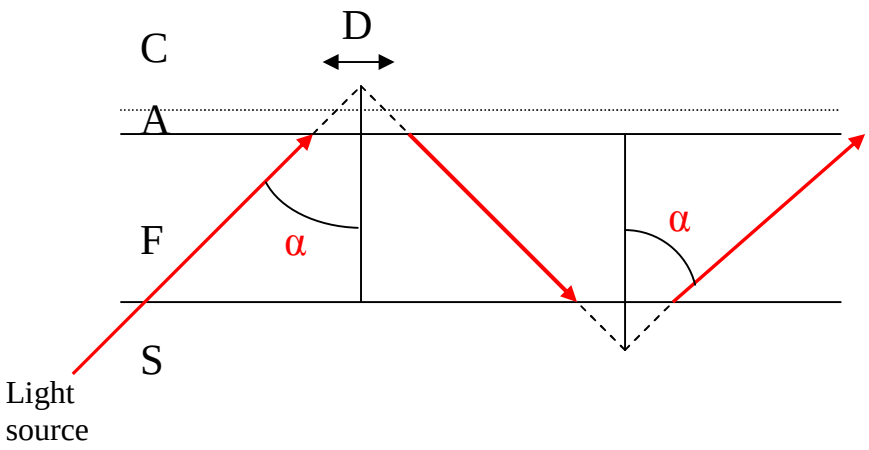

Figure A. 2: Laser light travelling through an optical waveguide. Light is confined within a high refractive index film (F) and will penetrate into the surrounding low refractive index material (S and C). A denotes an adsorbed adlayer, D the phase shift and α the angle of incidence.

A. 2 Waveguide and adlayer parameter calculations

A three layer model is used to calculate the waveguide parameters

$$\pi m = \frac{2\pi}{\lambda}\sqrt{n_F^2} - N^2 d_F - \arctan\left[\left(\frac{n_F}{n_S}\right)^{2p}\sqrt{\frac{N^2 - n_S^2}{n_F^2 - N^2}}\right] - \arctan\left[\left(\frac{n_F}{n_C}\right)^{2p}\sqrt{\frac{N^2 - n_C^2}{n_F^2 - N^2}}\right] \quad \text{(A2)}$$

where

p=1 and $N=N_{TM}$ for TM mode (A3)

p=0 and $N=N_{TE}$ for TE mode.

where TM is the transverse magnetic component of the propagating light, TE the transverse electric component and p the mode.

Adsorption of material onto the surface will form an adlayer with the parameters characterised using the four layer mode equation (Ramsden, 1995a). The refractive index of the adlayer, n_A is calculated using:

$$n_A = \left(\frac{\frac{FM(N_{TM})}{A(N_{TM})} - d_F}{\frac{FE(N_{TE})}{A(N_{TE})} - d_F} \left(\frac{1}{n_C^2} + \frac{1}{n_F^2} - \frac{1}{N_{TM}^2} \right) - \frac{1}{n_C^2} + \frac{1}{N_{TM}^2} \right)^{-1/2} \quad \text{(A4)}$$

and the thickness, d_A calculated using

$$d_A = \left(\frac{FE(N_{TE})}{A(N_{TE})} - d_F \right) \left(\frac{n_F^2 - n_C^2}{n_A^2 - n_C^2} \right) \quad \text{(A5)}$$

where

$$A(N) = \frac{2\pi}{\lambda} \sqrt{n_F^2 - N^2} \quad \text{(A6)}$$

$$FM(N) = \arctan\left(\frac{n_F^2}{n_S^2} \sqrt{\frac{N^2 - n_S^2}{n_F^2 - N^2}} \right) + \arctan\left(\frac{n_F^2}{n_C^2} \sqrt{\frac{N^2 - n_C^2}{n_F^2 - N^2}} \right) \quad \text{(A7)}$$

$$FE(N) = \arctan\left(\sqrt{\frac{N^2 - n_S^2}{n_F^2 - N^2}}\right) + \left(\sqrt{\frac{N^2 - n_C^2}{n_F^2 - N^2}}\right) \quad \text{(A8)}$$

A.3 Random sequential adsorption

As molecules adsorb onto a surface their shape will impact on the available surface for further adsorption. After a time adsorption will stop as the surface becomes jammed. This is the jamming limit (θ_J) (e.g. a sphere has $\theta_J \sim 0.547$). The available area is at first close to one but as the molecules start to adsorb the surface becomes more occupied and the corrections become increasingly prominent (Ricci et al., 1992). At a certain point the surface cannot accommodate further adsorption, despite there being space, and the jamming limit is reached (Ramsden, 1993; Evans, 1993; Ramsden et al., 1994; Lavalle et al., 2000).The equation used for fitting is

$$\phi(M, a) = \left(1 - x^3\right) / \left(1 - 0.812x + 0.2336x^2 + 0.0845x^3\right) \quad \text{(A9)}$$

where $x = \frac{\theta}{\theta_J}$, θ being related to M by M = θ m/a, where m is the mass per molecule, and θ_J is the jamming limit.

A.4 Mass calculations

In the situation where a specific protein with known polarisability adsorbs, forming an isotropic monolayer, the adsorbed mass can be calculated from the refractive indices

(Ramsden, 1993; Lukosz, 1998). The mass of the molecules in the adlayer is then given as:

$$M = \int_0^\infty (c_s(z) - c_{bulk})dz \qquad M = (c_A - c_{bulk}).d_A \qquad M = c_A d_A$$

Where C_s is the concentration of molecules in the adlayer (molecules per unit area) and C_{bulk} the bulk (liquid) concentration. The refractive index n_A of the adsorbed layer is related to c_A according to this equation:

$$n_A = n_c + c_A \frac{dn}{dc}$$

Where n_c is the refractive index of the media in which the molecules are dissolved, i.e. the buffer. The coefficient *dn/dc* depends on the Polarisability of the molecules and finally, eliminating c_A, the mass can be calculated as:

$$M = d_A \frac{n_A - n_C}{dn/dc}$$

The experimental waveguide system was used, the custom built setup used (built by Dr. Robert Horvath (Horvath et al., 2001; 2003) for setup details) for the cell experiments. The custom built setup enables the extraction of raw data and the calculation of additional parameters (Horvath et al., 2005).

Appendix B

Polyphenol control of cell spreading on glycoprotein substrates

JAMES MCCOLL, ROBERT HORVATH, **AMIRREZA AREF**, LEE LARCOMBE, IVA CHIANELLA, SARAH MORGAN, GLEB E. YAKUBOV and JEREMY J. RAMSDEN

B.1 Abstract

Cell–surface contacts are vital for many eukaryotic cells. The surface provides anchorage (facilitating spreading and proliferation), is involved in sensation, i.e., via mechano-, osmo- and chemoreceptors, and in addition nutrients may also be supplied via vessels adjacent the lamina. Hence, the ability to manipulate the surface characteristics provide a mechanism for directly influencing cell behaviour. Applications such as medical implants and tissue engineering require biocompatible, stable surfaces for controlling cell behaviour. Mucin-coated surfaces inhibit cell spreading compared with poly-l-lysine in vitro; hence, we show that a composite layer arrested from mucin-EGCg aggregate counters the inhibition. Although the anti-spreading effects of the glycoprotein substrate on cell behaviour are similar to those observed for pure polysaccharide surfaces, the reversal of cell spreading inhibition by the admixture of polyphenol/glycoprotein substrata is remarkable and unexpected.

Possible applications for a composite glycoprotein–polyphenol layer include medical devices, in particular for those operating at mucosal interfaces such as the oral, tracheal or gastrointestinal tract cavities, wound healing, cancer control and the controlled growth of therapeutic cell cultures.

B.2 Introduction

Cell surface interactions impact on cell shape, physiology and ultimately viability (Chen et al., 1998). Tissue engineering applications such as wound repair and tissue growth strive to mimic the assimilatory role of natural substrata whilst designers of biomedical coatings (such as those of certain implants and surgical instruments) may seek to assimilate or inhibit protein and cell attachment (Griffith, 2002). The use of natural components (i.e., produced by the body) for in vivo applications will reduce possible negative biocompatibility issues. To inhibit cell attachment many lessons can be learnt from natural systems, the mammalian repulsive mucus barriers for example actively remove invading cells from the mucosae (Shi et al, 2000). The major macromolecular component of the mucosal layer is mucin, a family of heavily glycosylated, high molecular weight glycoproteins with carbohydrate side chains that make up some 50–80% of the molecule by weight (Bansil et al., 1995). Indeed fibroblast and keratinocyte cultures grown on mucin-coated surfaces adhere poorly when compared with oxidised polystyrene (tissue culture polymers) or mucin surfaces that have their O-linked carbohydrates removed (Gabriel et al., 2005). Here the sugar moieties seem to play a pivotal inhibitory role, as cellulose-coated (Gekas et al., 2004; Faucheux et al., 1999) and dextran sulphate-coated surfaces (even when over-coated with fibronectin) (Wittmer et al., 2007) inhibit cell spreading. On the other hand, perhaps the most

extraordinary example of bioadhesion is the attachment of mussels to almost any surface type via their byssal threads. Even more remarkable is their ability to do this in an environment which is often extremely turbulent salt water. This is made possible through the use of a phenolic compound 3,4-dihydrophenyl-L-alanine (DOPA) which is cross-linked with various proteins to provide the adhesive. Indeed DOPA has also been shown to crosslink mucin. An important group of phenolic flavonoids are the catechins found in many fruits and vegetables, and persist in beverages such as tea (Shimizu and Weinstein, 2005). Epigallocatechin gallate (EGCg), found at high concentrations in green tea is a polyphenol known to cause flocculation of saliva and complexes with salivary proline-rich-proteins (Jobstl et al., 2004). It has been suggested that polyphenols may form aggregates with salivary glycoproteins. The metabolic activity and bioavailability of phytonutrients (of which EGCg is one of the most prominent) is controversial. EGCg has therefore been the target of numerous studies to investigate its antioxidant and metabolic activity, i.e., the effect on glucose metabolism. Here we investigate the cross-linking behaviour of mucin and EGCg. Spreading kinetics of fibroblasts on mucin coated and for the first time mucin mixed with EGCg coated surfaces are determined and used to assess the biocompatibility of these modified surfaces. Using dynamic light scattering (DLS) we infer that the presence of EGCg aggregates the mucin bulk solutions. Optical waveguide lightmode spectroscopy (OWLS) suggests that in addition to bulk solution aggregation the absorbed layer characteristics are also affected. Confocal microscopy, together with OWLS kinetic data suggests that EGCg is able to control cell spreading on mucin substrates.

B.3 Materials and methods

Chemicals and biochemicals

Pharmaceutical grade porcine gastric mucin (PGM) was purchased from Orthana Kemisk (Denmark). The commercial mucin preparation with a mean molecular mass estimated as 565 kDa [19] was dialysed to remove all salts and low molecular weight additives and lyophilized for storage. All solutions were made by dissolving weighed PGM in Elga ultrapure (resistance 18.2 MΩ cm, filtered through 200 nm pores) water.

Dulbecco's modified Eagle's medium with HAMS F12 (DMEM HAMS F12), foetal bovine serum (FBS), trypsin/EDTA, penicillin/streptomycin solution and glutamine were purchased from Invitrogen (UK). Hepes and natural occurring EGCg (Teavigo) were purchased from Sigma-Aldrich (UK). Cleaning solution "Cobas integra" was purchased from Roche (UK).

Dynamic light scattering

Measurements were performed using a PCS 4700 goniometer system (Malvern Instruments, UK) with dedicated software. All mucin solutions were filtered (0.2 μm, Minisart, UK), the temperature maintained at 25.0 ◦C and measurements conducted at 30 ◦, 60 ◦, 90 ◦ and 120 ◦ scattering angles.

Cell culture

McCoy fibroblast cells (ECCAC #CB3009, HPA, UK) were used for all experiments, cultured at 37 ◦C in a 5% CO2 environment with McCoy growth medium (MGM), comprising DMEM HAMS F12 with 10% FBS, 0.1% penicillin streptomycin and 0.2%

glutamine. Cells were detached using 0.05% trypsin/EDTA and collected using centrifugation.

Substrate modification

Sterilised (UV irradiated for 20 min under a laminar flow hood) 20 × 20 mm glass cover slips were coated with 0.1% (w/w) poly(L-lysine) (PLL) in water, 0.1% (w/w) mucin in water and 0.1% (w/w) mucin + 0.1% (w/w) EGCg in water. The mucin stock solution was prepared and pre-equilibrated overnight with EGCg added to the mucin stock solution and mixed 20 min before use. Solutions were applied to the substrata for 20 min, washed twice (first using water, then MGM) and incubated for 40 min (37 ◦C, 5% CO2 environment) in MGM. Waveguides were cleaned under sonication in Roche solution for 10 min, rinsed using ultrapure water and O2-plasma treated (20 mW for 2 min) before coating.

Cell attachment and spreading

Substrates (cover slips) were washed with fresh MGM before adding 1×10^5 cells to each cover slip. Following 30, 60 and 180 min of attachment and spreading cells were fixed using ice-cold methanol. 4×10^4 cells were added directly to the OWLS cuvette. Repeatable experiments confirmed the results (n=3). Cells were counted by eye using a haemocytometer, with the number of cells and surface coverage confirmed using phase-contrast microscopy inspection of the waveguide after the experiment.

Staining and confocal microscopy

The cytoplasm was visualised using a 1 µg/ml streptavidin-Alexa Fluor555 fluorescent conjugate (Molecular Probes) diluted in PBS which binds endogenous mitochondrial biotin. 500 µM Sytox green nuclear stain (Molecular Probes) diluted in DMSO (Sigma) counterstained the DNA and slides were mounted using a glycerolbased mountant (Dako, UK). Cells were imaged using a Zeiss laser scanning confocal microscope (LSM 510 Meta) with a minimum ×40 objective. The Sytox green nuclear stain was excited (488 nm) using an Argon ion laser with emission detected via a 505–550 nm band-pass filter and the Alexa Fluor555A excited (543 nm) using a HeNe laser source with detection through a 560 nm long-pass filter.

Optical waveguide lightmode spectroscopy

Smooth planar optical waveguides made from amorphous silica: titania at a ratio of approx. 2:1 and incorporating a shallow (5–10 nm) grating coupler were purchased from MicroVacuum, Hungary (type 2400, grating constant equal to 416.667 nm) and pre-equilibrated in MGM (buffered using 0.1 M Hepes, pH 7.4) overnight. The waveguides were assembled in a microcuvette (such that the waveguide formed the bottom of the cuvette) and mounted on a high precision (microradian resolution) mechanical goniometer of an integrated optical scanner equipped with temperature control. The polymer adsorption experiments were performed using the OWLS110 (Microvacuum, UK) whereas the cell experiments used a custom built setup with open cuvettes (Horvath et al., 2003; Horvath et al., 2005). The incoupling resonance peaks for the TM0 mode of the waveguides were measured every 40 s and saved for subsequent analysis. Biopolymer deposition Mucin and mucin/EGCg film assembly characteristics

were investigated by first flowing water then either 0.1% mucin or 0.1% mucin with 0.1% EGCg and finally pure water again through the microcuvette. Experiments were repeated three times. The wall shear rate of the fluids passing through the cuvette was 31 s^{-1}. The NTM(t) and NTE(t) values for the adsorption–desorption sequences were inserted into the two corresponding mode equations characterizing propagation of the guided light in a four layer structure: support, waveguiding film, protein adlayer assumed isotropic and cover. The two unknowns obtained (thickness and refractive index of the adlayer) were combined to yield the mass of protein adsorbed at the waveguide surface. The refractive index increment (dn/dc) of mucin dissolved in water, required for the mass determination (Ball and Ramsden, 1998) was separately determined at 632.816 nm, the wavelength of the light introduced into the optical waveguides, using a Rudolph J357 refractometer. The values were 0.14± 0.002 cm^3 /g for mucin and 0.20±0.004 cm^3/g for mucin/EGCg. The practical output of the kinetic adsorption–desorption experiments were plots of adsorbed mass of mucin versus time.

B.4 Results and discussion

The spreading kinetics of fibroblasts, were investigated using OWLS, a molecular microscopy technique that has been previously been used to measure the attachment and spreading of cells. Behaviour is dramatically different for mucin and mucin +EGCg layers (Fig. B1). The sigmoidal kinetics most likely correspond to cell spreading (Li et al., 1994) suggesting that the amount of high refractive index close to the substrate is highest for PLL, very low for mucin and is relatively high (when compared with mucin) for mucin+EGCg. The rate of physico-chemical association and initial spreading on mucin (0–10 min) is an order of magnitude smaller than that with mucin + EGCg or

with PLL (Fig. B1 legend). We can see that mucin sharply inhibits spreading compared with PLL, but the mucin + EGCg layer is practically as good an early spread-promoting substrate as PLL (Fig. B1). Confocal microscopy of cells living on identical substrates shows the organelle distribution of the cell (Fig. B2).

Confirming the OWLS data mucin clearly inhibits spreading compared with PLL. This is abolished by the admixture of EGCg and after 60 min the cells on mucin +EGCg are virtually indistinguishable from those on PLL. If EGCg were incorporated into the layer one might expect that it would desorb into the surrounding media over time. The possibility of EGCg leaching out of the substrate and leaving the cells on pure mucin is excluded by our failure to detect any free EGCg in the cover medium surrounding the cells using high performance liquid chromatography, with a detection limit of 1 μg/ml. OWLS and confocal microscopy data both support the conclusion that spreading is inhibited by mucin as observed for cellulose-coated substrates (Gekas et al., 2004; Wittmer et al., 2007) and the inhibition is initially abolished for the layer formed from the mucin + EGCg aggregate layer.

Analysing the OWLS peak width provides conformation of the spreading kinetics as the surface coverage, defined as the fraction of substratum covered by cell material (up to 150 nm above the surface for our experimental conditions) is obtained. The resonance peak overall width increases up to surface coverage of 50% of randomly placed objects and then decreases as the coverage increases further (Horvath et al., 2001; Cottier and Horvath, 2008). The peak width data clearly confirms that the cell covered area is larger for PLL and mucin +EGCg than for mucin (Fig. B3).

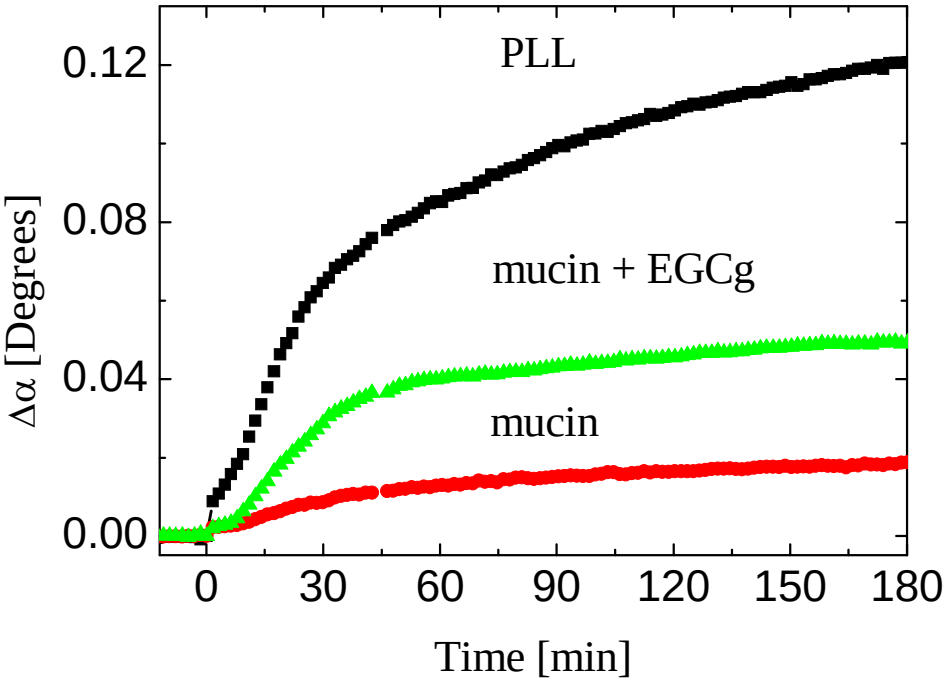

Figure B.1: Cell-substrata interactions monitored by OWLS (monitored as mean incoupling peak position shift with time). Fibroblasts spread on 0.1% PLL in water (top curve), 0.1% (w/w) mucin in water (lower curve) and 0.1% mucin + 0.1% EGCg in water (middle curve). Cells were added at time 0. 0-10minute data were fitted with linear least square fits yielding (PLL) $1.7x10^{-3} \pm 2x10^{-5}$, (mucin + EGCg) $1.1x10^{-3} \pm 5x10^{-5}$ (mucin) $1.7x10^{-4} \pm 9x10^{-5}$. For the interval 10 -30 minutes $\Delta\alpha$ values were, (PLL) $2.1x10^{-3} \pm 9x10^{-5}$, (mucin + EGCg) $1x10^{-3} \pm 2x10^{-5}$and $3x10^{-4} \pm 2x10^{-5}$(mucin).

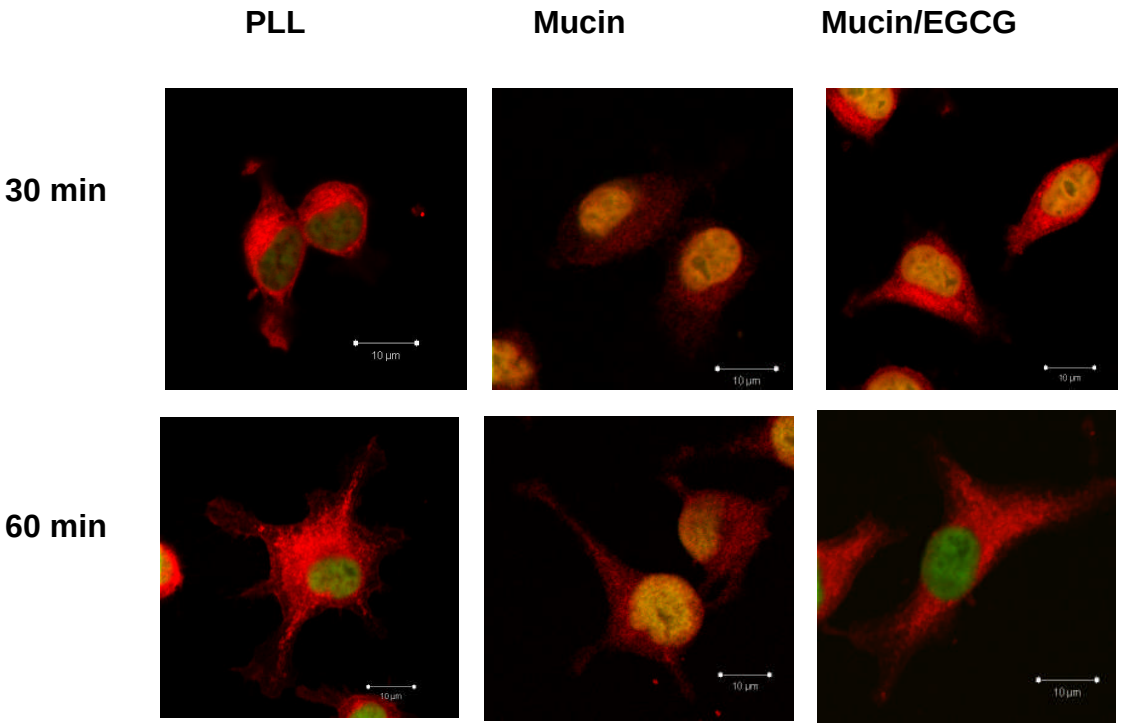

Figure B.2: Confocal microscopy images of fibroblast cells on poly-l-lysine, mucin and mucin/EGCg substrates after 30 and 60 minutes. Sytox (green) stains the nucleus and Alexa Fluor555A stains mitochondrial biotin, yellow indicates red on green staining. All images x400 magnification with 30 minute images zoomed (x4.5). White scale bars in the lower right hand corner correspond to 10µm for 30 and 60 minutes images.

For PLL and mucin + EGCg the initial rate of incoupling peak width change increases linearly over the first 30 min, whereas the mucin substrates exhibit twophase coverage kinetics, initially fast and then slow (Fig. B3). The incoupling peak position change suggests that the quantity (Fig. B1) and movement (Fig. B3) of optically refractive material, either intra-cellular (e.g., the nucleus or cyto-skeletal components) or extra-cellular towards the substratum during early cell spreading are key factors for long term

cell viability. This is clear if one compares Δα for PLL and mucin + EGCg at 60 min (Fig. B1), the 50% coverage point (from Fig. B3). There is a twofold increase in Δα for PLL, implying more highly optically refractive material is localised close to the surface for this substratum.

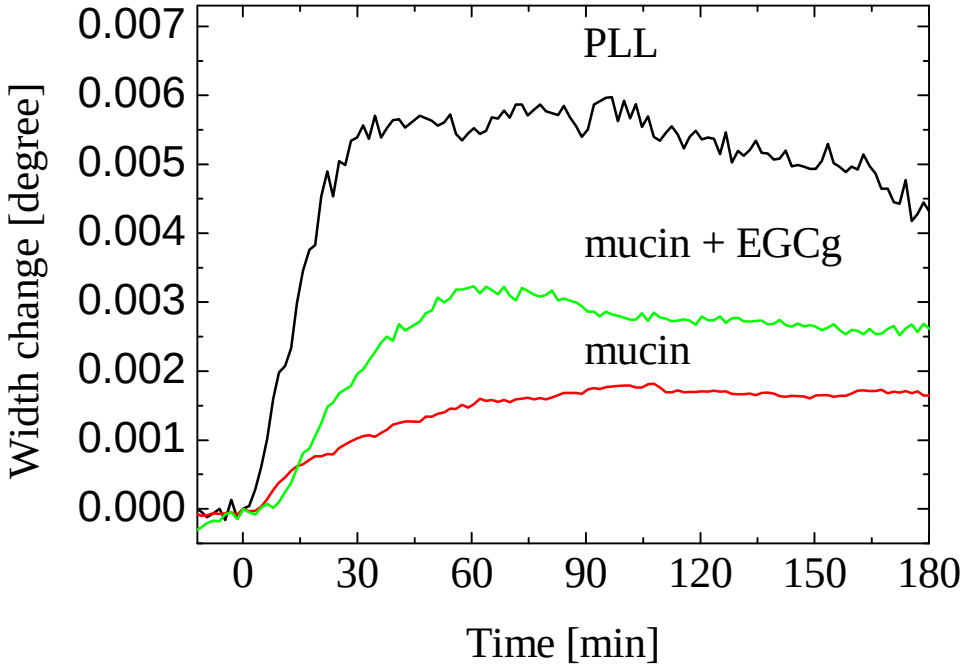

Figure. B.3: Cell-substrata interactions monitored via OWLS (incoupling peak width). Fibroblasts spread on 0.1% PLL in water (top curve), 0.1% (w/w) mucin in water (lower curve) and 0.1% mucin + 0.1% EGCg in water (middle curve). Cells were added at time 0. Notice that PLL and mucin + EGCg both reach a maximum peak width, which declines beyond 50%, whereas on mucin they never get that far. Linear least square fits to the interval 0-30 minutes gave rates of $2x10^{-4}\pm 8x10^{-6}$ deg/min and $9x10^{-5}\pm 3x10^{-6}$ deg/min for PLL and mucin + EGCg respectively. Mucin alone yields two phase, a fast initial are ($7x10^{-5}\pm 3x10^{-6}$deg/min) and a subsequent slow are $3x10^{-5}\pm 1x10^{-6}$ deg/min.

Cell attachment and spreading responds to substrate rigidity (Beningo et al., 2001; Engler et al., 2004) and the flavonoid-induced restoration of cell activity may be due to structural changes in the layer which alter the viscoelastic properties. On the other hand, upon contacting the substrate fibroblasts, and many other cell types will modify it by synthesising and releasing onto the surface proteins required for the extracellular matrix (Revel and Hay, 1963). We infer that for this cell type the synthesis and release of proteins at the surface is most likely not the primary driving force behind the results seen here as the timescales are too short, i.e., less than 1 h. The increase in $\Delta\alpha$ for mucin only substrates (10–30 min) suggests that more material is being localised close to the surface even as the surface coverage stops increasing.

B.5Conclusion

In summary, fibroblast cell attachment and spreading is greatly reduced on mucincoated substrates when compared with PLL but can be countered by incorporating a polyphenol flavonoid, EGCg, into the layer. It is, therefore, most likely that the substrate viscoelastic properties are the main influence on initial cell spreading. Of future interest would be the effect of surface elasticity on intracellular signalling pathways. Also there remain issues regarding the bioavailability of EGCg and the gastrointestinal tract behaviour of bioflavonoids. Of key interest here would be the role that EGCg plays in bacterial attachment at mucosal interfaces.

List of figures

2.7 Carbon nanomaterials were obtained from Thomas Swan, Page 60.

3.1 Chemical structure of all-*trans* retinoic acid, page 71.

3.2 Differentiation into neurons (Protocol A), Page 73.

3.3 Differentiation into new morphology (Protocol B), Page 74.

3.4 TERA2 cells were grown according to protocol A except that the concentration was 0.5 μM. The width of the image is 850 μm, Page 75.

3.5 TERA2 cells were grown according to protocol A, except that the storage temperature at 4 °C. The width of the image is 850 μm, Page 75.

3.6 Differentiation of neurons, protocol A (left) using fresh 10 μM retinoic acid. Protocol B (right) using 10 μM retinoic acid aged in the medium, both derived from undifferentiated TERA2 cells (centre). The widths of the images are 850 microns, Page 76.

3.7 Differentiation of TERA2 cells according to Protocol A. The number in the upper left-hand corner gives the number of days after initiating treatment with retinoic acid, Page 80.

List of tables

Abbreviations

bFGF	**basic fibroblast growth factor**
BMP4	**Bone morphogenic protein 4**
BSA	**Bovin serum albumin**
CNTs	**Carbon nanotubes**
DMSO	**Dimethyl sulfoxide**
ECCs	**Embryonal carcinoma cells**
ECM	**Extracellular matrix**
EGCs	**Embryonal germ cells**
EGF	**Epidermal growth factor**
ESCs	**Embryonal stem cells**
HEPES	**4-(2-hydroxyethyl)-1-piperazineethanesulfonic acid**
HSCs	**Hematopoietic stem cells**
MAPCs	**Multipotent adult progenitor cells**
MNPs	**Magnetic nanoparticles**
MRI	**Magnetic resonance imaging**
MSCs	**Mesenchymal stem cells**
NSCs	**Neural stem cells**
OWLS	**Optical waveguide lightmode spectroscopy**
PAH	**Poly allylamine hydrochloride**
PBS	**Phosphate buffered solution**
PLL	**Poly-l-Lysine**
PSS	**Poly sodium-4-styrene-sulfonate**

QCM	**Quartz crystal microbalance**
RA	**Retinoic acid**
RAR	**Retinoic acid receptor**
RBP	**Retinoic acid binding protein**
RGD	**Arginine-glycine-aspartate**
SAR	**Scanning angle reflectometry**
SDS	**Sodium dodecyl sulphate**
SEM	**Scanning electron microscopy**
SWNTs	**Single wall nanotubes**
TIRF	**Total internal reflection fluorescence**
VSV	**Vesicular stomatitis virus**

References:

Albrecht-Buehler, G. (1976) Filopodia of spreading three T3 cells. Do they have a substrate-exploring function? *J. Cell Biol*. 69, 275–286.

Alves, N. M., Gomez, R., Gomez, T., Mano, J. F. (2004) Viscoelastic behaviour of poly (methyl methacrylate) networks with different cross-linking degrees. *Macromolecules*. 37, 3735–3744.

Andrews, P.W. (1984) Retinoic acid induces neuronal differentiation of a human embryonal carcinoma cell line in vitro. *Developmental Biology*.103, 285-293.

Ansari, F., Horvath, R., Aref, A., Ramsden, J.J., (2008) Bacterial adsorption onto a thin Fe3O4 magnetic nanofilms. In *11th Annual Nanotechnology Conference and Trade Show, Boston, Massachusetts*, U.S.A., June 1-5, Page 66.

Baharvand, H., Kazemi Ashtiani, S., Valojerdi, M. R., Shahverdi, A., Taee, A., Sabour, D. (2004) Establishment and in vitro differentiation of a new embryonic stem cell line from human blastocyst. *Differentiation*. 72, 224–229.

Baharvand, H., Azarnia, M., Parivar, K., Kazemi Ashtiani, S. (2005) The effect of extra cellular matrix on embryonic stem cell-derived cardiomyocytes. *J Mol Cell Cardiol*. 38, 495-503.

Baharvand, H. (2006a) Embryonic Stem Cells: Establishment, Maintenance and Differentiation. In: Embryonic Stem Cell Research, ed. E.V. Grier, NOVA Publishers, p.1-63.

Baharvand, H., Kazemi Ashtiani, S., Taee, A., Massumi, M., Valojerdi, M. R., Eftekhari, P., Moradi, S. H. (2006b) Geration of New Human Embryonic Stem Cell Lines with Diploid and Triploid Karyotypes. *Development, Growth and Differentiation*. 48, 117-128.

Baharvand, H. and Zare, N. (2008). Nanotechnology application in stem cell biology and technology. In: Bionanotechnology, ed. D. Reisner, and J. Bronzino, CRC Press, p.1-43.

Baksh, D., Song, L., Tuan, R. (2007) Adult MSC: characterization, differentiation and application. *J Cellular and Molecular Medicine*. 8, 301-316.

Ball, V. and Ramsden, J. J. (1998) Buffer dependence of refractive index increments of protein solutions. *Biopolymers*. 46, 489–492.

Bansil, R., Stanlet, E and LaMont, J. T. (1995) Mucin biophysics. *A Rev Physiol.* 57, 635–657.

Bardsley, W.G. and Aplin, J.D. (1983) Kinetic analysis of cell spreading. I. Theory and modelling of curves. *J. Cell Sci.* 61, 365–373.

Barngrover, D. (1986) Substrata for Anchorage-dependent Cells. In Mammalian Cell Technology. ed. W. Thilly, Butter-worths, p. 131-149.

Bell, G.I., Dembo, M. and Bongrand, P. (1984) Cell adhesion. Competition between nonspecific repulsion and specific bonding. *Biophys. J.* 45, 1051–1064.

Beningo, K. A., Dembo, M., Kaverina, I., Small, V. and Wang, Y-L. (2001) Nascent focal adhesions are responsible for the generation of strong propulsive forces in migrating fibroblasts. *J Cell Biol.* 153, 881–887.

Beningo, K.A., Dembo, M. Wang Y.L. (2004) Responses of fibroblasts to anchorage of dorsal extraceluar matrix receptor. *Proc Natl Acad Sci.* 101, 8024-18029.

Bereiter-Hahn, J., L¨ uck, M., Miebach, T., Stelzer, H.K. and V¨oth, M. (1990) Spreading of trypsinized cells: cytoskeletal dynamics and energy require ments. *J. Cell Sci*. 96,171–188.

Berg, C. H., Rutland, M. W. And Arnebrant, T. (2003) Lubricating properties of the initial salivary pellicle-an AFM study. *Biofouling.* 19, 365–369.

Berg, C. H, Lindh, L. and Arnebrant, T. (2004) Intraoral lubrication of PRP-1, statherin and mucin as studied by AFM. *Biofouling*. 20, 63–165.

Berthelemy, N., Kerdjoudj, H., Gaucher, C., Schaaf, P. (2008) Polyelectrolyte films boost progenitor cell differentiation into endothelium-like monolayers. *Advance Materials*. 9999, 1-5.

Berry, C. C. and Curtis, A. (2003) Functionalisation of magnetic nanoparticles for applications in biomedicine. *Journal of Phys. D: Appl Phys*. 36, 198-206.

Binnih, B. and Rohrer, H. (1982) Scanning tunneling microscopy. *Helvetica Physica Acta*. 55, 38-47.

Bissell, M. J. and Barcellos-Hoff, M. H. (1987) The influence of extracellular matrix on gene expression: is structure the message? *J Cell Sci Suppl.* 8, 327-343.

Bjorklund, L. M., (2002) Embryonic stem cells develop into functional dopaminergic neurons after transplantation in a Parkinson rat model. *Proc Natl Acad Sci*. 99, 2344-2349.

Bongso, A. and Richards, M. (2006) History and perspective of stem cell research. *Best Practice & Research Clinical Obstetrics & Gynaecology*.18, 827–842.

Boskovic, B. (2007) Carbon nanotubes and Nanofibers. *Nanotechnology Perceptions*. 3, 141-158.

Bradley, A., Evans, M. J., Kaufman, M. H., Robertson, E. (1984) Formation of germline chimaeras from embryo-derived teratocarcinoma cell lines. *Nature*, 309, 255–256.

Braydich-Stolle, L., Hussain, s., Schlager, J. and Hofmann, M. (2005) In vitro cytotoxicity of nanoparticles in mammalian germline stem cells. *Toxicol Sci.* 88, 412-419.

Brooking, J., (2001) Transport of nanoparticles across the rat nasal mucosa. *J Drug Target.* 9, 267-279.

Bruinsma, R. (1996) Physical aspects of the adhesion of leukocytes. In: T.Riste and D. Sherrington (eds), Physics of Biomaterials: Fluctuations, Self-assembly and Evolution, pp. 61–101. Dordrecht: Kluwer.

Bruinsma, R. and Sackmann, E. (2001) Bioadhesion that the dewetting transition. C.R. Acad. Sci. Paris, S´er. IV, 2, 803–815.

Brustatori, M. (2001). Protein adsorption kinetics under anapplied electric field. PhD thesis, University of Michigan, Detroit, USA.

Bulte, J., and Kraitchman, D. (2004) Iron oxide MR contrast agents for molecular and cellular imaging. *NMR Biomed.* 17, 484-499.

Butler, M. A. (1988) Comparative Review of Microcarriers Available for the Growth of Anchorage-dependent Animal Cells. In Animal Cell Biotechnology. ed. R. Spier, and Griffiths, J. B. Academic Press, Vol. 3, pp 284-303.

Cacace, M. G., Landau, E. M., Ramsden, J. J. (1997) The Hofmeister series: salt and solvent effects on interfacial phenomena. *Q Rev Biophys*. 30, 241-278.

Caplan, A. (2006) Mesenchymal stem cells, In: Essentials of stem cell biology. Ed. R. Lanza. Academic Press.

Carpenter, M. K., Cui, X. Hu Z.-Y., Jackson, J., Sherman, S., Seiger A., Wahlberg, L.U. (1999) In vitro expansion of a multipotent population of human neural progenitor cells. *Exp Neurol.* 158, 265–278.

Chavany, C., Behmoaras, T., Puisieux, F., and Helene, C. (1994) Adsorption of oligonucleotides onto polyisohexycya nanocryslate nanoparticles protects them against nucleases and increases their cellular uptake. *Pharm Res*. 11, 1370-1378.

Chen, J., Hamon, M, A., Hu, H., Chen, Y., Rao, A., Eklund, P., Haddon, P. C.(1998) Solution properties of single-walled carbon nanotubes. *Sceince.* 282, 95-98.

Chen, F., Kathleen T Rousche and Rocky S Tuan. (2006) Technology Insight: adult stem cells in cartilage regeneration and tissue engineering. *Nature Clinical Practice Rheumatology.* 2, 373-382.

Cherukuri, P., Bachilo, M., Litovsky, S and Weisman, R. (2004) Near-infrared fluorescence microscopy of single-walled carbon nanotubes in phagocytic cells. *J Am Chem Soc.* 126, 15638-15639.

Chrissterson, C. E., Lindh, L. and Arnebrant, T. (2000) Film-forming properties and viscosities of saliva substitutes and human whole saliva. *Eur J Oral Sci.* 108, 418–425.

Chu, c., Zhang, X. Z., and van buskirk, R. (2002) Biodegradable hydrogel-textile hybrid for tissue engineering. National Textile Centre Research Briefs-material Competency: June 2002 (NTC Project: M01-B01).

Cottier, K. and Horvath, R. (2008). Imageless microscopy of surface patterns using optical waveguides. *App Phys. B.* 91, 319-327.

Cukierman, E., (2001) Taking cell-matrix adhesions to the third dimension. *Science.* 294, 1708-1712.

Cui, D., (2005) Effect of single wall carbon nanotubes on human HEK293 cells. *Toxicology letters.* 155, 73-85

Curtis, A.S. (2001) Cell reactions with biomaterials: the microscopies. *European cells & Materials.* 1, 59-65.

Dalby, M.J., Riehle, M. O., Johnstone, H., Affrossman, S., Curtis, A. (2002) Polymer-demixed nanotopography: control of fibroblast spreading and proliferation. *Tissue Eng.* 8, 1099-1108.

Dalby, M.J., Riehle, M., Sutherland, S., Agheli, H., Curtis, A. (2004) Changes in fibroblast morphology in response to nano-columns produced by colloidal lithography. *Biomaterials.* 25, 5415-5422.

Daley, G. (2006) Hematopoietic stem cells. In: Essential of stem cell biology, ed. R. Lanza. Academic Press.

DeLuca, L. M., Kosa, K. and Andrea, F. (1997) The role of Vitamin A in differentiation and skin carcinogenesis. *J. Nutr. Biochem*. 8, 426–437.

Dembo, M., Torney, D.C., Saxman, K. and Hammer, D. (1988) The reaction-limited kinetics of membrane-to-surface adhesion and detachment. *Proc R Soc Lond. B* 234, 55–83.

Dennis, J.E. (1999) A quadripotential mesenchymal progenitor cell isolated from the marrow of an adult mouse. *J Bone Miner Res.* 14, 700-709.

DeWild, M., Berner, S., Suzuki, H., Ramoino, L., Baratoff, A. and Jung, T. A. (2003) Molecular assembly and self-assembly: Molecular nanoscience for future technologies. *Ann N Y Acad Sci*. 1006, 291-305.

Dinesh, S., (2006) Stem cell attachment to layer-by-layer assembled TiO_2 nanoparticle thin films. *Biomaterials.* 27, 4294-4303.

Drager, U.C. and McCaffery, P. (1997) Retinoic acid and development of the retina. *Prog Retin Eye Res*. 16, 323–351.

Dunon. D et al. (1996) To stick or not to stick: the new leukocyte homing paradigm. *Current Opinion Cell Biol.* 8, 714–723.

Engler, A., Bacakova, L., Newman, C, Hategan, A., Griffin, M. and Discher, D.(2004) Substrate compliance versus ligand density in cell on gel responses. *Biophys J* 86, 617–628.

Evans, J. W. (1993) Random and cooperative sequential adsorption. *Rev Mo. Phys*. 65, 1281–1329.

Fang, Y., Ferrie, A. M., Fontaine, N. H., Mauro, J., Balakrishnan, J. (2006). *J Biophysics*. 91, 1925-1940.

Faucheux, N., Warocquier-Clérout, R., Duval, J. L., Haye, B., Nagel, M. D. (1999) cAMP levels in cells attached toAN69 and cuprophan: cAMP dependence of cell aggregation and the influence of serum. *Biomaterials.* 20, 159–165.

Feller, W. (1940) On the logistic law of growth and its experimental verifications in biology. *Acta Biotheoretica.* 5, 51–65.

Feynman, R. P. (1959).There's plenty of room at the bottom. (Accessed 10th September 2007).http://www.zyvex.com/nanotech/feynman.html.

Flemming, R. G., Murphy, C. J, Abrams, G. A., Goodman, S. L., Nealey, P. (1998) Effect of synthetic micro-and nano-structured surfaces on cell behaviour. *Biomaterials*. 20, 573-588.

Fogh, J. and Trempe G.(1975) New human tumour cell lines. In Human tumour cells in vitro. ed. J. Fogh , pp 115-159. Plenum Press.

Folkman, J. and Moscona, A. (1978). Role of Cell Shape in Growth Control. *Nature*. 273, 345-349.

Frangioni, J.V., and Hajjar, R.J. (2004) In vivo tracking of stem cells for clinical trials in cardiovascular disease. *Circulation.* 110, 3378-3383.

Fredrikkson, C., Kihlmann, S., Rodahl, M. and Kasemo, B. (1998). The piezoelectric quartz crystal mass and dissipation sensor: a means of studying cell adhesion. *Langmuir*. 14, 248–251.

Gabriel, M. O., Grunheid, T. and Zentner, A. (2005) Glycosylation pattern and cell attachment-inhibiting property of human salivary mucins. *J Periodontol*. 76, 1175-1181.

Gallagher, A. (2002) Interaction of animal cells with ordered nanotopography. *Transactions on nanobio science*. 1, 24-28.

Gardner, R. L., (2006) Present Perspective and future challenges. In: Essentials of stem cell biology, ed. R. Lanza. Academic Press.

Gekas, J., Hindié, M., Faucheux, N., Lanvin, O., Maziére, C., Fuéntes, V., Gouilleux-Gruart, V., David, B., Maziére, J-C., Lassoued, K. and Nagel, M-D. (2004) The inhibition of cell spreading on a cellulose substrate (cuprophan) induces an apoptotic process via a mitochondria-dependent pathway. *FEBS Lett.* 563, 103–107.

Gepstein, L. (2002) Derivation and Potential Applications of Human Embryonic Stem Cells. *Circulation Research.* 91, 866.

Gonsalves, K., Craig R. Halberstadt, Cato T. Laurencin, Lakshmi S. Nair. (2008) Biomedical Nanostructures. John Wiley & Sons, Inc.

Green, J. H. (1976) *An introduction to human physiology*. (4th edition), Oxford University press.

Griffith, L.G. (2002) Emerging design principles in biomaterials and scaffolds for tissue engineering. *Ann N Y Acad Sci*. 961, 83-95.

Grinnell, F. (1978). Cellular Adhesiveness and Extracellular Substrata. *Rev Cytol*. 53, 65-144.

Gryte, D. M., Ward, M. D. and Hu, W-S. (1993). Real-time measurement of anchorage-dependent cell adhesion using a quartz crystal microbalance. *Biotechnol Prog*. 9, 105–108.

Guarnaccia, S. P., Schnaar, R. L. Hepatocyte, M. (1982). Adhesion to Immobilized Carbohydrates. *J Biol Chem*. 257, 14288- 14292.

Guo, P. (2005) RNA nanotechnology: engineering, assembly and applications in detection, gene delivery and therapy. *Journal of nanoscience and nanotechnology*. 5, 1964-1982.

Gussoni, E., (1999) Dystrophin expression in the mdx mouse restored by stem cell transplantation. *Nature*. 401, 390-394.

Gutwein, L, and T.J. Webster. (2004) Increased viable osteoblast density in the presence of nanophase compared to conventional alumina and titania particles. *Biomaterials.* 25, 4175–4183.

Ham, R.G. and McKeehan, W.L., (1979) In: Methods in Enzymology, Vol. LVIII, Cell Culture. Ed. W. Jakoby and I.H. Pastan. Academic Press. p. 49.

Hamberg, L.M., (1996) Continuous assessment of relative cerebral blood volume in transient ischemia using steady state susceptibility-contrast MRI. *Magn Reson Med.* 35, 168-173.

Hanein, D. et al. (1993) Selective interactions of cels with crystal surfaces. *J.Cell Sci.* 104, 275–288.

Hartley, R.S., Margulis, M., Fishman, P.S., Lee, V.M.-Y., Tang, C.M. (1999) Functional synapses are formed between Ntera2 (NT2N, hNT) neurons grown on astrocytes. *J Comp Neurol*. 407, 1–10.

Hatton, M. N., Levine, M. J., Margarone, J. E. and Aguire, A.(1987) Lubrication and viscosity features of human saliva and commercially available saliva substitutes. *J Oral Maxillofac Surg.* 45, 496–499.

Heim, F., Chakfe, N., and Durand, B. (2002). Anew concept of a flexible textile heart valv prosthesis. Society for biomaterials, 28th Annual Meeting Transactions. p, 655.

Hermann, A. (2006) Epigenetic conversion of human adult bone mesodermal stromal cells into neuroectodermal cell types for replacement therapy of neurodegenerative disorders. Expert Opinion on Biological Therapy, Volume 6, pp. 653-670.

Hoehn, M., (2002) Monitoring of implanted stem cell migration in vivo: a highly resolved in vivo magnetic resonance imaging investigation of experimental stroke in rat. *Proc Natl Acad Sci U S A.* 99, 16267-16272.

Horrocks, G.M., Lauder, L. Stewart, R and Przyborski, SA. (2003) Formation of neurospheres from human embryonal carcinoma stem cells. *Biochem Biophys Res Comm.* 304, 411-416.

Horvath, R. J. V¨ or¨ os, R. Graf, G. Fricsovszky, M. Textor, L.R. Lindvold, N.D. Spencer, E. (2001) Reverse symmetry waveguides. *Appl Phys B* 72, 441-447.

Horvath, R; G. Fricsovszky, E. Papp; (2003). Application of the optical waveguide lightmode spectroscopy to monitor lipid bilayer phase transition. *Biosensors Bioelectronics.* 18, 415-428.

Horvath, R.; Henrik C. Pedersen, and Nina Skivesen (2004). Measurement of guided light-mode intensity: An alternative waveguide sensing principle. *Applied Physic Letter*. 84, 4044-4046.

Horvath, R. Henrik C. Pedersen, and Nina Skivesen (2005). Monitoring of living cell attachment and spreading using reverse symmetry waveguide sensing. *Applied Physic Letter*. 86, 071101.

Hu, Hui, Ni, Y., Montana, V., Haddon, R. and Parpura, V. (2004) Chemically functionalized carbon nanotubes as substate for neuronal growth. *Nano letters*. 4, 507-511.

Hug, T. S., Prenosil, J. E. and Morbidelli, M. (2000). Optical waveguide lightmode spectroscopy as a new method to study adhesion of anchorage-dependent cells as an indicator of metabolic state. *Biosens Bioelectron*. 16, 865–874.

Hug, T. S., Prenosil, J. E. and Morbidelli, M. (2002) Optical waveguide lightmode spectroscopy (OWLS) to monitor cell proliferation quantitatively. *Biotechnology and bioengineering.* 80, 213-221.

Janes, K., Calvo, P.and Alonso, M. J. (2001) Polysacharaide colloidal particles as delivery systems for macromolecules. *Adv Drug Deliv Rev*. 47, 83-97.

Javazon, E.H. (2001) Rat marrow stromal cells are more sensitive to plating density and expand more rapidly from single-cell-derived colonies than human marrow stromal cells. *Stem Cells*. 19, 219-225.

Jobstl, E., O'Connell, J., Fairclough, J. P. A., Williamson, M. P.(2004) Molecular Model for Astringency Produced by Polyphenol/Protein Interactions. *Biomacromolecules.* 5, 942–949.

Johnson, J., (2005) Oocyte generation in adult mammalian ovaries by putative germ cells in bone marrow and peripheral blood. *Cell.* 122, 303-315.

Jones-Villeneuve, E.M.V., McBurney, M.W., Rogers, K.A., Kalnins, V.I., (1982) Retinoic acid induces embryonal carcinoma cells to differentiate into neurons and glia, *J. Cell Biol*. 94, 253–262.

Karamuk, E et al., (2000). Structural and mechanical aspects of embroidered textile scaffolds for tissue engineering, Society of Biomaterial, Sixth World Biomaterials Congress Transactions.

Khademhosseini, A. (2008) Micro-and Nanoengineering of the Cell Microenvironment, Technologies and Applications. Artech House Publishers.

Khademhosseini, A. Langer, R. Borenstein, J and Vacanti, J. (2006) Microscale technologies for tissue engineering and biology. *Proc Natl Acad Sci U. S. A.* 103, 2480-2487.

Kommireddy, M., Shashikanth, M., Sriram, M., and Mills, D. (2006) Stem cell attachment to layer-by-layer assembled TiO_2 nanoparticle thin films. *Biomaterials* 27, 4296-4303.

Krause, D.S. (2001) Multi-organ, multi-lineage engraftment by a single bone marrow-derived stem cell. *Cell*. 105, 369-377.

Kurrat, R., Presonil, J. E. and Ramsden, J. J. (1997). Kinetics of human and bovine serum albumin adsorption at silica-titania surfaces. *J Coll Int Sci.* 185, 1–8.

Kuo, C and Tuan, R. (2003) Tissue Engineering with Mesenchymal Stem Cells. IEEE, Tissue engineerin, IEEE, *Engineering in Medicin and Biology*. p, 51-56.

Lagasse, E. (2000) Purified hematopoietic stem cells can differentiate into hepatocytes in vivo. *Nature medicine.* 6, 1229-1234

Langer, R., and Vacanti, J. P. (1993) Tissue engineering. *Science.* 260, 920-926.

Langmuir, I. (1918). The adsorption of gases on plane surfaces of glass, mica and latinum.*J Am Chem Soc*. 40, 1361–1403.

Lanza M.D, Winter, P., Caruthers, S. D., Morawski, A. M., Schmieder, A. H., Crowder, K. C. and Wickline, S. M. (2004) Magnetic resonance molecular imaging with nanoparticles. *Journal of Nuclear Cardiology*. 11, 733-743.

Lanza, R., Gearhart, J., Hogan, B., Melton, D., Pedersen, R. (2006) Essentials of stem cell biology. Academic Press.

Lavalle, G., Gergely, A., Lustig, and V. Ball.(2000) Critical analysis of the apoferritin adsorption at solid-liquid interfaces in the framework of a particular adsorption model. *J Chem Phys*. 113, 8212–8224.

Levenberg, S., Khademhosseini, A. Langer, R. (2006) Embryonic stem cell in tissue engineering. In: Essentials of stem cell biology.ed. R. Lanza. Academic Press.

Levine, M. J., Aguire, A., Hatton, M. N. and Tabak, L. A. (1987) Artificial slivas: present and future. *J Dent Res.* 66, 693–698.

Li, S-Y., Ramsden, J. J., Prenosil, J. E., and Heinzle, E. (1994). Measurement of adhesion and spreading kinetics of baby hamster kidney and hybridoma cells using an integrated optical method. *Biotechnol Prog*. 10, 520–524.

Li, W.J. (2002) Electrospun nanofibrous structure: a novel scaffold for tissue engineering. *J Biomed Mater Res*. 60, 613-621.

Li, W.J. (2003) Biological response of chondrocytes cultured in three-dimensional nanofibrous poly(epsilon-caprolactone) scaffolds. *J Biomed Mater Res.* 67A, 1105-1114.

Li, W.J., Richard Tuli, Chukwuka Okafor, Assia Derfoul, Keith G. Danielson, David J. Hall and Rocky S. Tuan. (2005) A three-dimensional nanofibrous scaffold for cartilage tissue engineering using human mesenchymal stem cells. *Biomaterial*. 26, 599-609.

Lovat, V., Pantarotto, D., Lagostena, L. (2005) Carbon nanotube substrates boost neuronal electrical signalling. *Nano Letters*. 5, 1107-1110.

Luthi P. O., Chopard B., A. Preiss, Ramsden J. J, (1998) A celluar automaton model for neurogenesis in *Drosophila*, *Physica D.* 118, 151-160.

Lyo, T., Maki, Y., Sasaki, N. and Nakata, M.(2004) Anisotropic viscoelastic properties of cortical bone. *J. Biomechanics.* 37, 1433–1437.

Macpherson, P. A, McBurney, M. W. (1995) P19 embryonal carcinoma cells: a source of cultured neurons amenable to genetic manipulation. *Methods: a companion to methods in Enzymology*. 7, 238-252.

Martínez-Mera, I., M.E. Espinosa-Pesqueira, R. Pérez-Hernández, (2007) *Mater Lett.* 61, 4447.

Mattson, M., Haddon, R. C., Rao, A. M. (2000) Molecular functionalization of carbon nanotubes and use as substrates for neuronal growth. *Journal of Molecular Neurosciences*. 123, 3838.

McColl, J. (2007) On some factors that effect the 'feel' of molecules. (Published PhD thesis). Cranfield University, England.

McColl, J., Horvath, R., Aref, A., Larcombe, L., Morgan, S., Chianella, I., Yakubov, G., and Ramsden, J. (2008) Polyphenol control of cell spreading on glycoprotein substrates. *Journal of Biomaterials Science: Polymer Edition, in press*.

McKeehan, W.L., (1984) Methods for Preparation of Media, Supplements, and Substrata for Serum-free. Animal Cell Culture. A.R. Liss, NY p.209.

McKenzie, J.L. (2004) Decreased functions of astrocytes on carbon nanofiber materials. *Biomaterials.* 25, 1309-1317.

Meng, J., Li Song, Jie Meng, Hua Kong, Guangjin Zhu, Chaoying Wang, Lianghua Xu , Sishen Xie, Haiyan Xu. (2006) Using single-walled carbon nanotubes nonwoven films as scaffolds to enhance long-term cell proliferation in vitro. *Journal of Biomedical materials research part A.* 79A, 298-306.

Mezey, E. (2003) Transplanted bone marrow generates new neurons in human brains. *Proc Natl Acad Sci U S A.*100, 1364-1369.

Miano, J.M., Berk, B.C., (2000) Retinoids—versatile biological response modifiers of vascular smooth muscle phenotype. *Circ Res*. 87, 355–362.

Moniaux, N., Andrianifahanana, M., Brand, R. E. and Batra, S. K. (2004) Multiple roles of mucins in pancreatic cancer, a lethal and challenging malignancy. *Brit J Cancer*. 91, 1633–1638.

Moore, M. T. and Levine, S. R. (2006) People Help Drive Progress. In: Essentials of Stem Cell Biology, ed. R. Lanza. Academic Press. p. 513.

Müller, G., Streicher, J and Müller, R, (1996) Homeotic duplicate of the pelvic body segment in regenerating tadpole tails induced by retinoic acid. *Dev Genes Evol*. 206, 344-348.

Nagy, A., Gocza, E., Diaz, E. M., Prideaux, V. R., Ivanyi, E., Markkula, M., Rossant, J. (1990) Embryonic stem cells alone are able to support fetal development in the mouse. *Development*. 110, 815-21.

Nagy, A., Rossant, J., Nagy, R., Abramov, N., Roder, W. (1993) Derivation of completely cell culture-derived mice from early-passage embryonic stem cells. *Proc Natl Acad Sci USA.* 90, 8424–8428.

N'Dri, N.A., Shyy, W and Tran-Son-Tay, R. (2002) Cell adhesion modeling: effect of the leukocyte rheology. Proc. 2nd Joint EMBS/BMES Conf.,23–26 October, Houston, pp. 362–365.

Niemeyer, C (2004) Nanobiotechnology: concepts, applications and perspectives, Wiley-VCH.

Niederreither, K., Abu-Abed, S., Schuhbaur, B., Petkovich, M., Chambon, P., and Dollé, P. (2002) Genetic evidence that oxidative derivatives of retinoic acid are not involved in retinoid signalling during mouse development. *Nature genetics*. 31,84-88.

Nimeri, G., Fredrikkson, C., Elwing, H., Liu, L., Rodahl, M. and Kasemo, B. (1998). Neutrophil interaction with protein –coated surfaces studied by an extended quartz crystal microbalance technique. *Coll Sur B Biointerfaces.* 11, 255–264.

Noy, N. (2000) Retinoid-binding proteins: mediators of retinoid action. *Biochem J.* 348, 481-495.

Nur, E. K. A. (2005) Three dimensional nanofibrillar surfaces induce activation of Rac. *Biochem Biophys Res Commun,* 331, 428-434.

Orlic, D., (2001) Bone marrow cells regenerate infarcted myocardium. *Nature.* 410, 701-705

Ozin, G. A., and Arsenault, A. C. (2005) Nanochemistry. Cambridge, RSC, Publishing.

Paradise, M. and Goswami, T. (2007) Carbon nanotubes – Production and industrial applications. *Mater Design*. 28, 1477-1489.

Park, K.H. (2003) Single-walled carbon nanotubes are a new class of ion channel blockers. *J Biol Chem*. 278, 50212-50216.

Payne, A.G. (2004) Using immunomagnetic technology and other means to facilitate stem cell homing. *Medical Hypotheses*. 62, 718-720.

Pennisi, E. (1998) How a growth control pathway takes a wrong turn to cancer. *Science*. 281, 1439–1441.

Pera, M. J., Cooper, S., Mills, J. and Parrington, J. M. (1989) Isolation and characterisation of a multipotent clone of human embryonal carcinoma-cells.*Differentiation.* 42, 10-23.

Perez-Vilar, J. and Hill, R. L.(1999) The structure and assembly of secreted mucins. *J Biol Chem*. 274, 31751–31754.

Pesen, D. and Hoh, J.H. (2005) Micromechanical architecture of the endothelial cell cortex. *Biophys. J.* 88, 670–679.

Poole, C. P. and Frank, O. J. (2003). Introduction to Nanotechnology. Wiley& Sons, Inc.

Pritinder, K. and Li, A. (2000) Adhesive properties of human basal epidermal cells: An analysis of keratinocyte stem cells, transit amplifying cells and postmitotic differentiating cells. *The Journal of Investigative Dermatology*. 114, 413-420.

Proctor, G. B. and Carpenter, G. H. (1998) The function of salivary proteins and the regulation of their secretion by salivary glands. *Biomed Rev.* 9, 3–5.

Przyborski, S. A, Morton, I. E, Wood, A, Andrews, P.W. (2000) Developmental regulation of neurogenesis in the pluripotent human embryonal carcinoma cell line NTERA-2. *Eur J Neurosci*. 12, 3521-3528.

Przyborski, S.A. (2001) Isolation of human embryonal carcinoma stem cells by immunomagnetic sorting. *Stem Cells*. 19, 500-504.

Przyborski, S.A, Christie, V.B, Hayman, M.W, Stewart, R., Horrocks, G.M. (2004) Human embryonal carcinoma stem cells: models of embryonic development in humans. *Stem Cells Dev*. 13, 400-408.

Przyborski, S.A. (2005) Differentiation of human embryonic stem cells after transplantation in immune-deficient mice. *Stem Cells*. 23, 1242-50.

Przyborski, S.A. (2007) Derivation and culture of human embryonal carcinoma stem cell line. Culture of human stem cells. Ed. Freshney, John Wiley & Sons, Inc.

Ramsden, J. J. Statist, J. (1993) Review of new experimental techniques for investigating random sequential adsorption. *Phys.* 73, 853–877.

Ramsden, J. J., Bachmanova, G. I. and Archakov, A. I.(1994) Kinetic evidence for protein clustering at a surface. *Phys Rev E.* 50, 5072–5076

Ramsden, J. J. (1995a). Experimental methods for investigating protein adsorption kinetics at surfaces. *Quart Rev Biophys.* 27, 41–105.

Ramsden, J. J. (1995b). Optical method for measurement of number and shape of attached cells in real time. *Cytometry*. 19, 97–102.

Ramsden, J. J. (1997). Dynamics of protein adsorption at the solid/liquid interface. *Recent Res Dev Phys Chem.* 1, 133–142.

Ramsden, J. J., and Mate, M., (1998) *Journal chemistry Society, Faraday Trans*. 94, 783-788.

Ramsden, J.J. (2000) MARCKS-a case of molecular exaptation? *Int. J. Biochem. Cell Biol.* 32, 475–479.

Ramsden, J. J., (2005) What is nanotechnology? *Nanotechnology Preceptions*. 1, 3-17.

Ramsden, J. J. (2006) High resolution molecular microscopy. in Proteins at Solid-Liquid Interfaces, edited by Ph. Dejardin, pp. 23–49 (Springer,Heidelberg).

Ramsden, J. J. (2008) *Biomedical Surfaces:* (1st ed), Norwood, Mass: Artech House.

Ratner, B. D., Hoffman, A., Schoen, F., Lemons, J.E. (2004) Biomaterials Science: An Introduction to Materials in Medicine.Academic Press.

Revel, J-P. and Hay, E. D. (1963) An autoradiographic and electron microscope study of collagen synthesis in differentiating cartilage. *Z Zellforsch.* 61, 110–114.

Revell, P. A., (2006) The biological effects of nanoparticles. *Nanotechnology Preceptions*. 2, 283-298.

Ricci, S. M., Talbot, J., Tarjus, G. and Viot, P. (1992). Random sequential adsorption of anisotropic particles. II. Low coverage kinetics. *J Chem Phys*. 97, 5219–5228.

Riviere, C., (2005) Iron oxide nanoparticle-labeled rat smooth muscle cells: cardiac MR imaging for cell graft monitoring and quantitation. *Radiology*. 235, 959-967.

Reynolds, B.A., Weiss, S. (1992a) Generation of neurons and astrocytes from isolated cells of adult mammalian central nervous system. *Science.* 255, 1707–1710.

Reynolds, B.A., Weiss, S., A. (1992b) Multipotent EGF-responsive striatal embryonic rogenitor cell produces neurons and astrocytes. *J Neurosci*. 12, 4565–4574.

Reynolds B.A., Weiss S., (1996) Clonal and population analyses demonstrate that an EGF-responsive mammalian embryonic precursor is a stem cell. *Dev Biol*. 175,1–13.

Roussel, P. h. and Delmotte, Ph. (2004) The diversity of epithelial secreted mucins. *Curr Organic Chem.* 8, 413–437.

Rosenthal, S., Tolinson, I., Adkins, E. (2001) Targeting cell surface receptor with ligand-conjugated nanocrystals. *J Am Chem Soc*. 124, 4586-4594.

Schaaf, P. and Talbot, J. (1989) .Surface exclusion effects in adsorption processes. *J Chem Phys*. 91, 4401–4409.

Schaaf, P.; Voegel, J-C and Senger, B. (1998). Irreversible deposition/adsorption processes on solid surfaces. *Ann De Phys*. 23, 1-89.

Schmeichel, K.L., and Bissell, M.J. (2003) Modelling tissue-specific signalling and organ function in three dimensions. *J Cell Sci.* 116, 2377-2388.

Schindler, M. (2005) A synthetic nanofibrillar matrix promotes in vivo-like organization and morphogenesis for cells in culture. *Biomaterials.* 26, 5624-5631.

Sekiya, I. (2002) Expansion of human adult stem cells from bone marrow stroma: conditions that maximize the yields of early progenitors and evaluate their quality. *Stem Cells.* 20, 530-541.

Senesi, G. S., E. D'Aloia, R. Gristina, P. Favia and R. d'Agostino. (2007) Surface characterization of plasma deposited nano-structured fluorocarbon coatings for promoting in vitro cell growth. *Surface science*. 601, 1019-1025.

Shapiro, E.M. (2006) In vivo detection of single cells by MRI. *Magn Reson Med*. 55, 242-249.

Shi Kam, N.W. (2004) Nanotube molecular transporters: internalization of carbon nanotube-protein conjugates into Mammalian cells. *J Am Chem Soc.* 126, 6850-6851.

Shi, L., Ardehali, R., Caldwell, K.D., Valint, P. (2000) Mucin coating on polymeric material surfaces to suppress bacterial adhesion. *Colloids Surface. B.* 17, 229-239.

Shih, C.C. (2002) Hematopoietic potential of neural stem cells. *Nature Mmedicine.* 8, 535-536.

Shimizu, M., Weinstein, I. B. (2005) Modulation of signal transduction by tea catechins and related phytochemicals. *Mutation Res.* 591, 147–160.

Shvedova, A. A. (2003) Exposure to carbon nanotube material: assessment nanotube cytotoxicity using human keratinocyte cells. *Journal of toxicology and environmental health.* 66, 1909-1926.

Slack, J. M. W. (2000) Stem cells in epithelial tissues. *Science.* 117, 1431–1433.

Smith, L. A., (2001) Embryo-Derived stem cell. *Stem cell*. 17, 435-462.

Smith, L. A. and Ma, P. X. (2004) Nano-fibrous scaffolds for tissue engineering. *Colloids and surfaces B.* 39, 125-131.

Smith, A.M., and Nie, S. (2005) Semiconductor Quantum Dots for Molecular and Cellular Imaging. *Tissue engineering and artificial organs.* 21,22-10.

Solter, D; Skreb, N; Damjanov, I. (1970) Extra uterine growth of mouse egg cylinders results in malignant teratoma. *Nature.* 227, 503–504.

Stevens, L. C. (1970) A new inbred subline of mice (129/terSv) with a high incidence of spontaneous congenital testicular teratomas. *J Natl Cancer Inst.* 50, 235–242.

Stewart, R, Christie, V and Przyborski, S.A. (2003) Manipulation of human pluripotent embryonal carcinoma stem cells and the development of neural subtypes. *Stem Cells.* 21,248-256.

Stoker, M. G. P., Rubin, H.(1967). Density dependent inhibition of cell growth in culture. *Nature.* 215,171-172.

Sun, S.Y., Lotan, R, (2002) Retinoids and their receptors in cancer development and chemoprevention. *Crit. Rev Oncol Hematol*. 41, 41–55.

Svendsen, C.N., Armstrong, R.J., Rosser, A.E., Chandran, S., Ostenfeld, T., M.A. Caldwell, (1998) A new method for the rapid and long term growth of human neural precursor cells, *J Neurosci Methods*. 85, 141–152.

Taylor, A.C. (1961) Attachment and spreading of cells in culture. *Exptl Cell Res. Suppl.* 8, 154–173.

Thompson, S, Stern, P.L, Webb, M, Walsh, F.S, Engstrom, W., Evans, E.P, Shi, W.K, Hopkins, B and Graham, C.F. (1984) Cloned human teratoma cells differentiate into neuron-like cells and other cell types in retinoic acid.; *J Cell Sci.* 72, 37-64.

Thomson, J. A., Itskovitz-Eldor, J., Shapiro, S. S., Waknitz, M. A., Swiergiel, J. J., Marshall, V. S., Jones, J. M. (1998) Embryonic stem cell lines derived from human blastocysts. *Science*. 282, 1145-7.

Tiefenthaler, K. and Lukosz, W. (1989) Sensitivity of grating couplers as integrated-optical chemical sensors. *J. Opt. Soc. Am. B* 6, 209.

Tiefenthaler, K. (1992) *Adv Biosensors*. 2, 261.

Tien, P. K. (1977) Integrated optics and new wave phenomena in optical waveguides. *Rev Mod Phys*. 49, 361-420.

Tourovskaia, T. Barber, T., Wickes, B. T., Hirdes, D., Grin, B., Castner, D. G. (2002) Micropatterns of chemisorbed cell adhesion-repellent films using oxygen plasma etching and elastomeric masks. *Langmuir*. 19, 4754–4764.

Turrsi, C. P., Faraoni, J. J., Menezes, M. And Serra, M. C.(2002) Analysis of potential lubricants for in vitro wear testing. *Dent Mater*. 22, 77–83.

Valentinuzzi, M. (2004) A primer for bioengineering. World scientific.

Vats, A., Tolley, N., Polark, J., (2002) Stem cell: source and application. *Clinical otolaryngology and allied science*. 27, 227-232.

Vescovi, B.A. Reynolds, D.D. Fraser, S. Weiss, (1993) Basic fibroblast growth factor regulates the proliferative fate of both unipotent (neuronal) and bipotent (neuronal/astroglial) epidermal growth factor-generated progenitor cells. *Neuron.* 11, 951–966.

Virtanen, I., Vartio, T., Badley, R.A. and Lehto, V.-P. (1982) Fibronectin in adhesion, spreading and cytoskeletal organization of cultured fibroblasts. *Nature.* 298, 660–663.

Vo-Dinh, T. (2006) Nanoprobes and nanobiosensors for monitoring and imaging individual living cells. *Nanomedicine*: *Nanotechnology, Biology, and Medicine.* 2, 22- 30.

Wangsness, R. K., (1986). Electromagnetic Field, 2nd edition., John Wiley& Sons, Inc., 405-421.

Watt, FM; Hogan, BL. (2000) Out of Eden: stem cells and their niches. *Science.* 287, 1427-30.

Webster, T. G., M.C. Waid, J.L. McKenzie, R.L. Price and J.U. Ejiofor, (2004) Nano-biotechnology: carbon nanofibres as improved neural and orthopaedic implants, *Nanotechnology* 15, 48–54.

Wesseling, J., van der Valk, S. W. and Hilkens, J. (1996) A mechanism for inhibition of E cadherin mediated cell cell adhesion by the membrane associated mucin episialin/MUC1. *Mol Biol Cell.* 7, 565–577.

Wilson, A and Trumpp, A. (2006) Bone-marrow haematopoietic-stem-cell niches. *Nature Reviews Immunology.* 6**,** 93-106

Witte R.P., Kao W.J., (2005) Keratinocyte-fibroblast paracrine interaction: the effects of substrate and culture condition. *Biomaterials.* 26, 3673–3682.

Wittmer, C. R., Phelps, J. A., Saltzman, W. M., Van Tassel, P. R.(2007) Fibronectin terminated multilayer films: Protein adsorption and cell attachment studies. *Biomaterials.* 28, 851–860.

Yoshimoto, H. (2003) A biodegradable nanofiber scaffold by electrospinning and its potential for bone tissue engineering. *Biomaterials*. 24, 2077-2082.

Zamir, E. and Geiger, B. (2001) Components of cell-matrix adhesions. *J Cell Science.* 114, 3577-3579.

Zuwei, Ma. and Masaya, T. (2005) Potential of nanofiber Matrix as tissue engineering scaffolds. *Tissue Engineering*. 11, 101-109.